Supporting information

Enzymatic Intermolecular Hetero-Diels Alder Reaction in the Biosynthesis of Tropolonic Sesquiterpenes

Qibin Chen,[1,#] Jie Gao,[1,#] Cooper Jamieson,[2] Jiawang Liu,[1] Masao Ohashi,[3] Jian Bai,[1] Daojian Yan,[1] Bingyu Liu,[1] Yongsheng Che,[4] Yanan Wang,[1] K. N. Houk [2*] and Youcai Hu[1, 5, 6*]

[1] State Key Laboratory of Bioactive Substance and Function of Natural Medicines, [5]NHC Key Laboratory of Biosynthesis of Natural Products, [6] CAMS Key Laboratory of Enzyme and Catalysis of Natural Drugs, Institute of Materia Medica, Chinese Academy of Medical Sciences & Peking Union Medical College, Beijing 100050, P. R. China

[2] Department of Chemistry and Biochemistry, [3] Department of Chemical and Biomolecular Engineering, University of California, Los Angeles, CA 90095, USA

[4] Institute of Medicinal Biotechnology, Chinese Academy of Medical Sciences & Peking Union Medical College, Beijing 100050, P. R. China

*E-mail: huyoucai@imm.ac.cn, houk@chem.ucla.edu

[#]These authors contributed equally to this work.

Table of contents

Experimental Procedures

Supplementary Tables

Supplementary Figures

Experimental Procedure

1. Strains and culture conditions

The endophytic fungus *Penicillium janthinillum* was isolated from the leaves of *Dracaena cambodiana* Pierre ex Gagnep and identified as we previously described.[1] It was maintained on Potato Dextrose Agar (PDA, BD) medium and stored at -80 °C with 20% glycerol. For compounds production and mRNA extraction, it was grown at 28 °C in Potato Dextrose Broth (PDB) medium (from BD) and shaken at 220 rpm for 4-5 days. *Aspergillus nidulans*, used as the heterologous expression host, was kindly donated by Prof. Wenbin Yin from Institute of Microbiology, Chinese Academy of Sciences. *A. nidulans* was cultured on CD plate (10 g/L glucose, 6 g/L $NaNO_3$, 0.52 g/L KCl, 0.52 g/L $MgSO_4 \cdot 7H_2O$, 1.52 g/L KH_2PO_4, 1 mL/L trace elements solution, 20 g/L agar) with supplementation of 10 mM uridine, 5 mM uracil, 0.5 mg/L pyridoxine, and 0.125 mg/L riboflavin at 37 °C for 3-4 days. *Saccharomyces cerevisiae* BJ5464-NpgA was used for *in vivo* homologous recombination to construct the *A. nidulans* overexpression plasmids. Yeast Extract Peptone Dextrose (YPD) medium (20 g/L peptone, 10 g/L yeast extract, 20 g/L dextrose) was used for routine growth, while uracil-dropout semisynthetic medium was used for selection of plasmids transformed into *S. cerevisiae*. *Escherichia coli* XL1-Blue was used for plasmid propagation, and *E. coli* BL21 (DE3) (Transgen Biotech, Beijing) was used for protein expression. The cultural media used for *E. coli* strains were LB broth (10 g/L tryptone, 5 g/L yeast extract, 10 g/L NaCl) and TB broth (12 g/L tryptone, 24 g/L yeast extract, 4 mL/L glycerol, 2.31 g/L KH_2PO_4, 12.54 g/L K_2HPO_4). Ampicillin or kanamycin was added to the media at concentrations of 100 μg/mL or 50 μg/mL if necessary.

2. General molecular biology experiments

Genomic DNA of *P. janthinillum* was prepared using the Plant Genomic DNA Kit (Tiangen, Beijing). For RNA extraction, mycelia of *P. janthinillum* were ground in liquid nitrogen, and dissolved in 1 mL Trizol (Invitrogen). The mixture was centrifuged at 12,000 rpm, 4 °C for 10 min, and the supernatant was transferred to a new tube containing 200 μL chloroform. After vortex mixing and centrifugation at 12, 000 rpm for 15 min, the supernatant was transferred and extracted once again with an equal volume of chloroform. 500 μL isopropanol was added to the supernatant, after which RNA was precipitated and washed with 1 mL 75% ethanol, and then resuspended in 40 μL RNase-free water. The residual genomic DNA was digested with RQ1 RNase-Free DNase (Promega) at 37 °C for 45 min, and RNA was purified by acid phenol (Ambion) extraction and ethanol precipitation. The cDNA was obtained by reverse transcription-polymerase chain reactions (RT-PCR) using PrimeScript™ RT Reagent Kit (Takara) with Oligo-dT primers. PCR for cloning were performed using Q5 high-fidelity DNA polymerase (New England Biolabs, NEB). PCR products were confirmed by DNA sequencing. The gene-specific primers were listed in Table S1. DNA restriction enzymes were used as recommended by the manufacturer (NEB).

3. Heterologous expression in *A. nidulans*

For heterologous expression in *A. nidulans*, plasmids pANU, pANR, and pANP, which contained auxotrophic markers for uracil (pyrG), riboflavin (riboB), and pyridoxine (pyroA), respectively, were used as backbones.[2] *glaA*, *gpdA*, and *amyB* were inserted as promoters. Genes of *eupfA*, *eupfB*, *eupfC*, *eupfD*, *eupfE*, *eupfF*, and *eupfG* with their own terminators (200-

500 bps) were amplified from the genomic DNA of *P. janthinillum*. The PacI/SwaI double-digested backbone and corresponding overlapping DNA fragments were assembled using yeast homologous recombination with *S. cerevisiae* BJ5464-NpgA.[3] The correct colonies checked by colony-PCR were combined, from which the plasmids were extracted using Zymoprep™ Yeast Plasmid Miniprep I Kit (Zymo Research), and transformed into *E. coli* XL-1-Blue for propagation. The plasmids extracted from *E. coli* transformants were checked by colony-PCR and enzymatic digestion, and confirmed by sequencing. The plasmids used for heterologous expression were listed in Table S2.

To prepare the protoplasts of *A. nidulans*, the spores of *A. nidulans* were inoculated into 50 mL liquid GMM medium (10 g/L glucose, 10 g/L yeast extract, 6 g/L nitrate salts, 0.52 g/L KCl, 0.52 g/L $MgSO_4 \cdot 7H_2O$, 1.52 g/L KH_2PO_4, 1 mL/L trace elements) supplemented with 10 mM uridine, 5 mM uracil, 0.5 μg/mL pyridoxine, and 0.125 μg/mL riboflavin, and germinated at 37 °C, 180 rpm for 5-6 hours. The germlings were harvested by centrifugation at 5,500 rpm, 4 °C for 3 min, and were washed with 25 mL Osmotic buffer (10 mM sodium phosphate buffer, 0.6 M $MgSO_4$, pH 7.0). The germlings were then resuspended in 25 mL Osmotic buffer containing 30 mg of Lysing enzyme from *Trichoderma harzianum* (Sigma-Aldrich) and 20 mg Yatalase (Takara), and shaken at 30 °C, 80 rpm for digestion. After 8-9 hours, the mixture was poured into a 50 mL tube and overlaid with 25 mL Trapping buffer (0.6 M sorbitol, 0.1 M Tris-HCl, pH 7.0). After centrifugation at 3,750 rpm, 4 °C for 15 min, the protoplasts were obtained from the middle layer which were further washed with triple volumes of STC buffer (1.2 M sorbitol, 10 mM $CaCl_2$, 10 mM Tris-HCl, pH 7.5) and resuspended in proper volume of STC buffer (100 μL protoplasts per transformation) for transformation.

For single transformation, plasmids were added into 100 μL protoplasts and incubated on ice for 50 min, after which 600 μL PEG solution (60% PEG4000, 50 mM $CaCl_2$ and 10 mM Tris-HCl with pH 7.5) was added and gently mixed, followed by additional incubation at room temperature for 20 min. Then the mixture was plated on dropout CD-sorbitol medium (10 g/L glucose, 6 g/L nitrate salts, 0.52 g/L KCl, 0.52 g/L $MgSO_4 \cdot 7H_2O$, 1.52 g/L KH_2PO_4, 1 mL/L trace elements, 1.2 M sorbitol, 15 g/L agar) and cultured at 37 °C for 2 days. Single transformant was transferred to solid CD plate and cultured for 3-4 days at 37 °C to harvest spores. The spores were inoculated into 25 mL liquid CD-ST medium (20 g/L soluble starch, 20 g/L casamino acids, 6 g/L nitrate salts, 0.52 g/L KCl, 0.52 g/L $MgSO_4 \cdot 7H_2O$, 1.52 g/L KH_2PO_4, 1 mL/L trace elements) and shaken for 4 days at 25 °C, 220 rpm for compounds production. The culture broth was extracted with ethyl acetate (EtOAc) for 3-4 times. The organic phase was concentrated to dried residue, which was dissolved in acetonitrile (MeCN) or methanol (MeOH) and subjected to UPLC-MS analysis.

4. Chemical complementation assays

To feed compounds to the heterologously overexpressed *A. nidulans* strains, spores of the *A. nidulans* transformed strain were inoculated in 25 mL of liquid CD-ST medium and shaken at 220 rpm, 25 °C. After 2 days, compounds (dissolved in DMSO) were added with a final concentration of 8 μM, and cultured for an additional 24 h, followed by extraction with EtOAc and analysis with UPLC-MS.

5. Protein expression and purification of EupfE and EupF

The intron-less sequence of *eupfE*, which was cloned from cDNA, was codon optimized based on the codon preference of *E. coli*, and the codon-optimized *eupfE* was synthesized and

ligated to the expression vector pET28a by GenScript Biotech Corp. (Nanjing, China). The resulting plasmid was transformed to *E. coli* BL21 (DE3) for His_6-tagged protein induction and purification.[1] The *E. coli* cells harboring the plasmid pET28a-*eupfE* were grown overnight in LB medium containing 50 μg/mL kanamycin at 37 °C. Then 1 mL of the overnight culture was inoculated into 1 L of fresh LB medium supplemented with 50 μg/ml kanamycin and incubated at 37 °C until the optical density at 600 nm (OD_{600} value) reached 0.55. Protein expression was induced with 50 μM of isopropyl-β-D-thiogalactopyranoside (IPTG, Sigma-Aldrich) and cultured for additional 20 h at 16 °C, 220 rpm. Cells were harvested by centrifugation at 4,000 rpm, 4 °C for 10 min, and re-suspended in 50 mL lysis buffer (50 mM Tris-HCl, pH 8.0, 10 mM imidazole, 150 mM NaCl and 10% glycerol) for disruption using a high-pressure homogenizer (ATS Engineering Limited). The lysate was centrifuged at 14,000 rpm, 4 °C for 10 min to remove the cellular debris, and the supernatant was subjected to Ni-NTA affinity chromatography at 4 °C following the manufacturer's protocols (GE Healthcare). The purified protein was concentrated and exchanged into buffer C (50 mM Bicine, pH 8.0, 150 mM NaCl) with Amicon® Ultra-15 Centrifugal Filters (10 K) before storage at -80 °C. The purity of protein was checked by SDS-PAGE, and the concentration was determined by NanoDrop (Thermo Scientific).

The intron-less sequence of *eupF* was synthesized using the sequence reported as it was suggestive as another putative DAase involved in the biosynthesis of eupenifeldin in *Phoma sp.* (CGMCC 10481).[4] The synthesized *eupF* was ligated to the pET28a vector and transformed into *E. coli* BL21 (DE3) for His_6-tagged protein induction and purification. TB broth was used for *E. coli* incubation (OD_{600} value reached 0.6) and protein induction (100 μM IPTG). The processes of protein induction and purification were the same as that of EupfE.

6. *In vitro* assays of EupfE and EupF

To characterize the function of EupfE, an *in vitro* reaction with a total volume of 100 μL reaction mixture containing 50 mM Bicine buffer (pH 8.0), 2 mM **4**, 3 mM NADPH, and 25 μM EupfE was carried out. The reaction was performed at 26 °C for 20 min and quenched with an equal volume of EtOAc. The EtOAc extracts were dried and dissolved in 30 μL MeCN for UPLC-MS analysis.

As the substrate of EupF, the unstable intermediate **5** should be prepared right before the *in vitro* reaction with EupF. To obtain **5**, a total volume of 200 μL reaction mixture containing 50 mM Bicine buffer (pH 8.0), 2 mM **4**, 3 mM NADPH, and 25 μM EupfE was incubated at 26 °C for 20 min. The reaction products were extracted with an equal volume of EtOAc for three times. The combined EtOAc extracts, which mainly contained **5**, were dried and re-dissolved in 4 μL DMSO, and subjected to *in vitro* assay with EupF immediately. The *in vitro* reaction with 100 μL reaction mixture, which contained 50 mM Bicine buffer (pH 8.0), 1 mM **8** or **10**, 50 μM EupF, and 4 μL newly prepared **5** (dissolved in DMSO, approximately 4 mM), was carried out at 26 °C for 2 h. The resulted products were extracted with an equal volume of EtOAc for three times. The dried EtOAc extracts were dissolved in 30 μL MeOH for UPLC-MS analysis.

To characterize the dehydration of EupF, an *in vitro* reaction with a total volume of 100 μL mixture containing 2 mM just prepared **5** and 30 μM EupF was carried out in PBS buffer (pH 7.5). The boiled EupF was used as control. The reactions were performed at 26 °C for 1, 2 and 3 hours, respectively. The reaction mixture was extracted with equal volume of EtOAc, and the extract was dissolved with 30 μL MeCN for UPLC-MS analysis (Figure S11). Since the

expected product **6** was extremely unstable, 1% glycerol was added to the *in vitro* reaction system to capture **6**. The *in vitro* reaction with glycerol was conducted with a total volume of 100 μL mixture containing 50 mM Bicine buffer (pH 8.0), 2 mM just prepared **5**, 1% glycerol and 30 μM EupF. The boiled EupF was used as control. The reactions were performed at 26 °C for 20, 40, 80 and 120 min, respectively. The reaction mixture was extracted with equal volume of EtOAc, and the extract was dissolved with 30 μL MeCN for UPLC-MS analysis.

7. **Site-specific mutation in EupF**

For site-directed mutagenesis, rolling-cycle PCR amplification (using the primers listed in Table S1) followed by subsequent DpnI digestion was conducted, according to the standard procedure of the QuikChange® XL Site-Directed Mutagenesis Kit. Each mutation was confirmed by sequencing. The resulting mutants of H37A, R51A, R92A, and R323A were expressed in *E. coli* BL21(DE3), purified and concentrated according to the procedures described above for the wild type proteins.

8. General procedures for chemical analyses

Optical rotations were acquired with a Rudolph Autopol V polarimeter. Circular Dichroism (CD) spectra were obtained on a JASCO J-815 CD spectropolarimeter and a Chirascan spectropolarimeter (Applied Photophysics). NMR spectra were recorded on Bruker AV-600 (600 HMz) or AV-800 (800 HMz) spectrometers, with TMS as an internal standard. HRESIMS data were determined on a Thermo Scientific™ Q Exactive™ Focus single stage quadrupole-orbitrap mass spectrometer. LC-MS analyses were conducted with a Waters ACQUITY H-Class UPLC-MS equipped with a PDA detector and a QDA mass detector (using positive and negative modes of electrospray ionization), with a Waters ACQUITY UPLC® BEH column (1.7 μm, C18, 2.1 × 50 mm ID) using the solvent gradient of 5−99% MeCN−H_2O (both with 0.02% formic acid, v/v) in 8 min followed by 99% MeCN−H_2O for 4 min at a flow rate of 0.4 mL/min. GC-MS analyses were performed on an Agilent Technologies 7890A-5975C GC/MS equipped with an HP-5MS capillary column (Agilent Technologies, 250 μm × 30 m, 0.25 μm) with the column temperature of 100 ºC and the gasification chamber temperature of 250 ºC. The following GC gradient was used: 2.0 min isothermal at 100 ºC, ramp to 180 ºC at 2 ºC/min, 0.0 min isothermal at 180 °C, ramp to 220 °C at 40 °C/min, then 43.0 min isothermal at 220 °C. The carrier gas flow rate was 2.0 mL/min, using high purity 99.999% helium gas (split ratio 5:1). The HPMSD chemical workstation NIST05.L standard mass spectrometry atlas and WILEY 275.L mass spectrometry atlas were used for retrieval. Semi-preparative HPLC separations were carried out with an SSI series III HPLC equipped with an SSI 1500 DAD detector, using a YMC Triart C18 column (5 μm, 10 × 250 mm), a SilGreen C18 column (5 μm, 10 × 250 mm), or a Waters XBridge™ Prep C_{18} (5 μm, 10 mm × 250 mm) column.

EtOAc and *n*-hexane used for extraction were analytical grade. MeCN used for semi-preparation HPLC separations was HPLC grade, while used for LC-MS analyses was LCMS grade. Other chemicals used in this study were analytical grade.

9. Isolation and structural characterization of metabolites

9.1 Neosetophomone B (1) and eupenifeldin (3)

To isolate neosetophomone B (**1**) and eupenifeldin (**3**), the wild type *P. janthinellum* was grown in liquid PDB medium at 28 ℃, 220 rpm for 5 days. The culture was filtered with a cheesecloth to obtain the mycelia, which were extracted with acetone-EtOAc (1:2, v/v) for three

times. The extracts were combined and evaporated under reduced pressure to yield the residue (1.95 g). The crude extract was dissolved in MeOH-DMSO (10:1, v/v) and subjected to semi-preparative HPLC separation (column: SilGreen C18, 5 μm, 10 × 250 mm ID; solvent: MeCN-H_2O, 70:30; flow: 3.5 mL/min; detector: 200, 256, 363 nm) to yield neosetophomone B (**1**, 2.1 mg, t_R = 10.2 min) and eupenifeldin (**3**, 40.4 mg, t_R = 14.8 min).

Neosetophomone B (**1**) was isolated as a white amorphous powder. Its (+)-ESIMS and (−)-ESIMS spectra showed ion peaks of *m/z* 385.2 $[M + H]^+$, and *m/z* 383.2 $[M - H]^-$ and 429.2 $[M - H + HCOOH]^-$, respectively. The molecular formula of **1** was determined as $C_{24}H_{32}O_4$ based on its (+)-HRESIMS data (*m/z* 385.23737 $[M + H]^+$, calcd for $C_{24}H_{33}O_4$ 385.23734, see Figure S24). Its ^1H (600 MHz, $CDCl_3$) and ^{13}C (150 MHz, $CDCl_3$) NMR data (see Table S3 and Figures S19-S20) was consistent with that of neosetophomone B[5]. Further interpretation of its HMBC and NOESY spectra (see Table S3 and Figures S21-S23) established its structure and configuration the same as that of neosetophomone B. The absolute configuration of **1** was assigned the same as that reported in the literature according to its optical rotation value $\{[\alpha]_D^{20}$ +73.3 (*c* 0.03, $CHCl_3$)} and CD spectrum (see Figure S25), since the absolute configuration of neosetophomone B had been determined by modified Mosher's ester method and confirmed via single-crystal X-ray diffraction in the literature.[5]

Eupenifeldin (**3**), isolated as a white amorphous powder, displayed a molecular formula of $C_{33}H_{40}O_7$ as suggested by its (+)-HRESIMS data (*m/z* 549.28387 $[M + H]^+$, calcd for $C_{33}H_{41}O_7$ 549.28468, see Figure S38). A comparison of its ^1H (600 MHz, $CDCl_3$), ^{13}C (150 MHz, $CDCl_3$) and 2D NMR data (see Table S5 and Figures S33-S37) with those reported in the literature revealed that the structure and configuration of **3** was consistent with that of eupenifeldin[5-7]. In addition, its optical rotation value $\{[\alpha]_D^{20}$ +317.8 (*c* 0.12, $CHCl_3$)} and CD spectrum (see Figure S39) were identical to those reported in the literature, respectively. Thus, the absolute configuration of **3** was assigned the same as that of eupenifeldin, whose absolute configuration was previously determined by X-ray and electronic circular dichroism (ECD)[7] and confirmed by vibrational circular dichroism (VCD)[5].

9.2 Stipitaldehyde (4)

To isolate stipitaldehyde (**4**), the spores of *A.nidulans* transformant harboring *eupfA*, *eupfB*, and *eupfC* were inoculated in 4 L liquid CD-ST medium and shaken at 220 rpm, 28 °C for 4 days. The culture was filtered through cheesecloth to separate the supernatant and the mycelia. The supernatant was acidified to pH 3.0 using 10 mM HCl, which was extracted with EtOAc for three times. The extracts were evaporated under reduced pressure to obtain the residue (0.92 g), which was separated by semi-preparative HPLC separation (column: YMC Triart C18, 5 μm, 10 × 250 mm ID; solvent: MeCN-H_2O (both with 0.02% formic acid, v/v), 27:73; flow: 3.5 mL/min; detector: 210, 247, 374 nm) to yield stipitaldehyde (**4**, 8.3 mg, t_R = 23.5 min).

Stipitaldehyde (**4**) was isolated as a yellow amorphous powder. It displayed ion peaks at *m/z* 181 $[M + H]^+$ and *m/z* 179 $[M - H]^-$ in (+)-ESI-MS and (−)-ESI-MS spectra, respectively. A comparison of its ^1H (600 MHz, acetone-d_6), ^{13}C (150 MHz, acetone-d_6) and 2D NMR data (see Table S6 and Figures S40-S43) with those reported in the literature revealed that the structure of **4** was consistent with that of stipitaldehyde, whose structure was confirmed by X-ray crystallographic analysis[8].

9.3 Stipitol (5)

To obtain sufficient amount of stipitol (**5**) for structural identification, a 10 mL-scaled *in vitro* assay of EupfE with **4** as the substrate was conducted. A reaction mixture containing 50 mM Bicine buffer (pH 8.0), 2 mM **4**, 3 mM NADPH and 25 μM EupfE was incubated at 26 °C for 20 min. The reaction products were extracted with an equal volume of EtOAc for three times. The extracts were combined and concentrated to dryness to give crude **5**, which were further dissolved in a mixture of C_6D_6-$(CD_3)_2SO$ (4:1) and subjected to NMR experiments immediately.

Stipitol **(5)** displayed a molecular weight of 182 as deduced by the LC-MS analysis {(+)-ESI-MS *m/z* 183 $[M + H]^+$; (−)-ESI-MS *m/z* 181 $[M - H]^-$}. A comparison of its ^1H (600 MHz, C_6D_6:$(CD_3)_2SO$ = 4:1), ^{13}C (150 MHz, C_6D_6:$(CD_3)_2SO$ = 4:1) and 2D NMR data (see Table S7 and Figures S44-S47) with those of stipitaldehyde (**4**), which had a molecular weight of 180, indicated that the aldehyde group in **4** was replaced by a -CH_2OH group in **5**. This deduction was supported by the upfield-shifted of C-9 (δ_C 59.1) and H_2-9 (δ_H 4.71, d, J = 2.8 Hz), as well as the HMBC correlations from H_2-9 to C-4, C-5, and C-6.

9.4 Methylation of Stipitol (5)

In order to verify the hypothesis that **5** can be dehydrated spontaneously and then attacked by nucleophilic reagents, **5** was dissolved in MeOH right after preparation and incubated at room temperature for 2 h. The reaction products were subjected to semi-preparative HPLC separation (column: YMC Triart C18, 5 μm, 10 × 250 mm ID; solvent: MeCN-H_2O (both with 0.02% formic acid, v/v), 27:73; flow: 3.5 mL/min; detector: 210, 247, 374 nm) to yield **6a** (1.5 mg, t_R = 11.5 min).

Compound **6a** displayed as a mixture of **6a-1** and **6a-2**, as deduced by the ^1H (600 MHz, CD_3OD) NMR and ^{13}C (150 MHz, CD_3OD) NMR spectra (see Table S8 and Figures S48-S49), which showed two sets of signals with a ratio of about 2:1, although it appeared as a single peak in the semi-preparative HPLC separation process and LC-MS analysis {(+)-ESI-MS *m/z* 199 $[M + H]^+$; (−)-ESI-MS *m/z* 197 $[M - H]^-$}. Further interpretation of the 2D NMR data (see Table S8 and Figures S50-S51) revealed them to be a pair of enol isomeric tautomer possessing a tropolone moiety. A comparison of their NMR data with those of **5** indicated **6a-1** and **6a-2** to be methylation products of **5**, which was consistent with its preparation procedure (dissolving **5** in methanol). This deduction was confirmed by the appearance of an additional methyl group (δ_C 58.4 in **6a-1** and δ_C 58.6 in **6a-2**, C-10; δ_H 3.37 in **6a-1** and δ_H 3.39 in **6a-2**, H_3-10) and the HMBC correlations from H_3-10 to C-9 in both of **6a-1** and **6a-2**.

9.5 1*E*, 4*E*, 8*Z*-humulene (7)

Spores of the *A. nidulans* mutant overexpressing *eupfG* were inoculated to 4 L liquid CD-ST medium and shaken at 220 rpm for 4 days at 28 °C. The culture broth and the mycelia were extracted with *n*-hexane for three times. The combined extracts were evaporated under reduced pressure to obtain the residue, which was subjected to GC-MS analysis.

Compound **7** was the major component of the *n*-hexane extracts, as shown in the GC-MS chromatogram (see Figure S8c). It displayed almost identical MS fragmentation characteristics as the 1*E*, 4*E*, 8*E*-humulene standard (Sigma) while showed different retention time from that of 1*E*, 4*E*, 8*E*-humulene standard (see Figure S8), which suggested **7** to be a configurational isomer of 1*E*, 4*E*, 8*E*-humulene. The configuration of **7** was further revealed by biosynthetic consideration: co-expressing *eupfD* (P450) and *eupfG* in *A. nidulans* led to the production of 1*E*, 4*E*, 8*Z*-humulenol (**8**) as the main product. Since the configuration of the $\Delta^{1(2)}$,

$\Delta^{4(5)}$, and $\Delta^{8(9)}$-double bonds in **8** was defined as 1*E*, 4*E*, 8*Z* (see Experimental Procedure **9.6**), the configuration of **7** was reasonably assigned as 1*E*, 4*E*, 8*Z*.

9.6 1*E*, 4*E*, 8*Z*-humulenol (8)

To isolate 1*E*, 4*E*, 8*Z*-humulenol (**8**), the *A.nidulans* heterologous transformant harboring *eupfD* and *eupfG* was cultured in 4 L liquid CD-ST medium and shaken at 220 rpm for 4 days at 28 °C. The culture broth and the mycelia were extracted with *n*-hexane for three times. The combined extracts were evaporated under reduced pressure to obtain the residue (0.31 g), which was separated by semi-preparative HPLC (column: YMC Triart C18, 5 μm, 10 × 250 mm ID; solvent: MeCN-H_2O; solvent gradient: 0-15 min, 70%-100% MeCN; 15-23 min, 100% MeCN; flow: 3.5 mL/min; detector: 210, 225, 250 nm) to yield 1*E*, 4*E*, 8*Z*-humulenol (**8**, 7.8 mg, t_R = 11.5 min).

1*E*, 4*E*, 8*Z*-humulenol (**8**), $[\alpha]_D^{20}$ +18.5 (*c* 0.21, MeOH), was isolated as a white amorphous powder. Its (+) ESI-MS spectrum displayed molecules at *m/z* 203 $[M + H - H_2O]^+$ and 221 $[M + H]^+$. The molecular formula of **8** was determined as $C_{15}H_{24}O$ according to its (+)-HRESIMS data (*m/z* 221.18948 $[M + H]^+$, calcd for $C_{15}H_{25}O$ 221.18999, see Figure S57, implying four indices of hydrogen deficiency. Analyses of its ^1H NMR (600 MHz, acetone-d_6), ^{13}C NMR (150 MHz, acetone-d_6) and 2D NMR data (Table S9 and Figures S52-S56) enabled the establishment of an eleven-membered macrocyclic sesquiterpene, featuring the $\Delta^{1(2)}$, $\Delta^{4(5)}$, and $\Delta^{8(9)}$-double bonds, which was structurally related to 1*E*, 4*E*, 8*E*-humulene[9]. The differences lay in an additional -OH group located at C-10 and the *Z*-geometry of the $\Delta^{8(9)}$-double bond. The deshielded shifts of H-10 (δ_H 4.22) and C-10 (δ_C 69.3), as well as the HMBC cross-peaks from HO-10 (δ_H 3.57, d, J = 4.2 Hz) to C-11, C-10, and C-9, from H-10 to C-1, C-11, C-9, C-8, and C-15, and from H-1, H_2-11, H-8, and H_3-15 to C-10, indicated the presence of the 10-OH group. The β-orientation of the 10-OH group and the 1*E*, 4*E*, 8*Z*-configuration of the three double bonds were defined according to the NOESY correlations, the coupling constant of $J_{4,5}$ (16.2 Hz), as well as biosynthetic consideration. The NOESY correlations of H_3-14/H-5/H-1 and H_3-14/H-8/H_3-15/HO-10 suggested these protons were on the same face of the macrocyclic ring, while correlations of H_3-13/H-4/H_3-12 and H-10/H-7α implied they were on the opposite face.

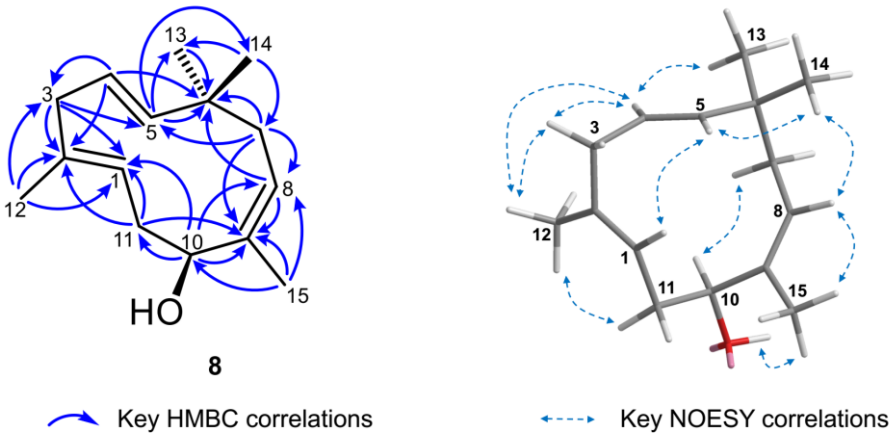

To determine the absolute configuration of **8**, which had only one chiral carbon (C-10), the theoretically calculated ECD spectra of *S*-**8** and *R*-**8** were compared with the experimental data (see Figure S58). Firstly, conformational analysis of *S*-**8** was carried out via Monte Carlo searching with the MMFF94 molecular mechanics force field using the Spartan14 software[10],

which showed three conformers having relative energy within 10 kcal/mol. The three conformers (Figure S59) were considered for further DFT calculations at B3LYP/6-31+G (d, p) level in methanol. Subsequently, the conformers were re-optimized using DFT at the WB97XD/DGDZVP level in methanol with the Gaussian program[11] (Tables S10). The WB97XD/DGDZVP harmonic vibrational frequencies were further calculated to confirm their stability. The energies, oscillator strengths, and rotational strengths of the first 20 electronic excitations were calculated using the TDDFT methodology at CAM-B3LYP/DGDZVP level in methanol. The final ECD spectra of *S*-8 were obtained according to the Boltzmann distribution theory and their relative Gibbs free energy (*Δ*G). As shown in Figures S60, in the region of 200–400 nm, the theoretically calculated ECD spectrum of *S*-**8** was agreed with the experimental CD spectrum of **8**. Thus, the absolute configuration of C-10 in **8** was determined as *S*.

9.7 1*E*, 4*E*, 8*E*-humulenol (10)

To obtain 1*E*, 4*E*, 8*E*-humulenol (**10**), a 4 L-scaled chemical complementation experiment was conducted. The *A. nidulans* transformant overexpressed *eupfD* was inoculated in 4 L of liquid CD-ST medium and shaken at 220 rpm, 28 °C for 2 days. Then 700 mg standard humulene (Sigma) was added and cultured for an additional 36 h. The culture broth and the mycelia were extracted with *n*-hexane for three times. The combined extracts were evaporated under reduced pressure to obtain the residue (0.38 g), which was separated by semi-preparative HPLC (column: YMC Triart C18, 5 μm, 10 × 250 mm ID; solvent: MeCN-H_2O, 50:50; flow: 3.5 mL/min; detector: 210, 225, 250 nm) to obtain 1*E*, 4*E*, 8*E*-humulenol (**10**, 3.1 mg, t_R = 50.6 min).

1*E*, 4*E*, 8*E*-humulenol (**10**), $[\alpha]_D^{20}$ +17.5 (*c* 0.04, MeOH), was isolated as a white amorphous powder. Its (+)-HRESIMS spectrum displayed a $[M + H - H_2O]^+$ peak at *m/z* 203.17944 $[M + H - H_2O]^+$ (calcd for $C_{15}H_{23}$ 203.17943, see Figure S66), suggesting a molecular formula of $C_{15}H_{24}O$. Interpretation of its ^{1}H NMR (800 MHz, acetone-d_6), ^{13}C NMR (200 MHz, acetone-d_6) and 2D NMR data (Table S11 and Figures S61-S65) established an eleven-membered macrocyclic sesquiterpene structure resembled that of 1*E*, 4*E*, 8*E*-humulene[9], with the only difference being the additional -OH group at C-10, which was supported by the downfielded chemical shift of C-10 (δ_C 78.5) and H-10 (δ_H 4.01), and the HMBC cross-peaks from HO-10 (δ_H 3.66, s) to C-9, C-10, and C-11, from H-10 to C-1, C-11, C-9, C-8, and C-15, and from H-1, H_2-11, H-8, and H_3-15 to C-10. The *E*-geometry of the $\Delta^{8(9)}$-double bonds was determined by NOESY correlations of H-5/H_3-14/H-7β/H_3-15 and H-4/H_3-13/H-8/H-10.

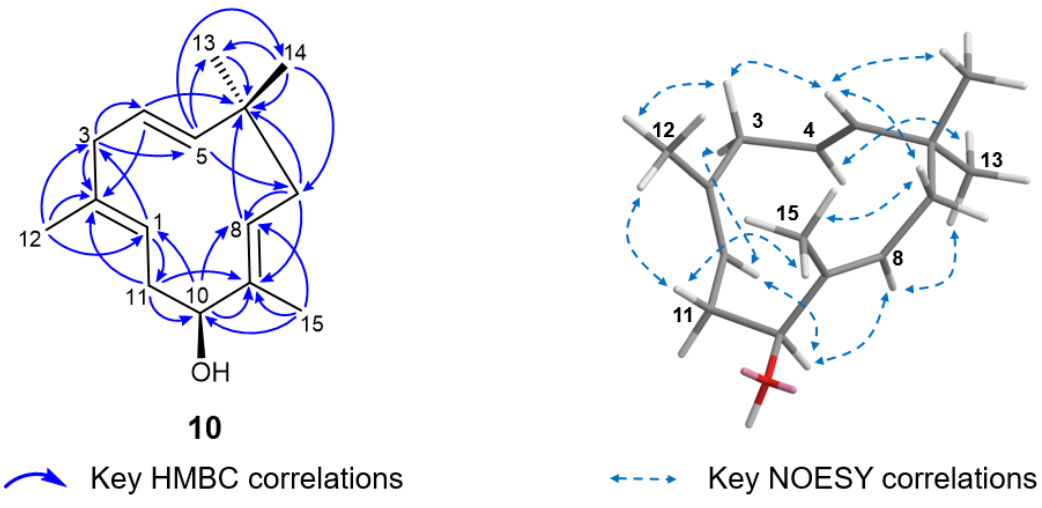

9.8 Epolone B (2) and isoepolone B (11)

To obtain epolone B (**2**) and isoepolone B (**11**), a 4 L-scaled chemical complementation experiment was conducted. The *A. nidulans* transformant overexpressed *eupfA/B/C/D/E/F* was inoculated in 4 L of liquid CD-ST medium and shaken at 220 rpm, 28 °C for 2 days. Then 700 mg humulene (Sigma) was added and cultured for an additional 36 h. The culture was filtered to obtain the mycelia, which were extracted with acetone-EtOAc (1:2, v/v) for three times. The extracts were evaporated under reduced pressure to obtain the residue (1.82 g), which was dissolved in MeOH-DMSO (10:1, v/v) and separated by semi-preparative HPLC (column: YMC Triart C18, 5 μm, 10 × 250 mm ID; solvent gradient: 0-5 min, 73% MeCN-H_2O; 5-60 min, 73-100% MeCN-H_2O; 60-75 min, 100% MeCN; flow: 3.5 mL/min; detector: 210, 254, 360 nm) to obtain epolone B (**2**, 3.2 mg, t_R = 9.6 min) and fraction A (t_R = 12.5~13.2 min). Fraction A was further purified by semi-preparative HPLC using the same column eluted with 50% MeCN-H_2O at a flow rate of 3.5 mL/min to yield isoepolone B (**11**, 1.1 mg, t_R = 58.3 min).

Epolone B (**2**) and isoepolone B (**11**) had the same molecular formula of $C_{24}H_{32}O_4$ as determined by their (+)-HRESIMS data (*m/z* 385.23660 $[M + H]^+$ for **2** and *m/z* 385.23627 $[M + H]^+$ for **11**, calcd for $C_{24}H_{33}O_4$ 385.23734, see Figures S31 and S72). Interpretation of their ^1H (600 MHz, $CDCl_3$), ^{13}C (150 MHz, $CDCl_3$) and 2D NMR data (see Tables S4, S12 and Figures S26-S30, S67-S71) established the same planar structure for **2** and **11**, which was the same as that of epolone B. Among them, the 1D and 2D NMR data of **2** was identical to that of epolone B. The NOESY correlations of H-4/H_3-13/H-8, H-9'α/H-1/H-10/H-8, H_3-14/H-5/H_3-15, and H-9'β/H_3-12/H-5 in **2** further suggested the relative configuration of **2** with an *S** configuration of C-10. It was worth to note that the relative configuration of C-10 of epolone B was wrongly drawn as *R** in a previous reference[12]. In fact, the relative configuration of epolone B was determined as same to that of pycnidione and epolone A, two co-isolated meroterpenoids, based on biosynthetic consideration. Since the relative configuration of the hydroxylated carbon in pycnidione and epolone A was defined as *S**, the corresponding carbon in epolone B should also be *S**. A subsequent literature which reported the biomimetic synthesis of an analogue of epolone B had amended the relative configuration of the hydroxylated carbon in epolone B as *S**,[13] which was consistent with our results. In addition, the optical rotation values {$[\alpha]_D^{20}$ +141.1 (*c* 0.33, $CHCl_3$) for **2** and $[\alpha]_D^{20}$ +101.3 (*c* 0.08, $CHCl_3$) for **11**} and CD spectra (see Figures S32 and S73) of **2** and **11** implied that they were epimers rather than enantiomers. For **11**, the NOESY correlations of H_3-14/H-5/H_3-15, H-9'β/H-1/H_3-15, H-4/H_3-13/H-8, and H-3α/H_3-12/H-9'α/H-10, together with the coupling constant of $J_{4,5}$ (15.9 Hz), suggested the *E*-geometry of the $\Delta^{4,5}$- and $\Delta^{8,9}$-double bonds, the α-orientation of H-10 and H_3-12, and the β-orientation of H-1 in **11**, which finalized **11** to be a 1,2-epimer of **2**.

10. Computational methodologies

Initial conformational searches were completed using Schrodinger's Maestro 2017-2 version 11.2.014.[14] These conformers were recalculated quantum mechanically in Gaussian 16 Rev. A.03 (sse4)[11] with the density functional PBE(0)-D3(BJ)/def2-TZVP.[15-19] This functional was chosen for its ability to reproduce both radical and concerted mechanisms.[20] This functional was chosen over wB97X-D and B3LYP to remove any biases towards a concerted mechanism. All reported structures are stationary points on the energy surface and characterized as transition states or minima by frequency calculations. Intrinsic reaction coordinate calculations were completed from TS-1. All reported energies were quasiharmonic corrected for enthalpy and entropy.[21-22] These corrections were made using the GoodVibes package.[23]

Supplementary Tables

Table S1. Primers used in this study.

Primer name	Sequence (5'→3')
For heterologous expression in *A. nidulans*	
pANU-eupfABC1	GCCTGAGCTTCATCCCCAGCATCATTACACCTCAGCAATGACAGATCAGGGCGCCAACC
pANU-eupfABC2	CTCGGTCTGTCATGCAGTTGACC
pANU-eupfABC3	CGTATGGTGCACACAATCGGCAG
pANU-eupfA4	CAGTGGAGGACATACCCGTAATTTTCTGGGCATTTAAATCGGTATACGTTGGCCAGGGT
pANU-eupfABC4	TGGGTCTCTCCCGTCACCCAAATCAATTCACCGGAGTCGGTATACGTTGGCCAGGGTGC
pANU-eupfABC5	ACTAACCATTACCCCGCCACATAGACACATCTAAACAATGGCCATGAATGTGGACAGCC
pANU-eupfABC6	TCATTTATAGCTCGTTCGGCACCTTTAATCATTTAAATTCTAGGCATTCTCTTGCGCCG
pANU-eupfABC7	TCTCCCTTCTCTGAACAATAAACCCCACAGAAGGCATTTATGGACAGCCTCAGCGGTGC
pANU-eupfABC8	CAGTGGAGGACATACCCGTAATTTTCTGGGCATTTAAATGCCCACTCTTCCCATGTGCC
pANR-eupfDE1	TAACCATTACCCCGCCACATAGACACATCTAAACAATGGGATCACTCGACTCTAAACCC
pANR-eupfDE2	CATAGGTCGCCAGGTACGACCAGTTCGGAAGATCAGGAAGTGTAACTGGCCTAGCGAGC
pANR-eupfDE3	GCCTGAGCTTCATCCCCAGCATCATTACACCTCAGCAATGGAGATCTTAGCTGCAGCAC
pANR-eupfDE4	CTAAAGGGTATCATCGAAAGGGAGTCATCCAATTTAAATGTATCGTGGACAGTTGGTGC
pANR-eupfD1	ACTAACCATTACCCCGCCACATAGACACATCTAAACAATGGAGATCTTAGCTGCAGCAC
pANR-eupfE2	TAAAGGGTATCATCGAAAGGGAGTCATCCAATTTAAATAAGTGTAACTGGCCTAGCGAG
pANP-eupfFG1	CTCCCTTCTCTGAACAATAAACCCCACAGAAGGCATTTATGGCCAGCCTCACGACCAAG
pANP-eupfFG2	TCATAGGTCGCCAGGTACGACCAGTTCGGAAGATCAGGAGTGCAGCGAGCATGACCTAG
pANP-eupfFG3	AGCCTGAGCTTCATCCCCAGCATCATTACACCTCAGCAATGCTTTTCACCGTGTCCCTC
pANP-eupfFG4	ATGAGACCCAACAACCATGATACCAGGGGATTTAAATGATAAGCGTGTCTTGACCTGTG
pANP-eupfF1	CTCCCTTCTCTGAACAATAAACCCCACAGAAGGCATTTATGCTTTTCACCGTGTCCCTC
pANP-eupfG2	GATGAGACCCAACAACCATGATACCAGGGGATTTAAATAGTGCAGCGAGCATGACCTAG
pANU-glaA-F	CCTGATCTTCCGAACTGGTC
pANU-glaA-R	TGCTGAGGTGTAATGATGCTG
pANR-gpdA-F	ACTCCGGTGAATTGATTTGG
pANR-gpdA-R	TGTTTAGATGTGTCTATGTGGC
pANP-amyB-F	GATTAAAGGTGCCGAACGAGC
pANP-amyB-R	AAATGCCTTCTGTGGGGTT
For RT-PCR	
pColdI-eupfE1	GGGAATTCCATATGATGGGATCACTCGACTCTAAACC
pColdI-eupfE2	TGCTCTAGATTACCACGGCTGTACCTCATC
RT-eupfE-check1	GGTGCCAATACTGGTCTAGG
RT-eupfE-check2	CACAAAGGCGGAAGTGAAG
pColdI-eupfF1	GGGAATTCCATATGATGCTTTTCACCGTGTCCC
pColdI-eupfF2	TGCTCTAGACTACAGATGGAACCCAGTAGTATC
For site-specific mutation in EupF	
H37A-F	CGAACCGTCTGCTGGCCCAATGGCCGAACG
H32A-R	CGTTCGGCCATTGGGCCAGCAGACGGTTCG
R51A-F	GTTGAAAACATTAGCGTGGCTCCGAACGGTAACCTGCT
R51A-R	AGCAGGTTACCGTTCGGAGCCACGCTAATGTTTTCAAC
R92A-F	TTTGACGAGTGGGTGGATGCTCTGATCGGTATTGGC
R92A-r	GCCAATACCGATCAGAGCATCCACCCACTCGTCAAA

R323A-F	GCGTGCGCGTTTGGTGCTACCGAGAAGGACAA
R323A-R	TTGTCCTTCTCGGTAGCACCAAACGCGCACGC

Table S2. Plasmids used in this study.

Plasmid name	**Vector**	**Genes**	**Aim**
pANU-eupfA	pANU	*eupfA* from gDNA (with the promoter *glaA*)	*A. nidulans* overexpression
pANU-eupfABC	pANU	*eupfA* from gDNA (with the promoter *glaA*) *eupfB* from gDNA (with the promoter *gpdA*) *eupfC* from gDNA (with the promoter *amyB*)	*A. nidulans* overexpression
pANR-eupfDE	pANR	*eupfD* from gDNA (with the promoter *glaA*) *eupfE* from gDNA (with the promoter *gpdA*)	*A. nidulans* overexpression
pANR-eupfD	pANR	*eupfD* from gDNA (with the promoter *gpdA*)	*A. nidulans* overexpression
pANR-eupfE	pANR	*eupfE* from gDNA (with the promoter *gpdA*)	*A. nidulans* overexpression
pANP-eupfFG	pANP	*eupfF* from gDNA (with the promoter *glaA*) *eupfG* from gDNA (with the promoter *amyB*)	*A. nidulans* overexpression
pANP-eupfF	pANP	*eupfF* from gDNA (with the promoter *amyB*)	*A. nidulans* overexpression
pANP-eupfG	pANP	*eupfG* from gDNA (with the promoter *amyB*)	*A. nidulans* overexpression
pColdI-eupfE	pColdI	*eupfE* from cDNA	Intron-less sequence cloning and protein purification
pColdI-eupfF	pColdI	*eupfF* from cDNA	Intron-less sequence cloning and protein purification
pET28a-eupfE	pET28a	*eupfE* from cDNA (codon optimized)	*E. coli* BL21(DE3) protein purification
pET28a-eupfF	pET28a	*eupfF* from cDNA (codon optimized)	*E. coli* BL21(DE3) protein purification
pET28a-eupF	pET28a	synthesized *eupF* (codon optimized)	*E. coli* BL21(DE3) protein purification

Table S3. NMR data of neosetophomone B (**1**).

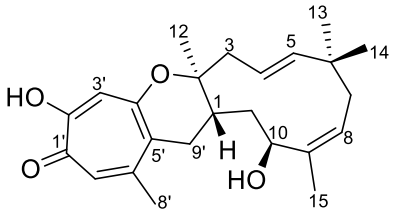

1

no	**1** [a]				Reported neosetophomone B [b]	
	δ_H mult (*J* in Hz)	δ_C type	HMBC	NOESY	δ_H mult (*J* in Hz)	δ_C type
1	1.77 overlap	33.2 CH	C-11, C-12	H-11*β*, H-9'*α*, H-9'*β*	1.77 m	33.0 CH
2		81.3 C				81.4 C
3*α*	2.70 d (15.0)	44.5 CH_2	C-2, C-4	H-3*β*, H_3-12	2.67 ddd (15.0, 2.9, 1.5)	44.3 CH_2
3*β*	2.30 dd (14.4, 10.2)		C-2, C-4, C-5, C-12	H-5, H_3-12	2.32 dd (15.0, 10.0)	
4	5.07 ddd (15.6, 10.2, 2.4)	120.0 CH	C-3, C-6	H-3*α*, H-7*α*, H_3-13	5.07 ddd (15.9, 10.0, 2.9)	119.8 CH
5	5.27 d (16.2)	144.8 CH	C-3, C-6, C-13, C-14	H-3*β*, H-10, H_3-14	5.28 dd (15.9, 1.5)	144.7 CH
6		38.7 C				38.6 C
7*α*	1.78 overlap	40.8 CH_2	C-5, C-6, C-8, C-9, C-14	H-8, H-10, H_3-12, H_3-13, H_3-14	1.78 dd (13.0, 7.3)	40.6 CH_2
7*β*	2.10 dd (12.0, 10.2)		C-5, C-6, C-8, C-9, C-13	H-5, H-7*α*, H-8, H-10, H_3-14	2.11 dd (13.0, 9.9)	
8	5.35 t (8.4)	127.2 CH	C-7, C-10, C-15	H-7*α*, H-7*β*, H_3-13, H_3-15	5.36 dd (9.9, 7.3)	127.0 CH
9		138.1 C				138.0 C
10	4.75 dd (9.6, 6.0)	67.2 CH	C-8, C-15	H-7*α*, H-7*β*, H-11*α*	4.76 dd (10.1, 6.1)	67.0 CH
11*α*	1.89 m	36.8 CH_2	C-1, C-2, C-9, C-10,	H-11*β*, H_3-12, H-9'*α*, H-9'*β*	1.89 dt (14.4, 6.1)	36.7 CH_2
11*β*	1.40 dd (13.8, 10.8)		C-2, C-9, C-10, C-9'	H-1, H-11*α*, H-9'*α*, H-9'*β*	1.42 ddd (14.4, 10.1, 1.1)	
12	1.14 s	19.6 CH_3	C-1, C-2, C-3	H-3*β*, H-11*α*, H-9'*α*	1.16 s	19.5 CH_3
13	0.91 s	21.8 CH_3	C-5, C-6, C-7, C-14	H-4, H-5, H-8, H-7*α*	0.92 s	21.6 CH_3
14	1.04 s	30.3 CH_3	C-5, C-6, C-7, C-13	H-5, H-7*α*, H-7*β*	1.05 s	30.2 CH_3
15	1.66 s	18.4 CH_3	C-8, C-9, C-10	H-8, H_3-13, H_3-14, H-9'*β*	1.67 s	18.3 CH_3
1'		172.8 C				172.4 C
2'		163.8 C				163.5 C
3'	6.96 s	113.7 CH	C-1', C-2', C-4', C-5'		6.97 s	113.7 CH
4'		161.3 C				161.3 C
5'		121.3 C				121.5 C
6'		149.8 C				150.0 C
7'	7.09 s	124.6 CH	C-1', C-2', C-5', C-6', C-8'	H-8'	7.10 s	124.6 CH
8'	2.35 s	27.2 CH_3	C-5', C-6', C-7'	H-7'	2.37 s	27.2 CH_3
9'*α*	2.44 dd (16.8, 13.2)	34.6 CH_2	C-1, C-11, C-5'	H-1, H-11*β*, H_3-12	2.46 dd (17.5, 12.5)	34.5 CH_2
9'*β*	2.65 dd (17.4, 5.4)		C-1, C-2, C-4', C-5', C-6'	H-1, H-11*α*, H-11*β*	2.67 dd (17.5, 5.4)	

[a] Measured in $CDCl_3$; 600 MHz for ^1H NMR and 150 MHz for ^{13}C NMR.

[b] Data reported in the literature[5] (measured in $CDCl_3$; 500 MHz for ^1H NMR and 100 MHz for ^{13}C NMR).

Table S4. NMR data of epolone B (**2**).

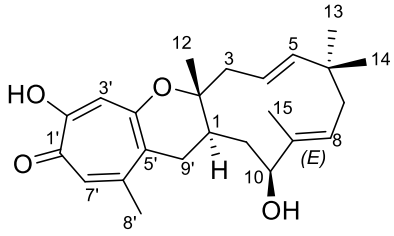

2

no	**2** [a]				Reported epolone B [b]	
	δ_H mult (*J* in Hz)	δ_C type	HMBC	NOESY	δ_H mult (*J* in Hz)	δ_C type
1	1.67 overlap	33.5 CH	C-2, C-3, C-10, C-11, C-12, C-9'	H-4, H-8, H-10, H-9'*α*	1.64 m	33.4 CH
2		81.5 C				81.3 C
3*α*	2.56 d (14.5)	42.6 CH_2	C-1, C-2, C-4, C-5, C-12	H-3*β*, H-4, H_3-12	2.56 bd (14.5)	42.6 CH_2
3*β*	2.25 overlap		C-4, C-5, C-12	H-3*α*, H-5, H-11*β*, H_3-12, H_3-15	2.23 bd (14.5, 10)	
4	5.03 dd (15.7, 10.6)	120.4 CH	C-2, C-3, C-5, C-6	H-3*α*, H-3*β*, H-7*α*, H_3-13, H_3-15	5.04 ddd (15.5, 10, 3)	120.3 CH
5	5.16 overlap	142.3 CH	C-3, C-4, C-6, C-7, C-13, C-14	H-3*β*, H-7*α*, H-11*β*, H_3-14, H_3-15	5.14 dd (15.5, 2)	142.2 CH
6		38.8 C				38.6 C
7*α*	2.21 overlap	40.7 CH_2	C-6, C-8, C-9, C-13, C-14	H-7*β*, H_3-14, H_3-15	2.22 dd (12.5, 6)	40.6 CH_2
7*β*	1.76 overlap		C-5, C-6, C-8, C-9, C-13	H-7*α*, H-8, H_3-13	1.77 dd (12.5, 5)	
8	5.17 overlap	123.7 CH	C-6, C-7, C-10, C-15	H-7*α*, H-7*β*, H-10, H_3-13, H_3-14	5.20 dd (6, 5)	123.8 CH
9		138.7 C				138.4 C
10	3.96 d (9.9)	77.9 CH	C-1, C-8, C-9, C-11, C-15	H-1, H-8, H-11*α*, H-9'*α*	3.94 bd (10)	77.9 CH
11*α*	1.15 dd (13.3, 9.3)	38.7 CH_2	C-1, C-2, C-9, C-10, C-9'	H-11*β*, H-9'*β*	1.12 bdd (14, 8)	38.7 CH_2
11*β*	1.72 overlap		C-1, C-2, C-9, C-10, C-9'	H-3*β*, H-5, H-11*α*	1.72 dd (14, 10)	
12	1.10 s	20.3 CH_3	C-1, C-2, C-3	H-3*α*, H-3*β*, H-5, H-11*β*, H-9'*β*	1.10 s	20.1 CH_3
13	0.99 s	24.2 CH_3	C-5, C-6, C-7, C-14	H-4, H-7*β*, H-8	0.99 s	24.1 CH_3
14	1.06 s	30.2 CH_3	C-5, C-6, C-7, C-13	H-7*α*, H-7*β*	1.06 s	30.0 CH_3
15	1.64 s	10.8 CH_3	C-8, C-9, C-10	H-5, H-7*α*	1.63 s	10.6 CH_3
1'		172.6 C				172.7 C
2'		163.3 C				163.1 C
3'	6.98 s	113.5 CH	C-1', C-2', C-4', C-5', C-9'		6.97 s	113.0 CH
4'		161.2 C				160.9 C
5'		120.4 C				119.9 C
6'		150.1 C				149.8 C
7'	7.10 s	124.5 CH	C-1', C-2', C-5', C-6', C-8'	H-8'	7.10 s	124.5 CH
8'	2.38 s	27.4 CH_3	C-5', C-6', C-7'	H-7'	2.39 s	27.2 CH_3
9'*α*	2.89 dd (17.5, 4.9)	31.4 CH_2	C-1, C-2, C-4', C-5', C-6'	H-1, H-10, H-9'*β*	2.88 dd (17, 5.5)	31.3 CH_2
9'*β*	2.35 overlap		C-1, C-2, C-11, C-4', C-5', C-6'	H-9'*α*, H_3-12	2.36 dd (17, 12.5)	

[a] Measured in $CDCl_3$; 600 MHz for ^1H NMR and 150 MHz for ^{13}C NMR.

[b] Data reported in the literature[12] (measured in $CDCl_3$; 500 MHz for ^1H NMR and 100 MHz for ^{13}C NMR).

Table S5. NMR data of eupenifeldin (**3**).

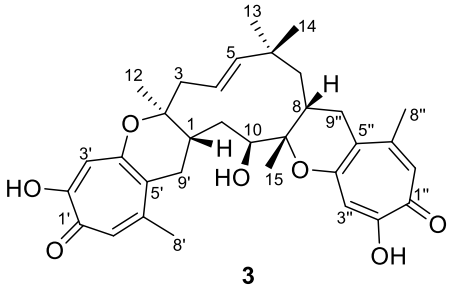

3

no	**3** [a]				Reported eupenifeldin [b]	
	δ_H mult (*J* in Hz)	δ_C type	HMBC	NOESY	δ_H mult (*J* in Hz)	δ_C type
1	2.16 overlap	41.7 CH	C-2, C-10, C-11, C-12, C-9'	H-9'*β*	2.22 ddd (14.0, 5.9, 4.4)	41.6 CH
2		80.7 C				80.7 C
3*α*	2.50 dd (13.2, 10.8)	46.4 CH_2	C-1, C-2, C-4, C-5, C-12	H-3*β*, H-5, H_3-12	2.53 dd (13.4, 11.1)	46.3 CH_2
3*β*	2.72 dd (13.2, 2.4)		C-1, C-2, C-4, C-5, C-12	H-3*α*, H-4	2.74 dd (13.4, 4.2)	
4	5.67 ddd (16.2, 10.8, 4.2)	125.9 CH	C-3, C-5, C-6, C-7	H-3*β*, H-7*α*, H-10, H_3-12, H_3-13	5.69 ddd (16.0, 11.1, 4.2)	125.8 CH
5	5.79 d (16.2)	144.1 CH	C-3, C-4, C-6, C-7, C-13, C-14	H-3*α*, H-8, H_3-14	5.81 d (16.0)	144.1 CH
6		35.1 C				35.0 C
7*α*	1.77 d (14.4)	46.7 CH_2	C-5, C-6, C-8, C-9, C-14	H-7*β*, H-10, H_3-13, H_3-14	1.79 d (14.7)	46.6 CH_2
7*β*	0.76 dd (14.4, 4.2)		C-5, C-6, C-8, C-9, C-14, C-9"	H-7*α*, H-8, H-9"*α*	0.78 dd (14.7, 4.3)	
8	1.81 brs	32.1 CH	C-6, C-7, C-5"	H-7*β*, H-11*α*, H_3-14, H_3-15, H-9"*α*, H-9"*β*	1.83 dd (5.3, 4.3)	32.0 CH
9		82.1 C				82.0 C
10	4.20 d (10.8)	70.9 CH	C-1, C-9, C-11, C-15	H-4, H-7*α*, H-11*β*, H_3-12	4.22 d (11.2)	70.8 CH
11*α*	1.53 t (11.4)	30.3 CH_2	C-2, C-10, C-9'	H-11*β*, H-9'*β*	1.53 dd (12.5, 11.2)	30.2 CH_2
11*β*	2.19 overlap		C-1, C-2, C-10, C-9'	H-8, H-11*α*, H-9'*β*	2.21 dd (12.5, 5.9)	
12	1.39 s	19.4 CH_3	C-1, C-2, C-3	H-3*α*, H-4, H-10	1.41 s	19.9 CH_3
13	1.05 s	29.8 CH_3	C-5, C-6, C-7, C-14	H-4, H-7*α*, H-7*β*	1.08 s	29.7 CH_3
14	1.08 s	27.3 CH_3	C-5, C-6, C-7, C-13	H-5, H-7*β*, H-8, H-9"*α*	1.11 s	27.2 CH_3
15	1.13 s	16.2 CH_3	C-8, C-9, C-10	H-8, H-11*α*, H-11*β*, H-9"*β*	1.15 s	16.1 CH_3
1'		172.5 C				172.2 C
2'		163.2 C				163.1 C
3'	6.94 s	113.7 CH	C-1', C-2', C-4', C-5'		6.99 s	113.8 CH
4'		160.4 C				160.6 C
5'		122.6 C				122.9 C
6'		150.7 C				150.7 C
7'	7.12 s	124.8 CH	C-1', C-2', C-5', C-6', C-8'	H-8'	7.17 s	124.8 CH
8'	2.39 s	27.5 CH_3	C-5', C-6', C-7'	H-7'	2.42 s	27.5 CH_3
9'*α*	3.37 dd (17.4, 13.8)	33.1 CH_2	C-1, C-4', C-5'	H-1, H-11*β*, H_3-12, H-8', H-9'*β*	3.40 dd (16.9, 14.0)	33.1 CH_2
9'*β*	2.39 overlap		C-1, C-2, C-11, C-4', C-5', C-6'	H-1, H-11*α*, H-9'*α*	2.42 d (16.9, 4.4)	
1"		173.4 C				173.3 C
2"		163.0 C				162.9 C
3"	6.90 s	112.9 CH	C-1", C-2", C-4", C-5"		6.93 s	112.8 CH

4"		159.6 C				159.5 C
5"		118.7 C				118.7 C
6"		151.5 C				151.5 C
7"	7.14 s	125.7 CH	C-1", C-2", C-5", C-6", C-8"	H-8"	7.17 s	125.6 CH
8"	2.36 s	27.6 CH_3	C-5", C-6", C-7"	H-7"	2.38 s	27.5 CH_3
9"*α*	2.35 overlap	34.4 CH_2	C-7, C-8, C-9, C-4", C-6"	H-9"*β*, H-7*α*, H-7*β*, H-8, H_3-14	2.37 d (17.2)	34.4 CH_2
9"*β*	2.83 dd (17.4, 5.4)		C-7, C-8, C-4", C-5", C-6"	H-9"*α*, H-8", H-8, H_3-15	2.86 dd (17.2, 5.3)	

[a] Measured in $CDCl_3$; 600 MHz for ^1H NMR and 150 MHz for ^{13}C NMR.

[b] Data reported in the literature[7] (measured in $CDCl_3$; 600 MHz for ^1H NMR and 150 MHz for ^{13}C NMR).

Table S6. NMR data of stipitaldehyde (**4**).

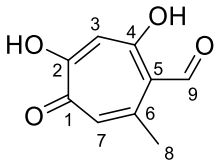

4

	4 [a]			Reported stipitaldehyde [b]	
no	δ_H mult (*J* in Hz)	δ_C type	HMBC correlations	δ_H mult (*J* in Hz)	δ_C type
1		177.8 C			176.2 C
2		165.6 C			165.9 C
3	6.78 s	110.8 CH	C-1, C-2, C-5	6.69 s	110.4 CH
4		177.5 C			174.7 C
5		115.8 C			115.8 C
6		151.6 C			149.2 C
7	6.83 s	125.9 CH	C-2, C-5, C-8	6.75 s	125.3 CH
8	2.71 s	26.2 CH_3	C-5, C-6, C-7, C-9	2.57 s	25.4 CH_3
9	10.15 s	198.2 CH	C-3, C-4, C-5	10.01 s	197.1 CH

[a] Measured in acetone-d_6; 600 MHz for ^{1}H NMR and 150 MHz for ^{13}C NMR.

[b] Data reported in the literature[8] (measured in DMSO-d_6; 500 MHz for ^{1}H NMR and 125 MHz for ^{13}C NMR).

Table S7. NMR data of stipitol (**5**).

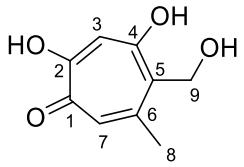

5

no	δ_H mult (*J* in Hz)	δ_C type	HMBC correlations
1		172.0 C	
2		165.7 C	
3	7.35 d (6.9)	113.6 CH	C-1, C-2, C-4, C-5
4		166.9 C	
5		131.1 C	
6		148.6 C	
7	6.95 brs	119.3 CH	C-1, C-2, C-5, C-6, C-8
8	2.32 s	26.3 CH_3	C-5, C-6, C-7
9	4.71 d (2.8)	59.1 CH_2	C-4, C-5, C-6

[a] Measured in a mixture of C_6D_6 and $(CD_3)_2SO$ (4:1, v/v); 600 MHz for ^{1}H NMR and 150 MHz for ^{13}C NMR.

Table S8. NMR data of **6a**[a].

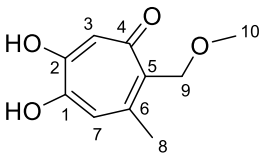

6a-1

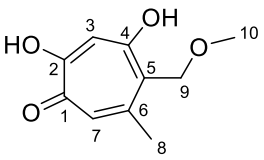

6a-2

	6a-1			**6a-2**		
no	δ_H mult (*J* in Hz)	δ_C type	HMBC correlations	δ_H mult (*J* in Hz)	δ_C type	HMBC correlations
1		167.1 C			173.5 C	
2		164.6 C			167.1 C	
3	6.70 s	115.3 CH	C-1, C-2, C-4, C-5	6.93 s	114.0 CH	C-1, C-4, C-5
4		184.5 C			168.5 C	
5		135.2 C			128.9 C	
6		151.9 C			152.4 C	
7	6.55 s	113.8 CH	C-1, C-2, C-5, C-8	7.03 s	120.7 CH	C-1, C-2, C-5, C-6, C-8
8	2.45 s	26.3 CH_3	C-5, C-6, C-7	2.53 s	26.3 CH_3	C-5, C-6, C-7
9	4.56 s	70.3 CH_2	C-4, C-5, C-6, C-10	4.58 s	69.3 CH_2	C-4, C-5, C-6
10	3.37 s	58.4 CH_3	C-9	3.39 s	58.6 CH_3	C-9

[a] Measured in CD_3OD; 600 MHz for ^1H NMR and 150 MHz for ^{13}C NMR.

Table S9. NMR data of 1*E*, 4*E*, 8*Z*-humulenol (**8**) [a].

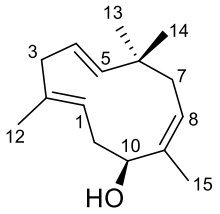

8

no	δ_H mult (*J* in Hz)	δ_C type	HMBC	NOESY
1	5.02 brt (8.1)	122.2 CH	C-2, C-3, C-10, C-11, C-12	H-3*α*, H-3*β*, H-10, H_2-11
2		143.0 C		
3*α*	2.44 dd (12.0, 6.6)	41.8 CH_2	C-1, C-2, C-4, C-5, C-12	H-1, H-4, H-5, H_3-12
3*β*	2.50 dd (12.0, 7.2)			H-1, H-5, H_3-12
4	5.67 dt (16.2, 7.2)	127.5 CH	C-2, C-3, C-6	H-3*α*, H-3*β*, H_3-12, H_3-13
5	5.42 brd (16.2)	144.0 CH	C-3, C-4, C-6, C-13, C-14	H-1, H-3*β*, H_3-14
6		37.5 C		
7*α*	2.09 t (12.6)	43.8 CH_2	C-5, C-6, C-8, C-9, C-13, C-14	H-7*β*, H-10
7*β*	1.69 m			H-7*α*, H-8, H_3-13, H_3-14
8	5.27 brd (12.6)	124.7 CH	C-6, C-7, C-9, C-10, C-15	H-7*β*, H_3-14, H_3-15
9		138.3 C		
10	4.22 dt (10.2, 4.2)	69.3 CH	C-1, C-8, C-9, C-11, C-15	H-7*α*, H_2-11, HO-10
11	2.28 m	34.8 CH_2	C-1, C-2, C-9, C-10	H_3-12, H_3-15
12	1.63 s	17.6 CH_3	C-1, C-2, C-3,	H-3*α*, H-3*β*
13	1.03 s	28.5 CH_3	C-5, C-6, C-7, C-14	H-7*α*, H-4
14	1.04 s	24.7 CH_3	C-5, C-6, C-7, C-13	H-8
15	1.70 s	18.2 CH_3	C-8, C-9, C-10	H-8
HO-10	3.57 d (4.2)		C-9, C-10, C-11	H-10, H_2-11, H_3-15

[a] Measured in acetone-d_6; 600 MHz for ^{1}H NMR and 150 MHz for ^{13}C NMR.

Table S10. Free energies (*Δ*G) and Boltzmann distribution abundances of conformers of *S*-**8**.

Conf.	WB97XD/DGDZVP Gibbs free energy (298.15 K)		
	G (Hartree)	ΔG (Kcal/mol)	Boltzmann Distribution
C1	-660.747239	0.0000	0.513
C2	-660.747142	0.0610	0.463
C3	-660.74437	1.8000	0.025

Table S11. NMR data of 1*E*, 4*E*, 8*E*-humulenol (**10**) [a].

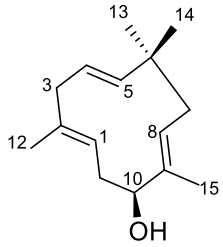

10

no	δ_H mult (*J* in Hz)	δ_C type	HMBC	NOESY
1	4.91 t (7.8)	123.9 CH	C-2, C-3, C-10, C-11, C-12	H-10, H-11*α*, H-11*β*
2		140.0 C		
3	2.47 d (7.5)	41.2 CH_2	C-1, C-2, C-4, C-5, C-12	H-1, H-4, H-5, H_3-12
4	5.58 dt (16.0, 7.2)	128.1 CH	C-2, C-3, C-6	H_2-3, H_3-13
5	5.20 d (15.8)	142.0 CH	C-3, C-4, C-6, C-7, C-13, C-14	H_2-3, H-7*β*, H_3-14
6		37.6 C		
7*α*	1.82 brd (12.4)	42.5 CH_2	C-5, C-6, C-8, C-9	H-7*β*, H_3-13
7*β*	2.19 brt (11.7)		C-5, C-6, C-8, C-9, C-13	H-7*α*, H_3-14, H_3-15
8	5.04 brd (9.0)	124.7 CH	C-6, C-7, C-10, C-15	H-10, H_3-13
9		137.0 C		
10	4.01 m	78.5 CH	C-1, C-8, C-9, C-11, C-15	H-1, H-8, H-11*α*, H-11*β*
11*α*	2.36 dt (13.4, 6.8)	33.0 CH_2	C-1, C-2, C-9, C-10	H-1, H-10, H-11*β*, H_3-12
11*β*	2.03 d (11.0, 6.8)		C-1, C-2, C-9, C-10	H-1, H-11*α*, H_3-12, H_3-15
12	1.65 s	18.0 CH_3	C-1, C-2, C-3,	H_2-3, H-11*α*
13	1.08 s	24.6 CH_3	C-5, C-6, C-7, C-14	H-4, H-7*α*, H-8
14	1.06 s	29.7 CH_3	C-5, C-6, C-7, C-13	H-5, H-7*α*, H-7*β*
15	1.45 s	10.9 CH_3	C-8, C-9, C-10	H-7*β*, H-11*β*
10-OH	3.66 s		C-9, C-10, C-11	H-10, H-11*α*, H-11*β*, H_3-12, H_3-15

[a] Measured in acetone-d_6; 800 MHz for ^{1}H NMR and 200 MHz for ^{13}C NMR.

Table S12. NMR data of isoepolone B (**11**) [a].

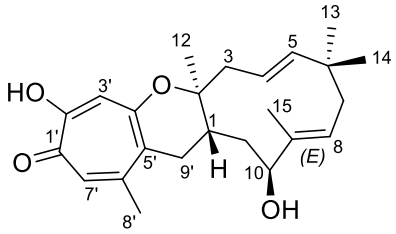

11

no	δ_H mult (*J* in Hz)	δ_C type	HMBC	NOESY
1	2.01 m	29.4 CH	C-2, C-3, C-10, C-11, C-12, C-9'	H-9'*β*, H$_3$-15
2		82.1 C		
3*α*	2.58 d (14.5)	42.8 CH$_2$	C-1, C-2, C-4, C-5, C-12	H-3*β*, H$_3$-12
3*β*	2.18 overlap		C-1, C-4, C-5, C-12	H-3*α*, H-5, H$_3$-12
4	5.07 ddd (15.9, 9.8, 1.9)	120.8 CH	C-3, C-5, C-6	H-3*α*, H-3*β*, H$_3$-13
5	5.15 d (15.9)	141.9 CH	C-3, C-4, C-6, C-7, C-13, C-14	H-3*β*, H$_3$-14, H$_3$-15
6		38.9 C		
7*α*	1.84 dd (12.5, 4.7)	40.9 CH$_2$	C-5, C-6, C-8, C-9, C-13	H-7*β*, H-8, H$_3$-14
7*β*	2.22 overlap		C-5, C-6, C-8, C-9, C-13, C-14	H-5
8	5.41 dd (11.1, 4.7)	120.8 CH	C-7, C-10, C-15	H-7*α*, H-7*β*, H$_3$-13
9		139.4 C		
10	4.36 d (6.4)	73.7 CH	C-1, C-8, C-9, C-11, C-15	H-11*α*, H-9'*α*
11*α*	1.56 overlap	34.7 CH$_2$	C-1, C-9, C-10, C-9'	H-1, H-9'*α*, H-9'*β*, H-10
11*β*	1.50 overlap		C-1, C-2, C-9, C-10, C-9'	H-9'*β*
12	1.11 s	20.6 CH$_3$	C-1, C-2, C-3	H-3*α*, H-9'*α*
13	1.04 s	24.3 CH$_3$	C-5, C-6, C-7, C-14	H-4, H-7*α*, H-8
14	1.09 s	30.0 CH$_3$	C-5, C-6, C-7, C-13	H-5, H-7*α*, H-7*β*
15	1.55 s	16.5 CH$_3$	C-8, C-9, C-10	H-1, H-5
1'		172.4 C		
2'		163.4 C		
3'	7.00 s	113.5 CH	C-1', C-2', C-4', C-5'	
4'		161.2 C		
5'		122.0 C		
6'		150.1 C		
7'	7.11 s	124.3 CH	C-1', C-2', C-5', C-6', C-8'	H-8'
8'	2.39 s	27.4 CH$_3$	C-5', C-6', C-7'	H-7', H-9'*β*
9'*α*	2.26 overlap	34.2 CH$_2$	C-1, C-2, C-11, C-4', C-5', C-6'	H-9'*β*, H-11*α*, H$_3$-12
9'*β*	3.22 dd (17.8, 4.7)		C-1, C-2, C-4', C-5', C-6'	H-1, H-11*β*, H-9'*α*

[a] Measured in $CDCl_3$; 600 MHz for ^{1}H NMR and 150 MHz for ^{13}C NMR.

Supplementary Figures

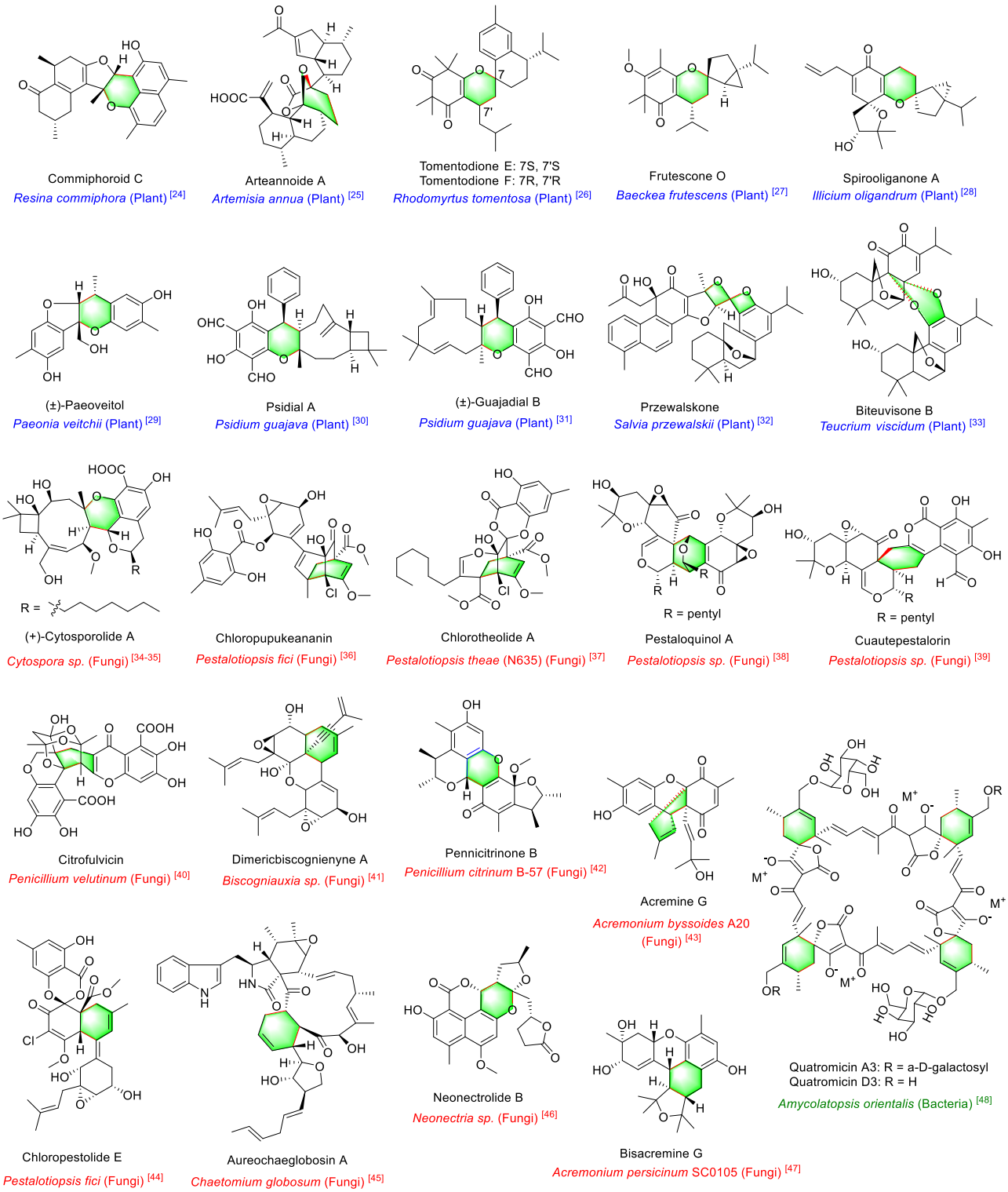

Figure S1. Natural products probably biosynthesized *via* intermolecular Diels-Alder cycloadditions isolated from plants, fungi, and bacteria[24-48].

A)

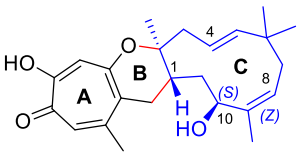

Neosetophomone B

(Absolute configuration)

Neosetophoma sp. (MSX50044)[5]

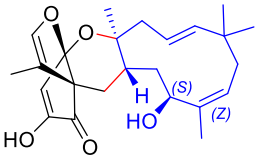

Neosetophomone A

(Absolute configuration)

Neosetophoma sp. (MSX50044)[5]

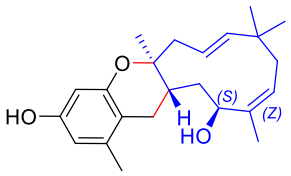

Pughiinin A

Kionochaeta ramifera BCC 7585 [49]

Kionochaeta pughii BCC 3878 [50]

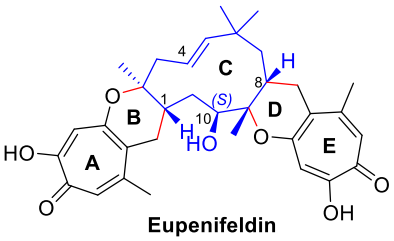

Eupenifeldin

(Absolute configuration)

Eupenicillium brefeldianum ATCC 74184 [6]

Kionochaeta ramifera BCC 7585 [49]

Phoma sp. [7]

Phoma sp. XZ068 [51]

Neosetophoma sp. (strain MSX50044) [5]

An unidentified ascomycete [52]

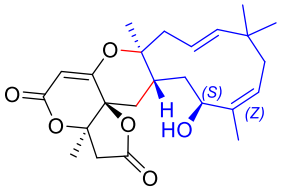

Phomanolide B

(Absolute configuration)

Phoma sp. [7]

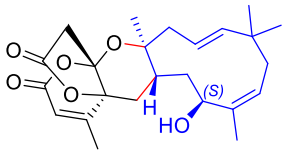

Phomanolide E

(Absolute configuration)

Phoma sp. [4]

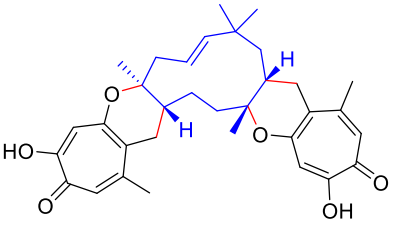

Dehydroxyeupenifeldin

Neosetophoma sp. (MSX50044) [5]

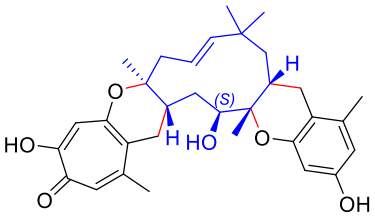

Noreupenifeldin B

Neosetophoma sp. (MSX50044) [5]

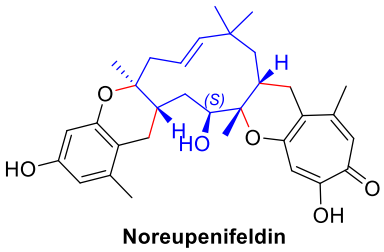

Noreupenifeldin

An unidentified ascomycete producing eupenifeldin [52]

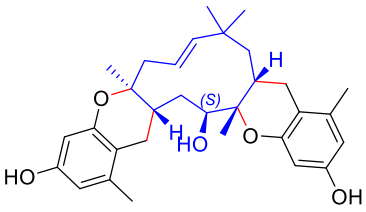

Ramiferin

Kionochaeta ramifera BCC 7585 [49]

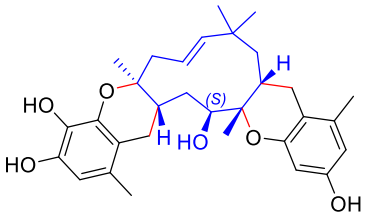

22-hydroxyramiferin

Neosetophoma sp. (MSX50044) [5]

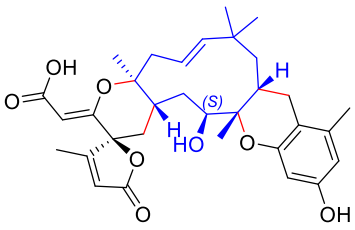

Phomanolide A

(Absolute configuration)

Phoma sp. [7]

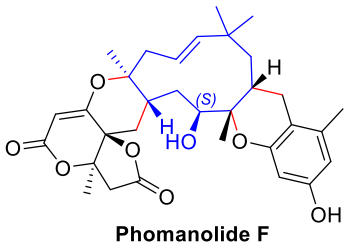

Phomanolide F

(Absolute configuration)

Phoma sp. [4]

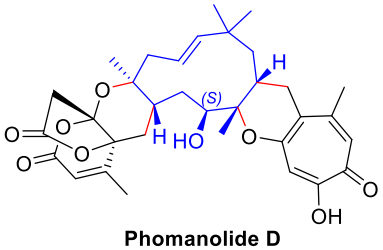

Phomanolide D

(Absolute configuration)

Phoma sp. [4]

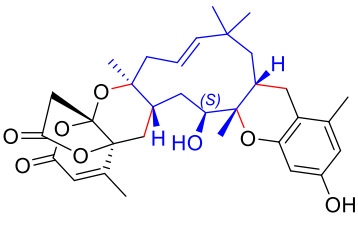

Phomanolide C

(Absolute configuration)

Phoma sp. [4]

To be continued…

Continued…

B)

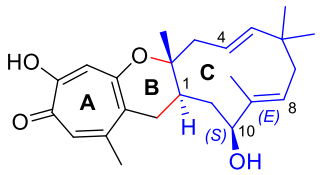

Epolone B

OS-F69284 (ATCC 74390) [12]

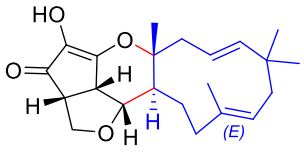

Xenovulene A

Acremonium strictum [53]

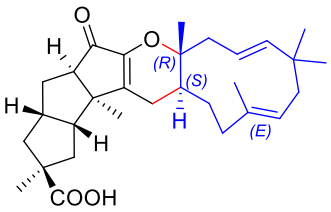

Sterhirsutin A

(Absolute configuration)

Stereum hirsutum [54]

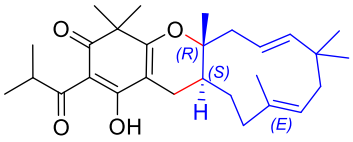

(+)-Hyperjapone A

(Absolute configuration)

Hypericum japonicum [55]

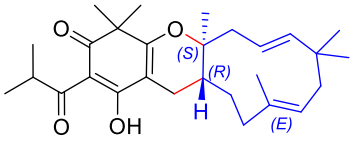

(–)-Hyperjapone A

(Absolute configuration)

Hypericum japonicum [55]

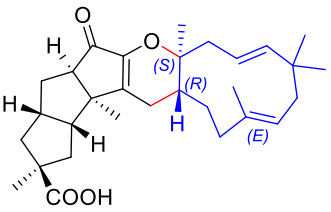

Sterhirsutin B

(Absolute configuration)

Stereum hirsutum [54]

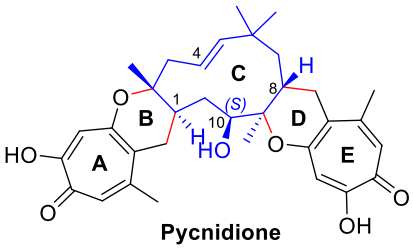

Pycnidione

(Absolute configuration)

Phoma sp. [56]

OS-F69284 (ATCC 74390) [12]

Phoma sp. H4-77 [57]

Diaporthe sp. [58]

Gloeotinia sp. FKI-3416 [59]

Theissenia rogersii 9203120 [60]

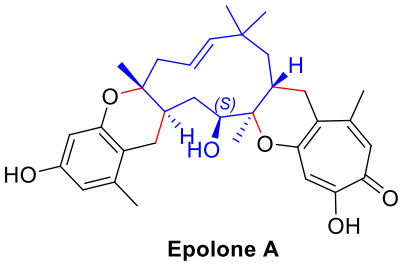

Epolone A

OS-F69284 (ATCC 74390) [12]

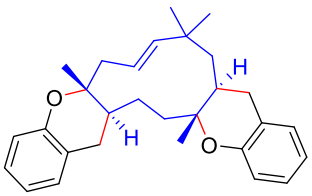

(±)-Lucidene

Uvaria lucida ssp. *lucida* [61]

Figure S2. Natural meroterpenoids possibly derived from intermolecular Diels-Alder reactions with humulene and polyketone-derived fragments. These compounds can be classified into two groups according to the configurations of the 1,2- and 8,9- double bonds in the humulene, which usually serve as the dienophiles in the DA reactions. **A) *trans-Z* or *trans-cis* type**, in which 1*E*, 4*E*, 8*Z*-humulene is engaged, resulting in the *trans*-fused B/C rings and *cis*-fused C/D rings; **B) *trans-E* or *trans-trans* type**, in which 1*E*, 4*E*, 8*E*-humulene is engaged, resulting in the *trans*-fused B/C rings and *trans*-fused C/D rings. Notably, the absolute configurations of some of these compounds are not determined in the original literature (such as noreupenifeldin, pughiinin A, ramiferin, epolone A, and epolone B), which are uniformed based on biosynthetic consideration in this figure. The sources of the compounds are listed below the structures[4-7, 12, 49-61].

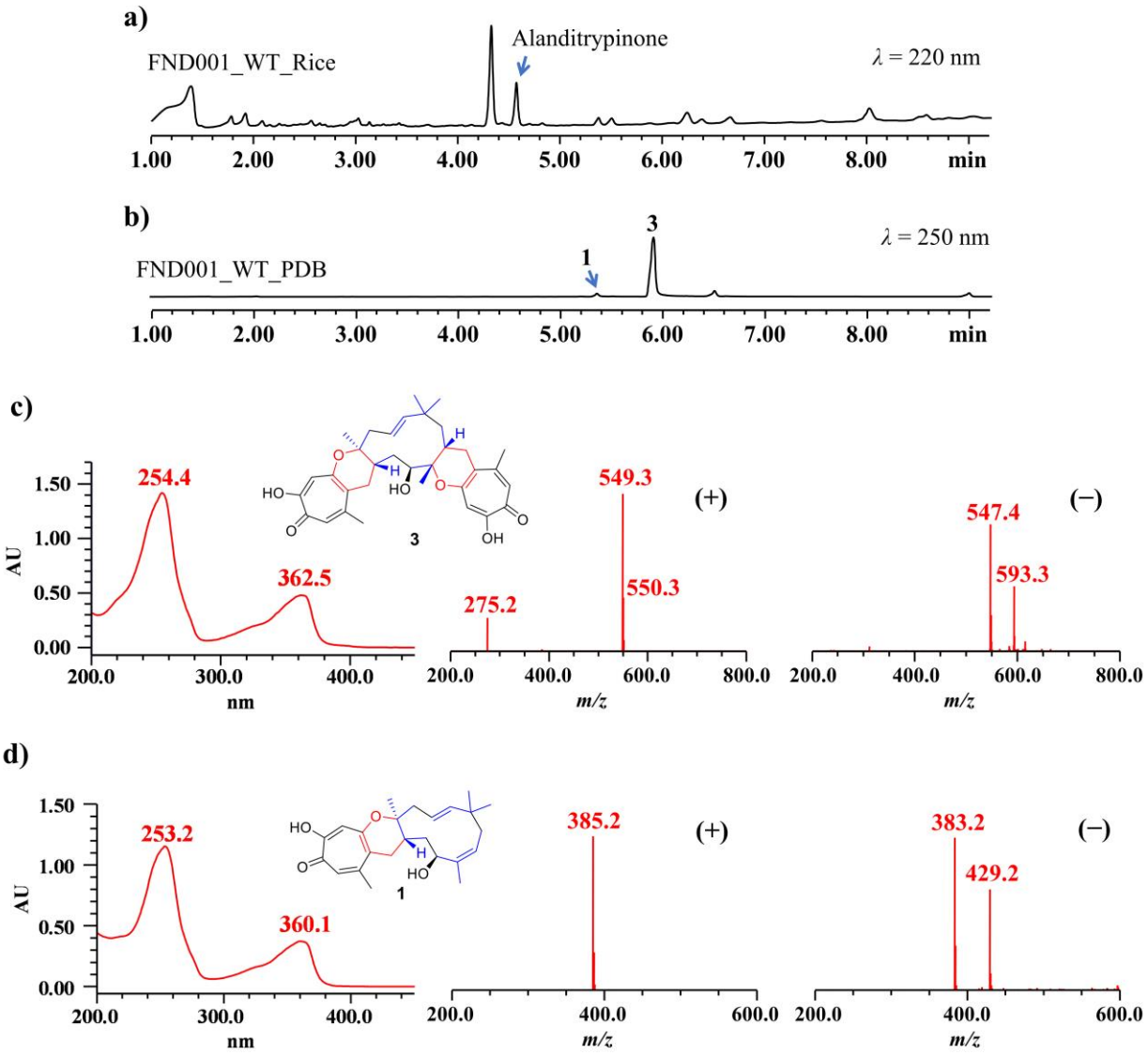

Figure S3. LC-MS analysis of the metabolites from wild type *Penicillium janthinellum* (FND001). a) UPLC chromatogram of the extracts from the rice fermentation of *P. janthinellum*. **b)** UPLC chromatogram of the extracts from the *P. janthinellum* cultured in PDB medium. **c)** Extracted UV spectrum and ESIMS data of **3**. The (+)-ESIMS and (-)-ESIMS spectra showed ion peaks of *m/z* 549.3 $[M + H]^+$, 547.4 $[M - H]^-$ and 593.3 $[M - H + HCOOH]^-$, respectively, suggesting a molecular weight of 548 matched with eupenifeldin (**3**); **d)**.Extracted UV spectrum and ESIMS data of **1**. The (+)-ESIMS and (-)-ESIMS spectra showed ion peaks of *m/z* 385.2 $[M + H]^+$, 383.2 $[M - H]^-$ and 429.2 $[M - H + HCOOH]^-$, respectively, suggesting a molecular weight of 384 matched with neosetophomone B (**1**).

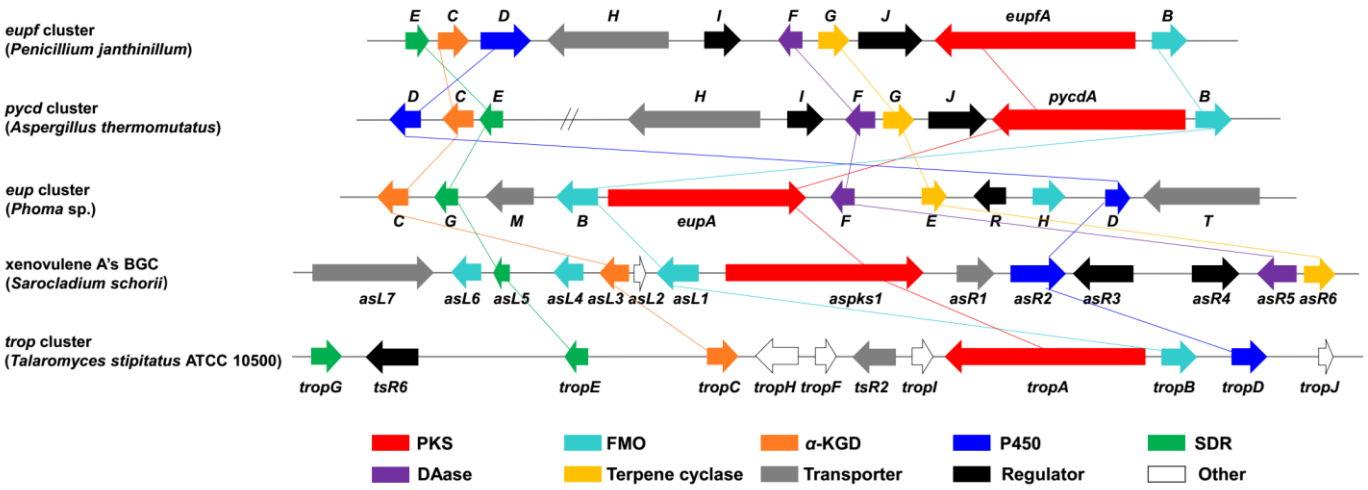

Gene	Size (bp)	Predicted function	Protein homologue, Origin	Similarity/identity (%)
eupfA	8226	NR-PKS (SAT-KS-AT-PT-ACP-MT-R)	XP_026613065.1, *Aspergillus thermomutatus*	92/88
			EupA (QCO93110.1), *Phoma* sp.	73/58
			Aspks1 (AWM95789.1), *Sarocladium schorii*	72/58
			TropA (B8M9J9.1), *Talaromyces stipitatus* ATCC 10500	59/43
eupfB	1578	FAD-dependent monooxygenase	XP_026613066.1, *Aspergillus thermomutatus*	85/80
			AsL1 (AWM95796.1), *Sarocladium schorii*	75/66
			EupB (QCO93109.1), *Phoma* sp.	74/64
			TropB (B8M9J8.1), *Talaromyces stipitatus* ATCC 10500	59/44
eupfC	1148	α-ketoglutarate-dependent dioxygenase	XP_026609887.1, *Aspergillus thermomutatus*	86/85
			AsL3 (AWM95787.1), *Sarocladium schorii*	79/72
			EupC (QCO93106.1), *Phoma* sp.	68/62
			TropC (B8M9K5.1), *Talaromyces stipitatus* ATCC 10500	62/52
eupfD	1987	cytochrome P450 monooxygenase	XP_026609888.1, *Aspergillus thermomutatus*	95/94
			EupD (QCO93115.1), *Phoma* sp.	64/54
			AsR2 (AWM95791.1), *Sarocladium schorii*	46/28
			TropD (B8M9J6.1), *Talaromyces stipitatus* ATCC 10500	45/29
eupfE	963	short-chain dehydrogenase/reductase	XP_026609886.1, *Aspergillus thermomutatus*	92/89
			EupG (QCO93107.1), *Phoma* sp.	82/68
			TropE (B8M9K8.1), *Talaromyces stipitatus* ATCC 10500	58/43
			AsL5 (AWM95785.1), *Sarocladium schorii*	44/32
eupfF	1104	putative hetero Diels-Alderase	XP_026613062.1, *Aspergillus thermomutatus*	96/92
			EupF (QCO93111.1), *Phoma* sp.	81/67
			AsR5 (AWM95794.1), *Sarocladium schorii*	75/64
eupfG	1295	humulene synthase	XP_026613063.1, *Aspergillus thermomutatus*	94/92
			EupE (QCO93112.1), *Phoma* sp.	82/70
			AsR6 (AWM95795.1), *Sarocladium schorii*	75/62
eupfH	4778	ABC transporter	XP_026613060.1, *Aspergillus thermomutatus*	91/88
			EupT (QCO93116.1), *Phoma* sp.	81/71
			AsL7 (AWM95783.1), *Sarocladium schorii*	79/67
eupfI	1566	transcription factor	XP_026613061.1, *Aspergillus thermomutatus*	79/75
			AsR4 (AWM95793.1), *Sarocladium schorii*	71/49
eupfJ	2851	transcription factor (MHR superfamily)	XP_026613064.1, *Aspergillus thermomutatus*	92/90
			XP_024682557.1, *Aspergillus novofumigatus* IBT 16806	86/82

Figure S4. Bioinformatics analysis of the *eupf* gene cluster and homologs.

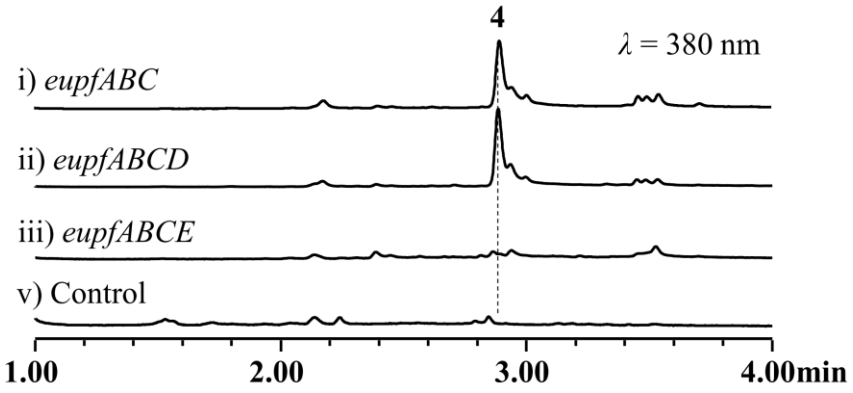

Figure S5. LC-MS analysis of the metabolites from the heterologously overexpressed *A. nidulans* strains. Heterologous expression of *eupfABC* in *A. nidulans* led to the major production of **4** (trace i). Comparing to the metabolism spectrum of *A. nidulans* overexpressing *eupfABCD* which was almost identical with that of *eupfABC* mutant (trace ii), compound **4** disappeared in *A. nidulans* mutant overexpressing *eupfABCE* (trace iii), which indicated that **4** could be a substrate of EupfE.

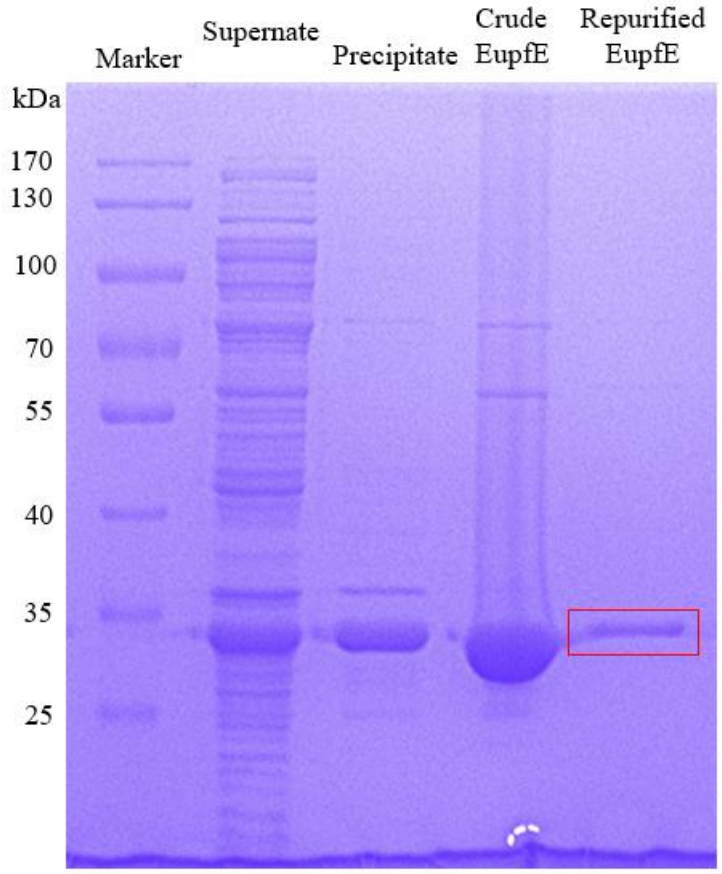

Figure S6. SDS-PAGE gel (10%) of the purified EupfE. EupfE (SDR, 31 kDa) was purified from *E. coli* BL21(DE3) with N-terminal His_6-tag using pET28a vector.

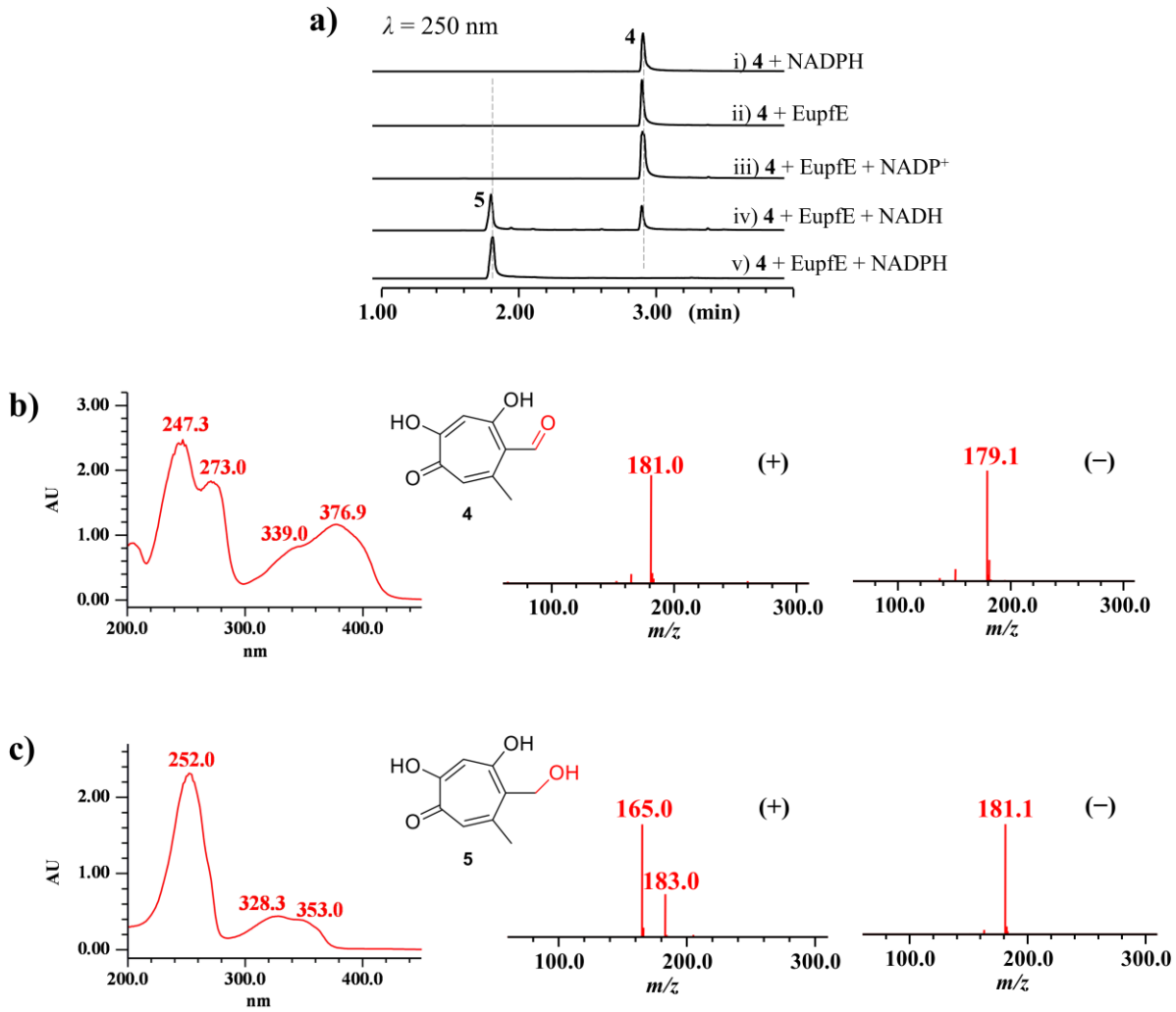

Figure S7. LC-MS analysis of products in *in vitro* assays of EupfE. a) UPLC chromatograms of the resulted products from *in vitro* assays of EupfE, in which **4** was partly or completely converted to **5** in the presence of NADH (trace iv) or NADPH (trace v), respectively. **b)** UV and ESIMS data of **4. c)** UV and ESIMS data of **5.** The ESIMS data suggested a molecular weight of 180 and 182 for compounds **4** and **5**, respectively. Comparing with the UV absorption of **4**, the significant blue shift of UV absorption of **5** suggested the aldehyde group in **4** was reduced to a hydroxymethyl group in **5**.

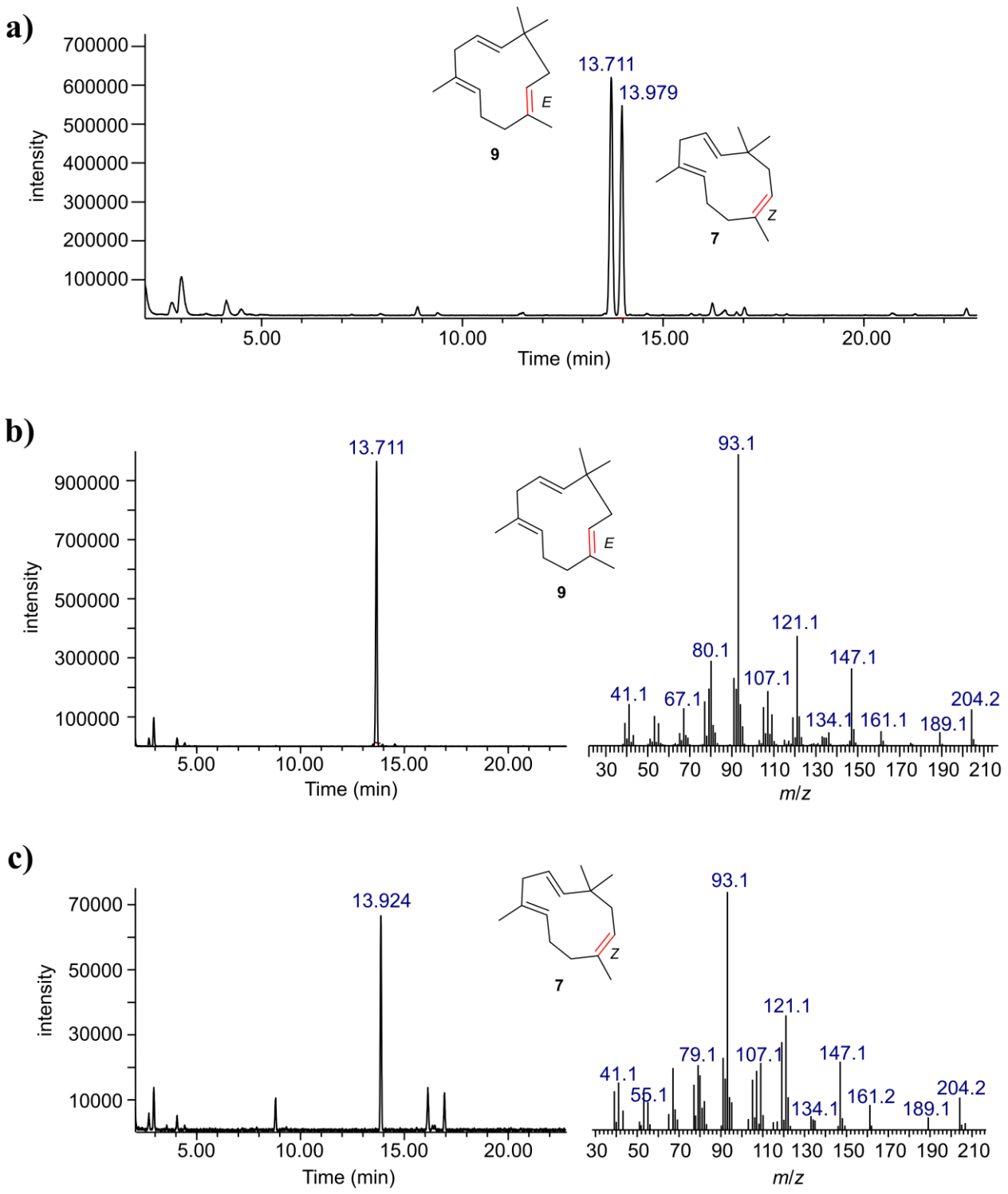

Figure S8. GC-MS analysis of the extracts from the *A. nidulans* mutant overexpressing *eupfG* and the standard 1*E*, 4*E*, 8*E*-humulene (9). a) GC-MS chromatogram of a mixture of the standard 1*E*, 4*E*, 8*E*-humulene (**9**, from Sigma) and the *n*-hexane extracts of the *A. nidulans* mutant overexpressing *eupfG*. **b)** GC-MS chromatogram of the standard **9** and the extracted MS spectrum of **9**. **c)** GC-MS chromatogram of the *n*-hexane extracts of the *A. nidulans* mutant overexpressing *eupfG*, which contained compound **7** as major product, and the extracted MS spectrum of **7**.

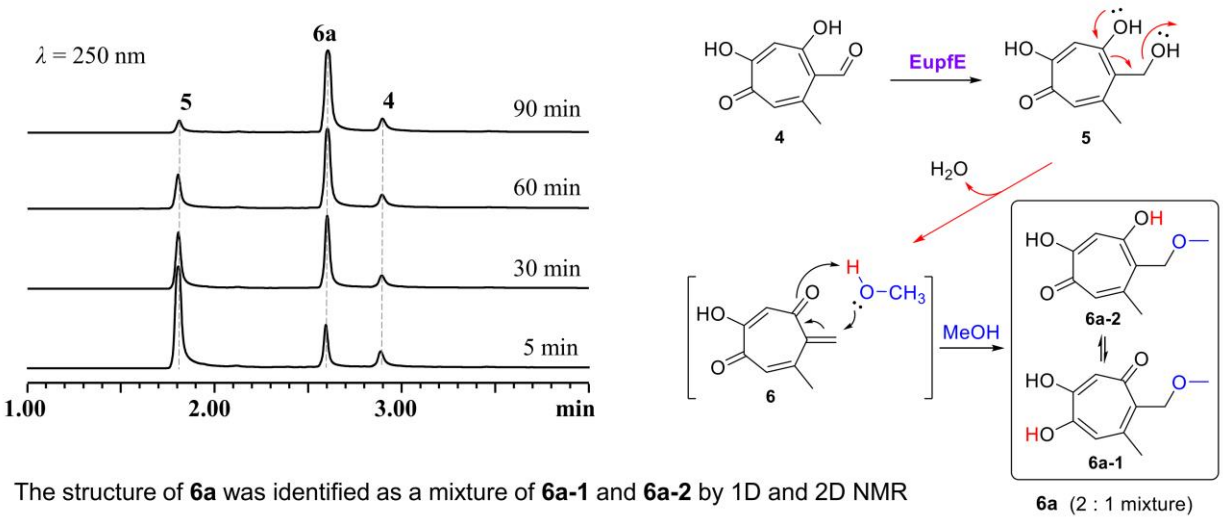

Figure S9. Stability assay of compound 5 in methanol. To obtain **5**, the *in vitro* reaction was conducted in a 100 μL system containing 50 mM Bicine buffer (pH 8.0), 3 mM NADPH, 2 mM **4**, and 25 μM EupfE. The reaction mixture was incubated at 26 °C for 20 min, which was subsequently extracted with EtOAc and concentrated to dryness to obtain the crude compound **5**. The crude compound **5** was dissolved in MeOH and analyzed by UPLC-MS at 5 min, 30 min, 60 min and 90 min, respectively. The time-dependent transformation from **5** to **6a** suggested that compound **5** was extremely unstable in polar aprotic solvent.

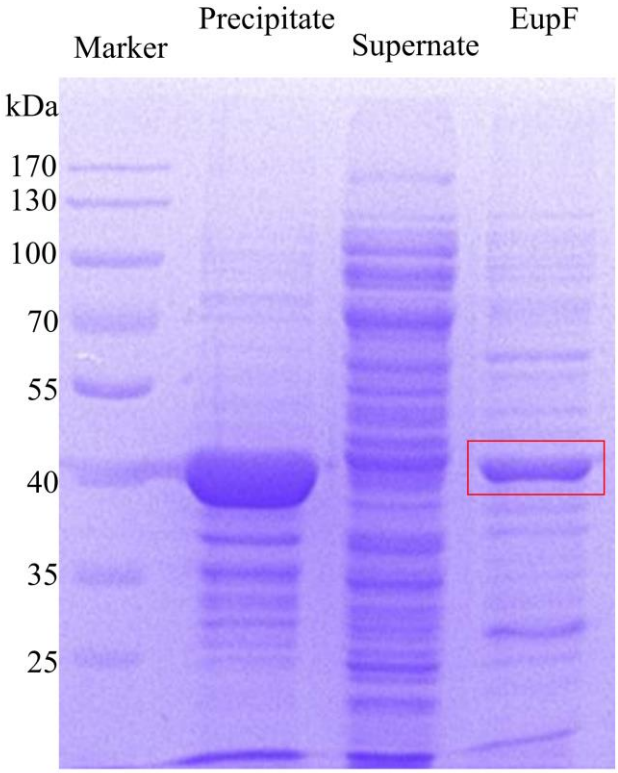

Figure S10. SDS-PAGE gel (10%) of the purified EupF. EupF (DAase, 42 kDa) was purified from *E. coli* BL21(DE3) with N-terminal His_6-tag using pET28a vector.

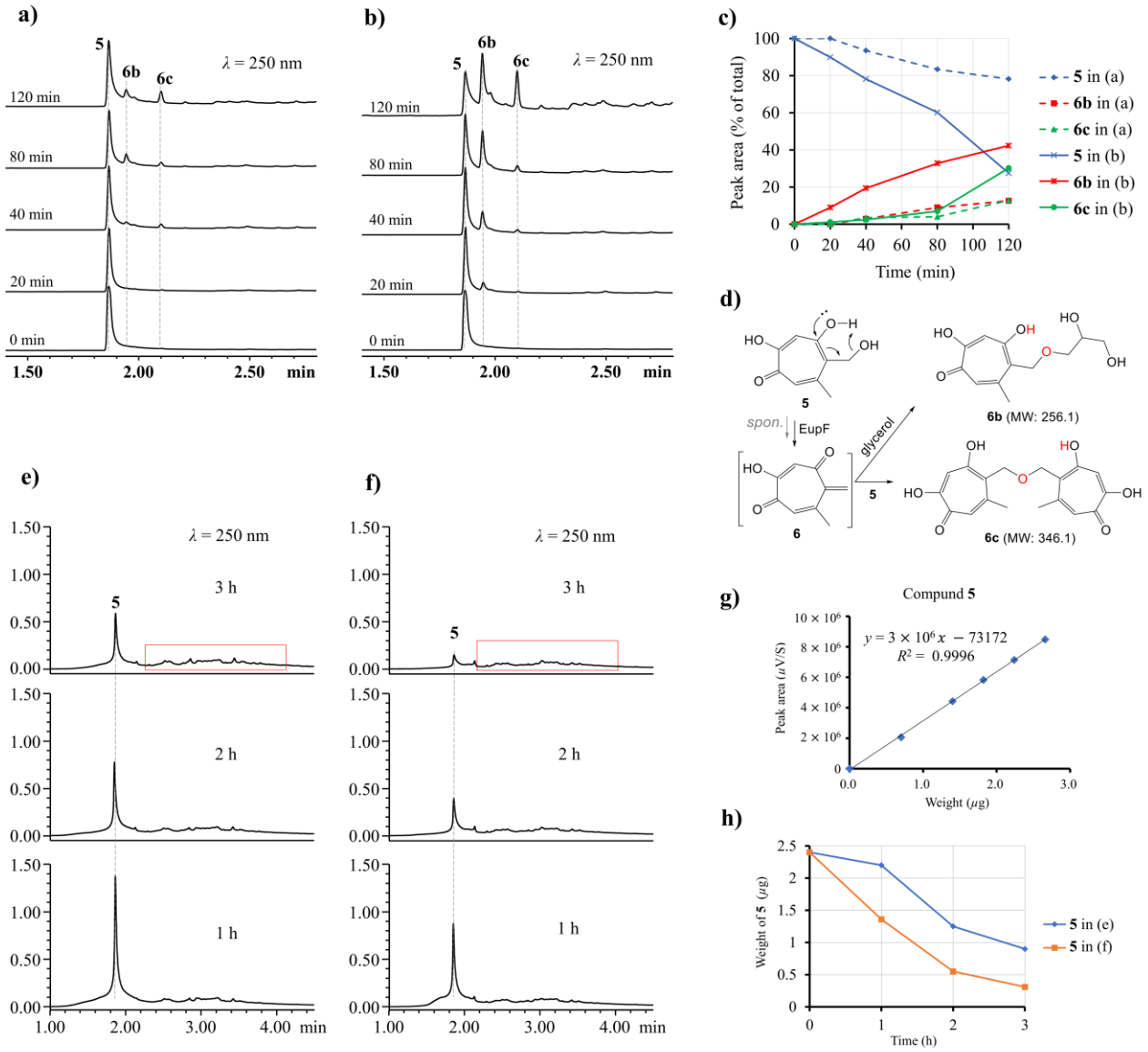

Figure S11. ***In vitro*** **assay of EupF with 5 as substrate.** Since the expected product **6** was extremely unstable, 1% glycerol was added in the *in vitro* reaction system (a) and (b) to capture **6**. **a)** Time-course analysis of the dehydration of **5** with boiled EupF in Bicine buffer with 1% glycerol. **b)** Time-course analysis of the dehydration of **5** with EupF in Bicine buffer with 1% glycerol. **c)** Changes of the percentage peak area of **5**, **6b**, and **6c** in assays a) (dashed lines) and b) (solid lines). 72.5% of **5** was converted to two main products, **6b** and **6c**, in the presence of EupF, while only 21.8% of **5** could be spontaneously transformed. **d)** Proposed structures of **6b** and **6c** which were inferred from their UV absorption and molecular weight. **e)** Time-course analysis of the dehydration of **5** with boiled EupF in PBS buffer without glycerol. **f)** Time-course analysis of the dehydration of **5** with EupF in PBS buffer without glycerol (Red rectangular box showed a series of polymers with UV absorption similar to that of **5**). **g)** Concentration standard curve of **5** ($y = 3\times10^6x - 73172$, $R^2 = 0.9996$; y: peak area; x: weight of **5**.). **h)** Time-course consumption of **5** in assays e) and f), which was calculated on the basis of the standard curve as shown in g). These results revealed that EupF could significantly accelerate the dehydration of **5**.

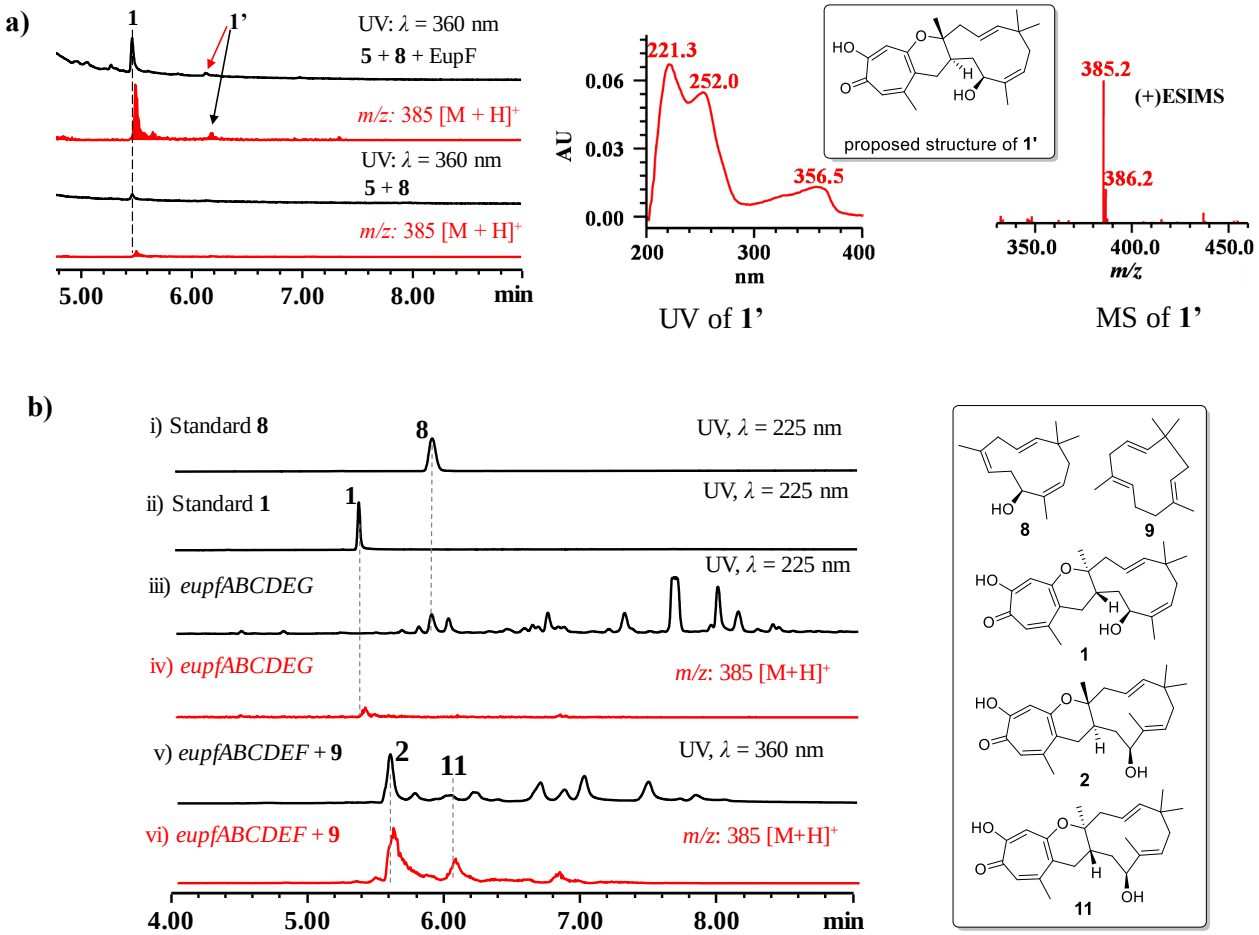

Figure S12. LC-MS traces of a) *in vitro* assays of EupF with 5 and 8 as substrates; and b) extracts from the *A. nidulans* mutants overexpressing *eupf* genes. a) A very tiny peak (**1'**, t_R = 6.18 min) with same UV and MS characteristics (*m/z*: 385 $[M + H]^+$) as those of **1** was detected in the *in vitro* EupF assay. **1'** was proposed as a diastereomer of **1** even it was not isolated due to its tiny amount. **b)** Co-expressing *eupfABCDEG* (without *eupfF*) in *A. nidulans* led to the production of apparent **8** without **1** or **1'** detected in HPLC (only tiny **1** was detected by extracted *m/z*: 385, traces iii-iv), which suggested EupF/EupfF was required for the Diels-Alder reaction. **2** and **11** were isolated from *A. nidulans* co-expressing *eupfABCDEF* feeding **9**.

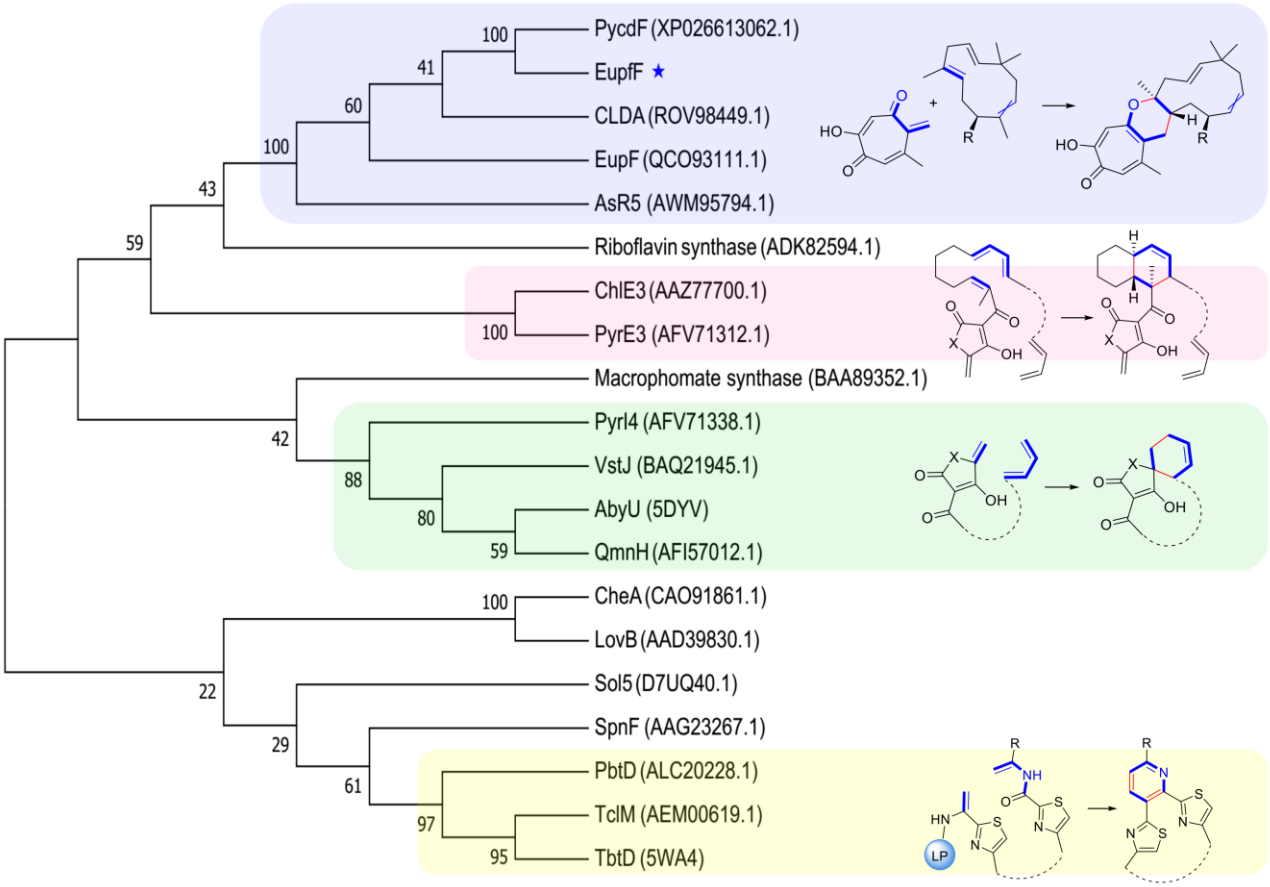

Figure S13. Neighbor joining method based phylogenetic analysis of intramolecular and intermolecular DAases using MEGA7.0 software. Protein names and accession numbers are shown at the leaves of the tree. The phylogenetic relationship of intermolecular DAases is relatively independent with intramolecular DAases. Enzymes that catalyze Diels-Alder reactions between tropolone *o*-quinone methide and humulene showed close phylogenetic relationship.

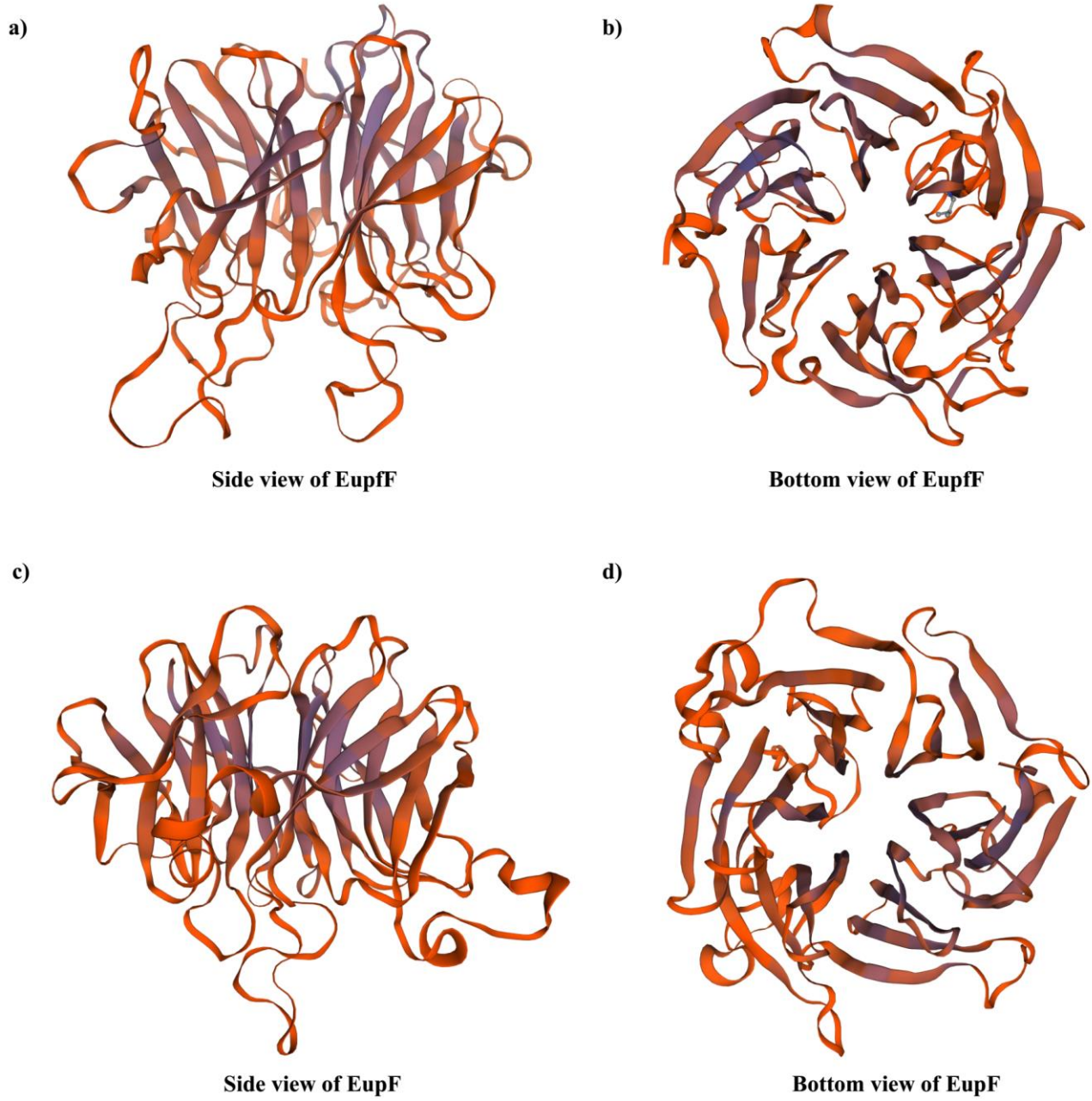

Figure S14. Models of EupfF and EupF computed with SWISS-MODEL and template 2p4o.1.A. The 3D models of EupfF and EupF suggested that these two proteins showed similarity in conformation with a six-bladed propeller.

```
EupfF                [1]   -  M  L  F  T  V  S  L  L  L  S  G  L  L  A  V  S  P  S  L  S  A  V  L  P  -  -  -  -  -  [ 30]
EupF QCO93111.1      [1]   -  M  R  Y  H  L  S  A  L  V  L  V  F  T  A  F  R  E  T  L  T  A  P  T  P  -  -  -  -  -  [ 30]
PycdF XP026613062.1  [1]   -  M  R  S  T  V  S  S  L  L  L  G  F  L  A  V  S  P  S  L  S  A  V  V  P  -  -  -  -  -  [ 30]
CLDA ROV98449.1      [1]   -  M  P  S  L  V  T  S  V  A  L  G  F  L  A  Y  M  P  T  L  S  T  M  I  P  -  -  -  -  -  [ 30]
AsR5 AWM95794.1      [1]   M  R  R  S  F  L  I  S  A  A  L  G  L  S  M  S  T  P  A  L  A  A  S  I  Q  S  V  L  G  Y  [ 30]

EupfF                [31]  -  -  -  -  -  -  -  -  -  -  -  -  -  -  -  -  -  R  A  S  S  A  T  -  -  -  -  G  S  V  P  [ 60]
EupF QCO93111.1      [31]  -  -  -  -  -  -  -  -  -  -  -  -  -  -  -  -  -  G  N  N  -  -  -  -  -  -  -  -  T  I  P  [ 60]
PycdF XP026613062.1  [31]  -  -  -  -  -  -  -  -  -  -  -  -  -  -  -  -  -  R  N  S  N  A  T  -  -  -  -  G  S  V  P  [ 60]
CLDA ROV98449.1      [31]  -  -  -  -  -  -  -  -  -  -  -  -  -  -  -  -  -  R  A  N  N  A  T  S  H  A  T  G  A  I  P  [ 60]
AsR5 AWM95794.1      [31]  L  R  P  T  S  H  H  H  A  P  C  A  D  D  V  V  L  K  Q  S  A  G  S  D  S  A  A  P  D  P  [ 60]

EupfF                [61]  L  P  E  R  L  L  H  H  W  P  N  G  T  W  V  E  N  I  A  V  R  P  N  G  N  L  L  L  T  T  [ 90]
EupF QCO93111.1      [61]  L  P  N  R  L  L  H  Q  W  P  N  G  T  W  V  E  N  I  S  V  R  P  N  G  N  L  L  V  T  T  [ 90]
PycdF XP026613062.1  [61]  L  P  E  R  L  L  H  H  W  P  N  G  T  W  V  E  N  I  A  V  R  P  N  G  N  L  L  L  T  T  [ 90]
CLDA ROV98449.1      [61]  L  P  S  R  L  L  H  H  W  P  N  G  T  W  V  E  N  I  S  V  R  P  N  G  N  L  L  V  T  T  [ 90]
AsR5 AWM95794.1      [61]  L  P  S  R  V  V  H  N  W  P  N  G  T  W  I  E  N  I  S  V  R  P  N  G  N  L  L  V  S  Q  [ 90]

EupfF                [91]  S  T  P  N  G  T  V  W  H  V  K  K  P  W  T  D  T  P  E  V  E  L  A  Y  N  F  D  E  W  V  [120]
EupF QCO93111.1      [91]  S  T  P  D  G  S  V  W  Q  V  K  E  P  W  K  E  N  P  E  V  E  R  V  F  N  F  D  E  W  V  [120]
PycdF XP026613062.1  [91]  S  T  P  N  G  T  V  W  H  V  K  K  P  W  T  D  T  P  E  V  E  L  A  Y  N  F  D  E  W  V  [120]
CLDA ROV98449.1      [91]  S  T  P  N  G  T  V  W  H  V  K  E  P  W  S  E  T  P  D  V  E  L  A  Y  N  F  D  E  W  V  [120]
AsR5 AWM95794.1      [91]  S  T  P  R  G  R  V  W  Q  V  K  E  P  W  L  D  E  P  K  V  E  L  A  Y  D  F  D  E  W  V  [120]

EupfF                [121] D  R  L  I  G  I  G  E  T  T  P  D  K  Y  I  V  V  G  S  R  F  Y  S  P  D  A  Y  S  S  H  [150]
EupF QCO93111.1      [121] D  R  L  I  G  I  G  E  T  Q  D  D  K  Y  V  V  V  G  S  R  F  Y  S  T  D  A  Q  S  S  H  [150]
PycdF XP026613062.1  [121] D  R  L  I  G  I  G  E  T  T  P  D  K  Y  I  V  V  G  S  R  F  Y  S  P  E  A  Y  S  S  Q  [150]
CLDA ROV98449.1      [121] D  R  L  I  G  I  G  E  T  T  P  D  K  Y  V  V  V  G  S  R  F  Y  N  P  S  A  Y  S  S  Q  [150]
AsR5 AWM95794.1      [121] D  R  I  I  G  I  G  E  T  T  P  D  K  Y  V  V  V  G  S  R  F  Y  S  L  D  P  Q  S  S  Q  [150]

EupfF                [151] V  D  R  T  F  A  A  M  E  L  D  F  T  -  -  K  E  P  P  S  T  R  M  V  A  W  M  P  E  A  [180]
EupF QCO93111.1      [151] V  A  R  T  F  C  A  M  E  L  D  F  S  G  N  T  T  E  P  S  A  R  L  I  A  W  M  P  E  S  [180]
PycdF XP026613062.1  [151] V  D  R  T  F  A  A  M  E  L  D  F  T  -  -  T  D  T  P  S  A  R  M  A  A  W  M  P  E  A  [180]
CLDA ROV98449.1      [151] V  E  R  T  F  V  A  L  E  L  D  F  S  -  D  G  D  E  P  T  A  R  V  V  S  W  F  P  E  A  [180]
AsR5 AWM95794.1      [151] V  E  R  T  F  C  A  M  E  L  D  F  T  -  K  G  E  K  P  S  A  R  L  V  A  R  F  P  H  A  [180]

EupfF                [181] E  L  L  Q  G  V  A  A  L  P  W  D  R  S  I  V  L  I  S  D  Q  Y  V  L  R  P  R  Y  K  Q  [210]
EupF QCO93111.1      [181] Y  L  L  Q  G  V  A  A  L  P  W  D  R  D  T  V  L  I  S  D  Q  Y  V  L  R  P  R  A  V  Q  [210]
PycdF XP026613062.1  [181] A  L  L  Q  G  V  A  A  L  P  W  N  R  S  T  V  L  I  S  D  Q  Y  V  L  R  P  R  Y  Q  Q  [210]
CLDA ROV98449.1      [181] S  L  L  Q  S  V  A  A  L  P  W  K  S  T  T  V  L  I  S  D  Q  Y  V  L  R  P  R  E  T  Q  [210]
AsR5 AWM95794.1      [181] N  L  L  Q  S  V  S  A  L  P  W  D  R  S  V  V  L  I  S  D  Q  Y  L  L  H  P  R  A  D  W  [210]

EupfF                [211] V  D  W  T  P  S  P  G  Q  I  W  R  L  D  T  K  T  G  D  Y  E  L  V  M  T  D  Y  A  E  M  [240]
EupF QCO93111.1      [211] I  D  W  T  P  S  P  G  Q  I  W  V  L  D  T  R  T  G  E  Y  G  L  V  M  T  D  Y  A  E  L  [240]
PycdF XP026613062.1  [211] V  D  W  T  P  S  P  G  Q  I  W  R  L  D  T  Q  T  G  D  Y  E  L  V  M  T  D  Y  A  E  M  [240]
CLDA ROV98449.1      [211] L  D  W  T  P  A  P  G  Q  I  W  R  L  D  T  L  T  G  K  K  E  I  V  M  T  N  Y  A  E  L  [240]
AsR5 AWM95794.1      [211] E  D  L  T  P  G  P  G  Q  I  W  R  L  D  T  K  T  G  H  H  E  I  V  M  T  N  Y  A  E  M  [240]

EupfF                [241] N  T  T  Y  A  H  G  P  D  V  G  I  N  G  I  R  I  L  G  N  E  L  Y  W  V  N  Q  D  N  G  [270]
EupF QCO93111.1      [241] N  T  T  Y  A  K  G  P  D  V  G  I  D  G  I  K  I  R  D  H  D  L  F  W  V  N  Q  D  D  S  [270]
PycdF XP026613062.1  [241] N  T  T  Y  A  H  G  S  D  V  G  I  D  G  I  R  I  L  G  N  E  L  Y  W  V  N  Q  D  T  G  [270]
CLDA ROV98449.1      [241] N  T  T  Y  A  H  G  E  D  V  G  V  N  G  I  K  I  R  D  H  Y  L  Y  W  V  N  Q  D  T  G  [270]
AsR5 AWM95794.1      [241] N  T  T  Y  N  H  G  L  D  V  G  I  N  G  I  K  I  H  G  D  H  L  Y  W  I  N  M  D  T  G  [270]

EupfF                [271] G  V  Y  R  V  E  I  Q  K  N  G  H  P  V  P  P  -  A  V  P  E  V  V  S  V  V  E  S  Q  L  [300]
EupF QCO93111.1      [271] G  I  Y  R  V  K  I  D  D  A  G  V  P  V  A  P  -  V  K  P  Q  L  V  A  S  Y  N  -  T  M  [300]
PycdF XP026613062.1  [271] G  I  Y  R  V  A  I  Q  K  N  G  Y  P  V  P  P  -  A  V  P  E  V  V  S  V  V  E  S  Q  L  [300]
CLDA ROV98449.1      [271] G  V  Y  K  I  E  I  D  D  E  G  Y  P  V  P  P  -  A  I  P  E  T  I  T  V  V  D  -  T  L  [300]
AsR5 AWM95794.1      [271] G  A  Y  R  V  R  I  D  K  Y  G  Y  P  T  P  L  N  A  V  P  E  T  L  G  V  A  E  D  A  L  [300]
```

To be continued…

Continued…

```
EupfF                [301] W D D F A F G - - - - - - - P G D E D L L W V T G L N A V Y A [330]
EupF QCO93111.1      [301] W D D M A F D - - - - - - - P F N E N V I W A T G L N A V F A [330]
PycdF XP026613062.1  [301] W D D F A F G - - - - - - - P G N K D L L W A T G L N A V Y A [330]
CLDA ROV98449.1      [301] W D D F G F G - - - - - - - P N G A D T I W S T G L N S V W A [330]
AsR5 AWM95794.1      [301] W D D F A M H G T R I G E E S D D T T M F A T S I V N L M A [330]

EupfF                [331] V S K K N G T A V V V D G V G T S N N M S F P G P T S C Q F [360]
EupF QCO93111.1      [331] A T - L D G Q I V P V D G V G T S D N L T L P G P T A C A F [360]
PycdF XP026613062.1  [331] V S T K N G T A V V V D G V G T S N N L S F P G P T A C Q F [360]
CLDA ROV98449.1      [331] V S P D N G T A V T V T G V G T S D N L S F P G P T A A Q F [360]
AsR5 AWM95794.1      [331] I S P E N G T I V P L A G V G T S E P M G F P G P T S A Q F [360]

EupfF                [361] G R T K H D S N V L Y V T G N L Y S V P D S L L D V K I G G [390]
EupF QCO93111.1      [361] G R T E K D K S I L Y V T G N L L T V P E S L L D V K L G G [390]
PycdF XP026613062.1  [361] G R T K Y D S N V L Y V T G N L Y S V P D N L L D V K I G G [390]
CLDA ROV98449.1      [361] G R T Q K D S N I L Y V T G N L Y D V P D S L L D L T L R G [390]
AsR5 AWM95794.1      [361] G R T E K D S H I L Y V T G K L F N V P P S I R D V V I Q G [390]

EupfF                [391] W V R A I D T T G F H L [402]
EupF QCO93111.1      [391] W - - - - - - - - - - - [402]
PycdF XP026613062.1  [391] W V R A I D T T G F H L [402]
CLDA ROV98449.1      [391] W V R A V D T T G F H F [402]
AsR5 AWM95794.1      [391] W V R A I D T T G F H F [402]
```

Figure S15. Multiple sequence alignment of EupfF with its homologous proteins.
The proteins EupF (QCO93111.1), PycdF (XP026613062.1), CLDA (ROV98449.1), and AsR5 (AWM95794.1) from *Phoma* sp., *Aspergillus thermomutatus*, *Cytospora leucostoma*, and *Sarocladium schorii*, respectively, showed closed phylogenetic relationship (Figure S13) and highly homology (Figure S4) with EupfF, which were supposed to possess similar catalytic activity for the intermolecular hetero-Diels-Alder cycloaddition. Since His, Lys, and Arg have been reported as potential active sites for dehydration and Diels-Alder reaction, the conserved residues of H37, R51, R92, and R323 (labeled in red), which approached the protein catalytic cavity of EupF according to the 3D models computed with SWISS-MODEL (Figure S14), were selected for mutation sites in the subsequent site-specific mutagenesis experiments.

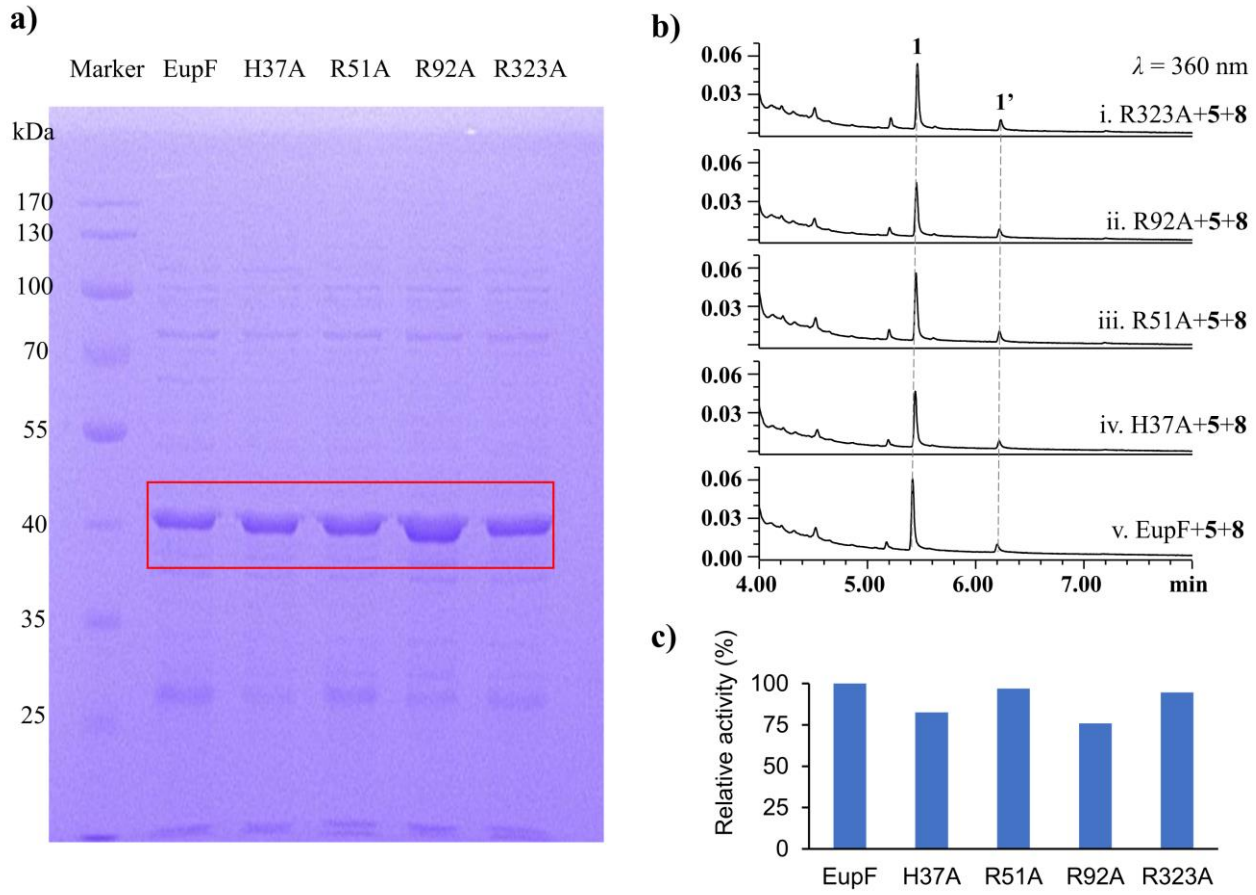

Figure S16. Site-specific mutagenesis experiments of EupF. a) SDS-PAGE gel (10%) of the purified mutants. **b)** *In vitro* assay of EupF and its mutants with **5** and **8** as substrates. **c)** Relative activity of EupF and its mutants in enzymatic reactions. Mutants of H37A, R51A, R92A, and R323A showed similar catalytic activity as the wild-type EupF, which suggested these amino acid residues might not be catalytic sites of EupF.

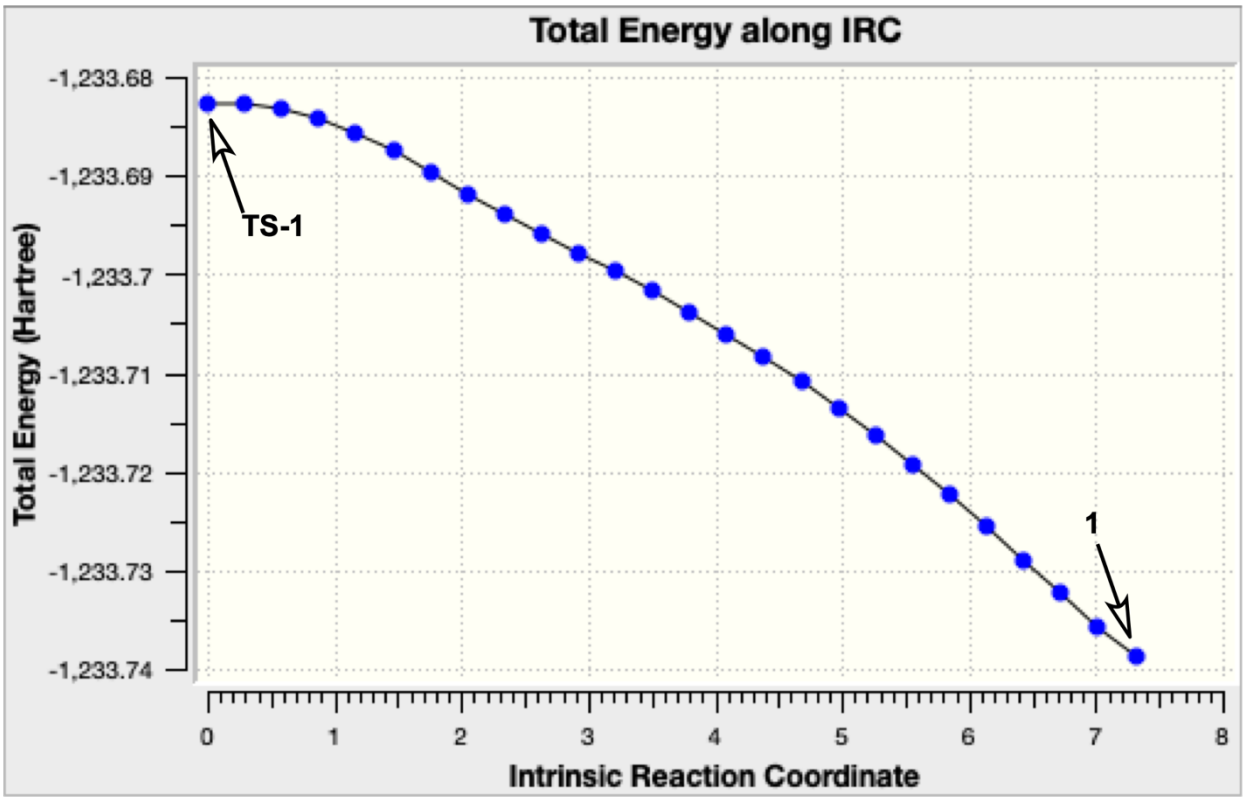

Figure S17. Computed intrinsic reaction coordinate connecting TS-1 to product 1 without intervening minima. The calculation was done at the PBE(0)-D3(BJ)/def2-TZVPP level of theory.

Coordinates of computed structures

TS-2 Eopt -1233.681891

C	0.503263	0.337787	-0.692665
C	0.356160	-0.943904	-0.211528
C	1.052707	-2.079570	-0.892667
C	2.386645	-2.182333	-0.195169
C	3.424340	-1.433518	-0.544030
H	2.422583	-2.795190	0.701306
C	-0.297814	-1.185266	1.097389
H	0.316570	-0.811125	1.923532
H	-1.245808	-0.635751	1.149131
H	-0.502258	-2.242458	1.257876
C	0.486636	1.537056	0.207736
H	0.304846	2.453612	-0.356419
H	-0.304577	1.463315	0.956862
C	4.694908	-1.204932	0.220807
C	5.869235	-1.128449	-0.752972
H	6.013990	-2.088880	-1.253115
H	6.794233	-0.876792	-0.227054
H	5.701025	-0.374924	-1.525789
C	4.964830	-2.287049	1.256176
H	4.167314	-2.342143	2.000793

H	5.057641	-3.267106	0.782850
H	5.896696	-2.076521	1.787043
C	4.523295	0.147161	0.972269
H	3.785397	-0.009990	1.761461
H	5.476957	0.367695	1.468432
C	4.149936	1.308775	0.110687
H	4.934814	1.647328	-0.564109
C	2.992847	1.975967	0.051408
C	1.813822	1.690731	0.950592
H	1.996175	0.764600	1.505905
O	1.620852	2.769132	1.859017
C	2.822331	3.123818	-0.897326
H	2.125883	2.873673	-1.704884
H	2.411936	3.997688	-0.384771
H	3.320879	-0.811166	-1.432070
H	1.136491	0.436965	-1.571756
H	1.193252	-1.849483	-1.950836
H	0.470750	-2.996760	-0.813699
H	3.772658	3.401935	-1.353937
H	2.465956	2.951187	2.279665
C	-2.662214	-1.150282	-0.873180
C	-3.784406	-1.762713	-0.203859
C	-3.243190	1.369389	-0.558106
C	-4.847967	-1.223529	0.423540
C	-4.406041	1.304080	0.154904
C	-5.186080	0.208040	0.631905
H	-3.732537	-2.846377	-0.214235
H	-4.868676	2.248368	0.421143
O	-6.229228	0.399033	1.268229
O	-5.761614	-2.012679	0.976171
H	-6.401598	-1.367953	1.363368
C	-2.790277	2.769646	-0.885791
H	-3.466644	3.502813	-0.450851
H	-2.768420	2.931384	-1.966738
H	-1.788870	2.970466	-0.502687
C	-2.447859	0.288120	-1.066154
C	-1.295384	0.543868	-1.810291
H	-1.046990	1.557346	-2.094188
H	-0.966560	-0.242885	-2.473673
O	-1.773942	-1.914266	-1.288494

TS-1 Eopt -1233.682632

C	-0.644829	-1.110587	0.595615
C	-0.364325	-0.267967	1.645092
C	0.051823	1.133980	1.316395
C	-1.230320	1.889779	1.079646

C	-1.830053	1.940072	-0.102036
H	-1.725827	2.281031	1.964112
C	-0.663838	-0.597439	3.060776
H	-1.677691	-0.261360	3.315058
H	-0.617397	-1.669337	3.251929
H	0.038290	-0.097284	3.726074
C	-1.630109	-2.236025	0.680680
H	-1.389556	-3.042540	-0.016695
H	-1.656546	-2.680394	1.676981
C	-3.234435	2.385967	-0.394304
C	-3.276526	3.073941	-1.757065
H	-2.686170	3.993014	-1.739296
H	-4.302664	3.335181	-2.029454
H	-2.867938	2.434179	-2.542606
C	-3.785429	3.330967	0.664650
H	-3.822210	2.859770	1.649569
H	-3.173161	4.232223	0.740496
H	-4.804064	3.631893	0.406981
C	-4.121794	1.107342	-0.401387
H	-4.180687	0.746263	0.627180
H	-5.134801	1.417382	-0.688606
C	-3.672807	0.024549	-1.326525
H	-3.758284	0.266198	-2.384994
C	-3.183996	-1.185858	-1.037397
C	-3.036846	-1.724566	0.366008
H	-3.269993	-0.934280	1.087960
O	-3.907323	-2.831555	0.564164
C	-2.786451	-2.127959	-2.133850
H	-1.700154	-2.264872	-2.168664
H	-3.222236	-3.117793	-1.977197
H	-1.307549	1.510928	-0.956057
H	-0.585688	-0.649556	-0.386988
H	0.660270	1.126648	0.406245
H	0.641460	1.569097	2.123038
H	-3.104260	-1.755450	-3.108055
H	-4.793192	-2.555402	0.312713
C	2.743498	-0.510095	1.227846
C	3.878068	0.380014	1.254064
C	2.584228	-0.998828	-1.322004
C	4.675000	0.828192	0.263700
C	3.591654	-0.227967	-1.827762
C	4.587146	0.579095	-1.200071
H	4.108090	0.735224	2.253111
H	3.707389	-0.217259	-2.906337
O	5.451912	1.158133	-1.868471
O	5.686228	1.640951	0.545096

H	6.075707	1.821397	-0.344375
C	1.760984	-1.722054	-2.356956
H	2.061700	-1.430188	-3.361373
H	1.878876	-2.805666	-2.272661
H	0.695917	-1.501154	-2.245878
C	2.233537	-1.217484	0.049870
C	1.205472	-2.100781	0.372929
H	0.790377	-2.748002	-0.386585
H	1.173483	-2.466671	1.389709
O	2.125506	-0.672646	2.293858

8 Eopt -660.695367

C	1.500247	1.323546	-0.876744
C	0.739351	2.284526	-0.353637
C	-0.577203	2.631094	-1.009630
C	-1.608809	1.755673	-0.333760
C	-1.682680	0.463739	-0.621474
H	-2.157138	2.173532	0.505879
C	0.964424	2.908707	0.984695
H	0.141781	2.663211	1.665999
H	1.894780	2.590409	1.452889
H	0.981416	3.999970	0.897618
C	2.555352	0.549839	-0.159099
H	3.295928	0.138780	-0.849191
H	3.103356	1.158667	0.562874
C	-2.312113	-0.641188	0.169849
C	-3.093399	-1.569473	-0.758720
H	-3.953994	-1.046348	-1.182099
H	-3.460707	-2.445142	-0.215760
H	-2.476978	-1.917784	-1.590222
C	-3.230913	-0.132378	1.269701
H	-2.692649	0.498915	1.980878
H	-4.055288	0.450903	0.852455
H	-3.657464	-0.971067	1.826018
C	-1.132276	-1.408198	0.842587
H	-0.684558	-0.736937	1.578188
H	-1.570650	-2.247394	1.398736
C	-0.100929	-1.942926	-0.097946
H	-0.464890	-2.718487	-0.770654
C	1.184944	-1.603633	-0.241209
C	1.904508	-0.596036	0.624034
H	1.193198	-0.141186	1.321993
O	2.949531	-1.232848	1.352371
C	2.030994	-2.264822	-1.287564
H	2.286178	-1.562142	-2.087801
H	2.975493	-2.615773	-0.864843

H	-1.078350	0.107133	-1.454714
H	1.209455	0.933063	-1.849789
H	-0.532259	2.402772	-2.076928
H	-0.818903	3.691873	-0.900536
H	1.511386	-3.110656	-1.739218
H	2.565619	-1.984347	1.812750

1 Eopt -1233.743197

C	0.269548	0.945860	0.636967
C	-0.044692	-0.132992	1.676889
C	1.120555	-1.071186	1.986702
C	1.812173	-1.577579	0.767778
C	3.128261	-1.549530	0.621877
H	1.176304	-1.928280	-0.039885
C	-0.620503	0.417185	2.971753
H	-0.783981	-0.399768	3.676552
H	0.063085	1.133295	3.430396
H	-1.576768	0.913685	2.803585
C	1.378258	1.943984	0.987340
H	1.066106	2.937985	0.653413
H	1.504175	2.032507	2.069604
C	3.930749	-1.810816	-0.613862
C	3.112515	-2.426814	-1.737323
H	2.273143	-1.788544	-2.019753
H	2.716246	-3.400143	-1.438727
H	3.735265	-2.573593	-2.623679
C	5.107048	-2.721857	-0.267104
H	5.723371	-2.284312	0.523361
H	4.753632	-3.694876	0.081741
H	5.743572	-2.882394	-1.141435
C	4.501121	-0.428563	-1.043116
H	4.977879	0.020333	-0.165772
H	5.305619	-0.613382	-1.763346
C	3.528610	0.519467	-1.674360
H	3.459482	0.442548	-2.757903
C	2.766639	1.456096	-1.100750
C	2.763574	1.718127	0.385128
H	3.251064	0.884681	0.893574
O	3.472275	2.925593	0.670089
C	1.930273	2.374129	-1.938493
H	2.147209	2.245992	-2.999393
H	0.861261	2.196185	-1.792474
H	3.726089	-1.198581	1.465196
H	0.560159	0.404127	-0.269332
H	0.697904	-1.895845	2.571976
H	1.833468	-0.551906	2.633234

H	2.119213	3.416983	-1.669031
H	4.341080	2.852463	0.265787
C	-2.120319	-0.507550	0.475540
C	-3.046663	-1.569387	0.284070
C	-3.386119	1.414850	-0.449318
C	-4.279598	-1.623016	-0.275148
C	-4.563305	0.833558	-0.827222
C	-5.073481	-0.513481	-0.842328
H	-2.655513	-2.510200	0.667362
H	-5.310388	1.504121	-1.240475
O	-6.177415	-0.758042	-1.309709
O	-4.939854	-2.785523	-0.345998
H	-4.396747	-3.484421	0.033220
C	-3.315538	2.904131	-0.674431
H	-4.282448	3.291825	-0.988657
H	-3.010084	3.435656	0.230039
H	-2.586461	3.155050	-1.450495
C	-2.217261	0.815108	0.121820
C	-1.020496	1.696863	0.347356
H	-0.860373	2.319921	-0.535399
H	-1.212201	2.406232	1.163418
O	-1.021061	-1.010386	1.087457

6				Eopt	-572.985275
C	-0.685204	-1.484270	0.172125		
C	0.755367	-1.551331	0.020203		
C	-1.074025	1.126424	0.079360		
C	1.667182	-0.568814	-0.080844		
C	0.193202	1.577231	0.178205		
C	1.463871	0.909319	0.015340		
H	1.132696	-2.568162	0.034304		
H	0.336201	2.641410	0.334018		
O	2.495056	1.572260	-0.027569		
O	2.952492	-0.868798	-0.215369		
H	3.405662	0.002640	-0.209932		
C	-2.165146	2.151259	0.188504		
H	-1.761477	3.114212	0.496629		
H	-2.663263	2.293640	-0.774715		
H	-2.926988	1.840094	0.906004		
C	-1.501330	-0.254486	-0.135242		
C	-2.722291	-0.518130	-0.620477		
H	-3.424145	0.260452	-0.886364		
H	-3.023263	-1.546872	-0.770254		
O	-1.280694	-2.498542	0.488846		

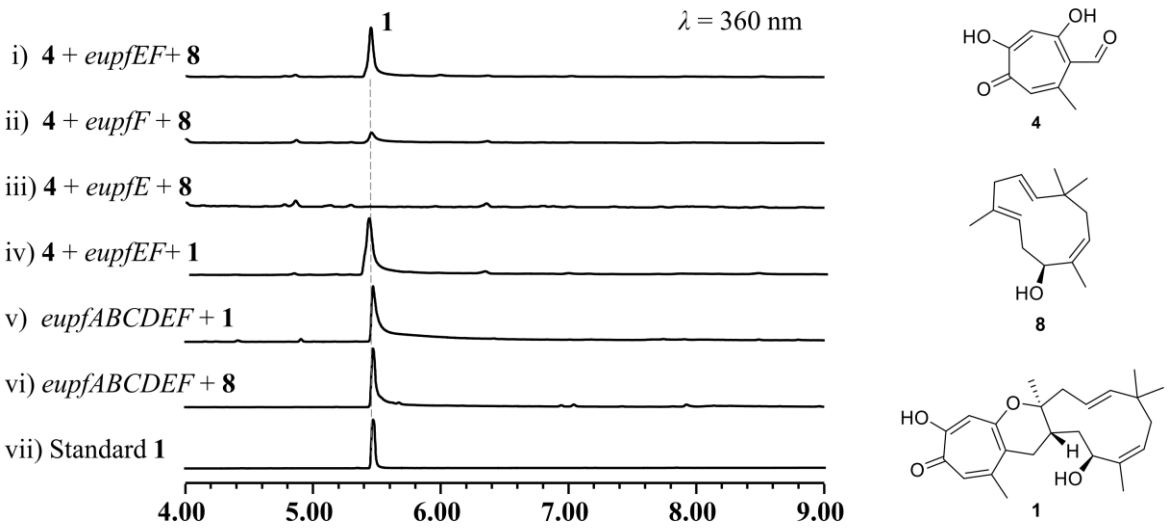

Figure S18. Feeding experiments of compounds 1, 4 and 8 to *A. nidulans* mutants. 3 was not detected in all these feeding experiments, suggesting other or additional enzymes were required for the right side DA reaction in the biosynthesis of **3**.

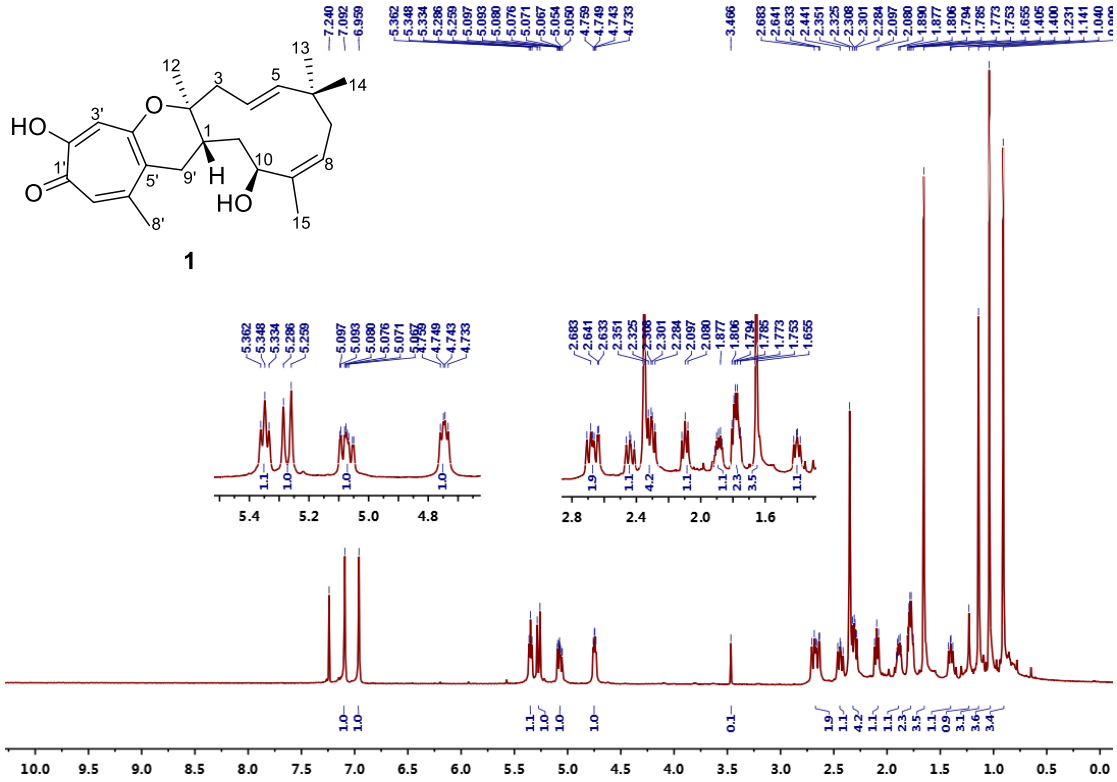

Figure S19. ^{1}H NMR (600MHz) spectrum of **1** in $CDCl_3$.

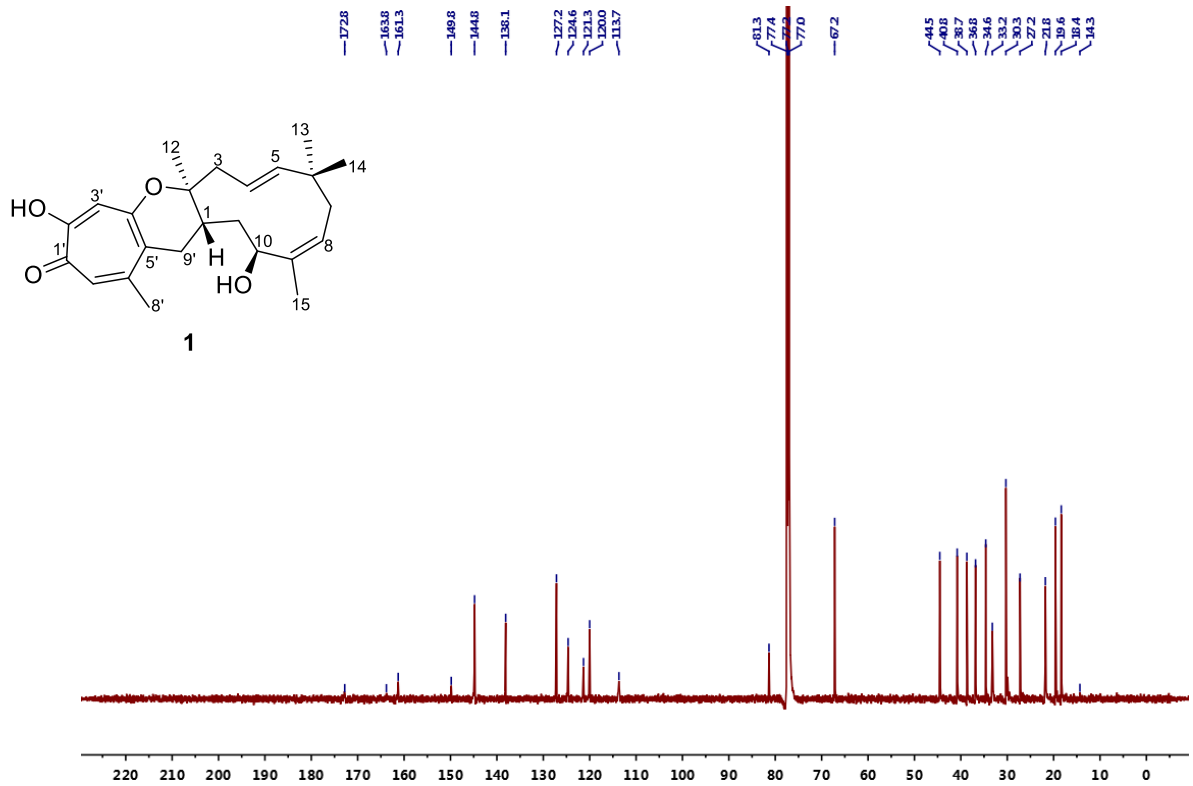

Figure S20. ^{13}C NMR (150MHz) spectrum of **1** in $CDCl_3$.

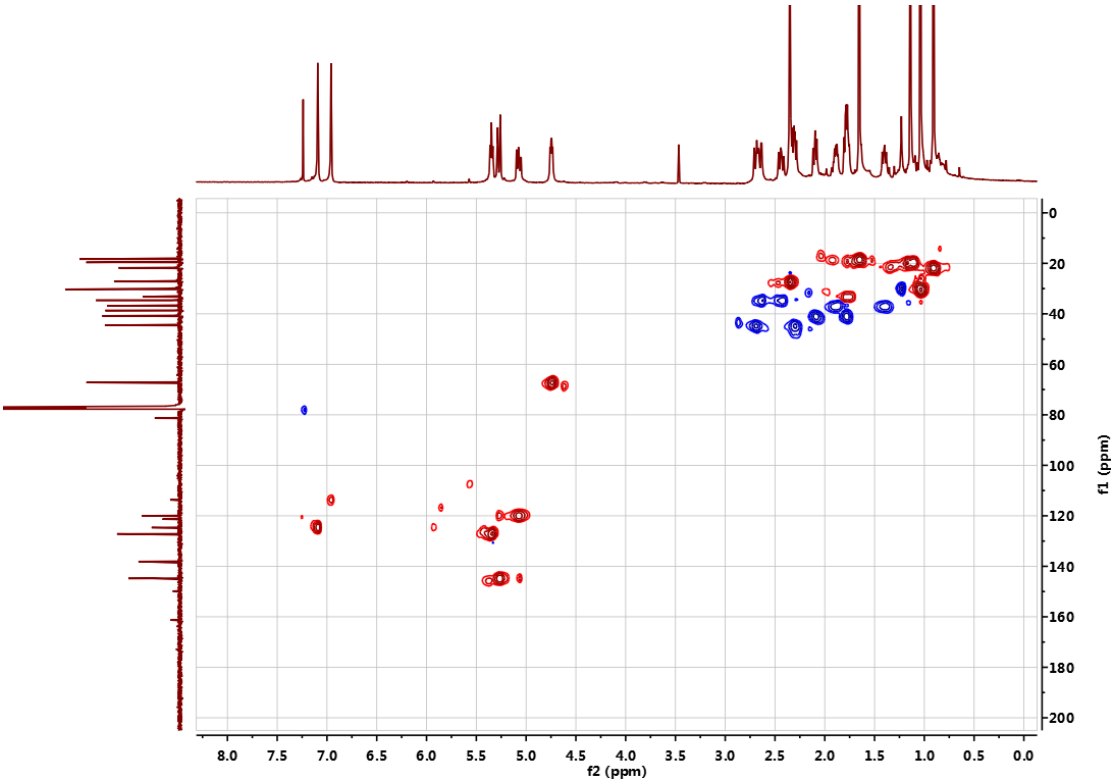

Figure S21. HSQC (600MHz) spectrum of **1** in $CDCl_3$.

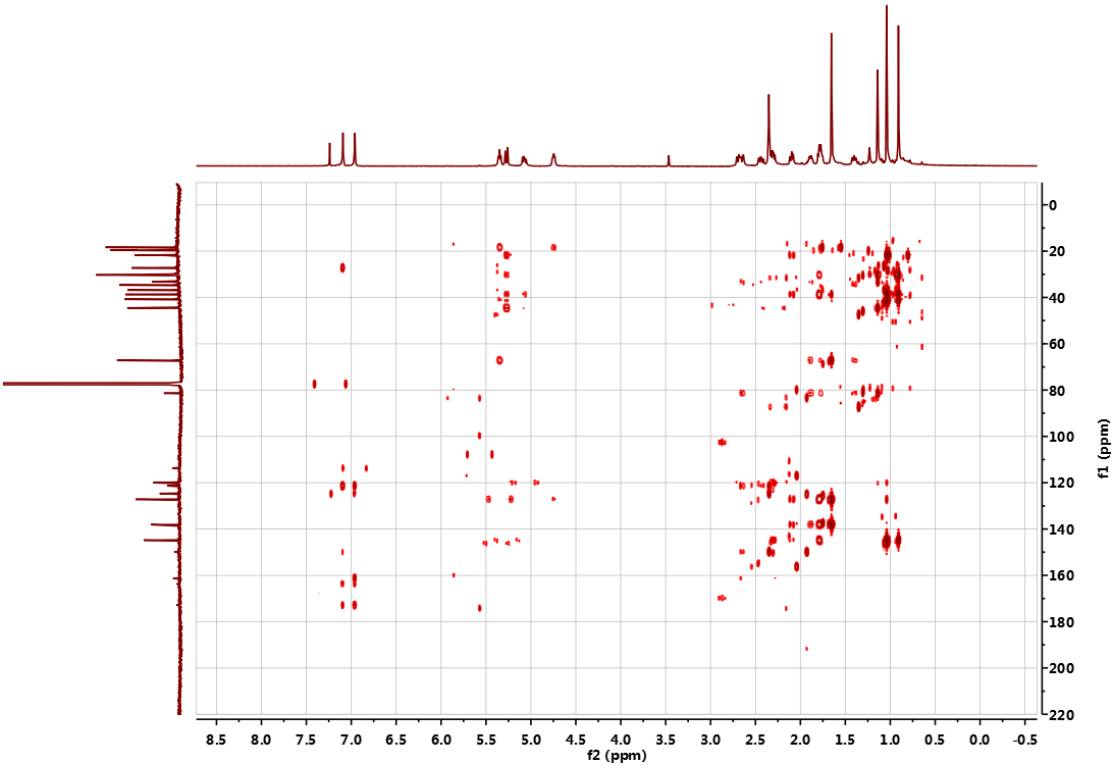

Figure S22. HMBC (600MHz) spectrum of **1** in $CDCl_3$.

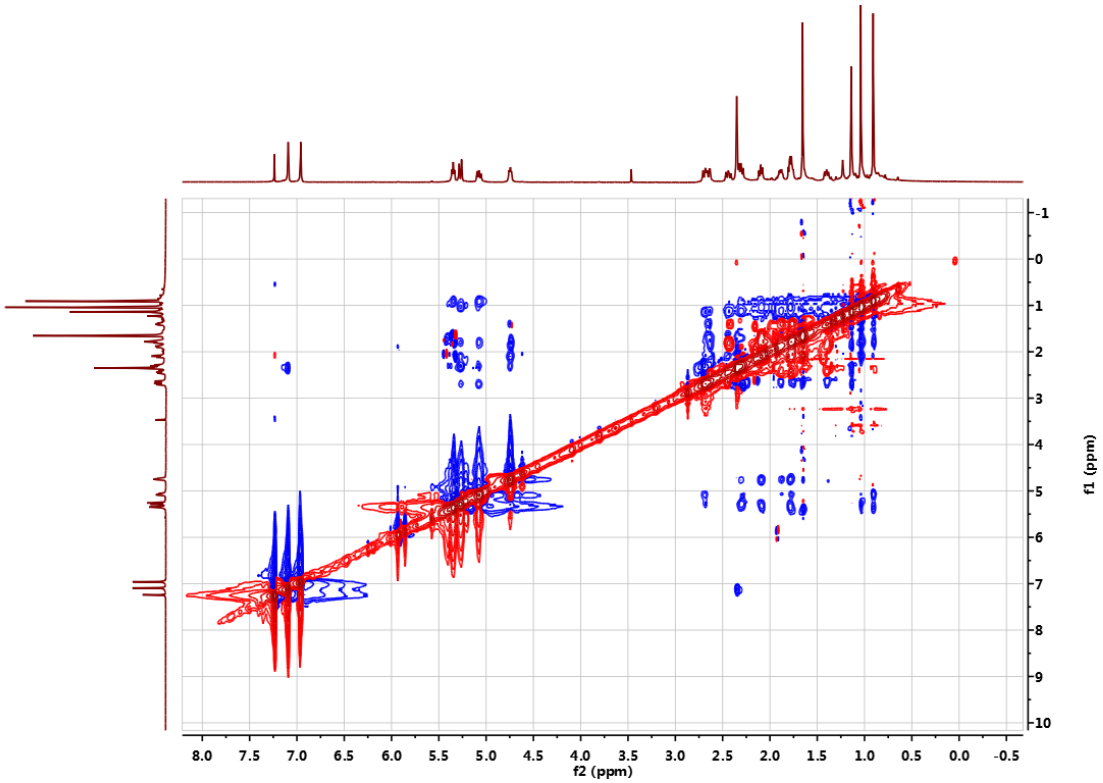

Figure S23. NOESY (600MHz) spectrum of **1** in $CDCl_3$.

Thermo Qexactive Focus Report

compound NO. : CUP-13
Method : LCMS(compound)-low

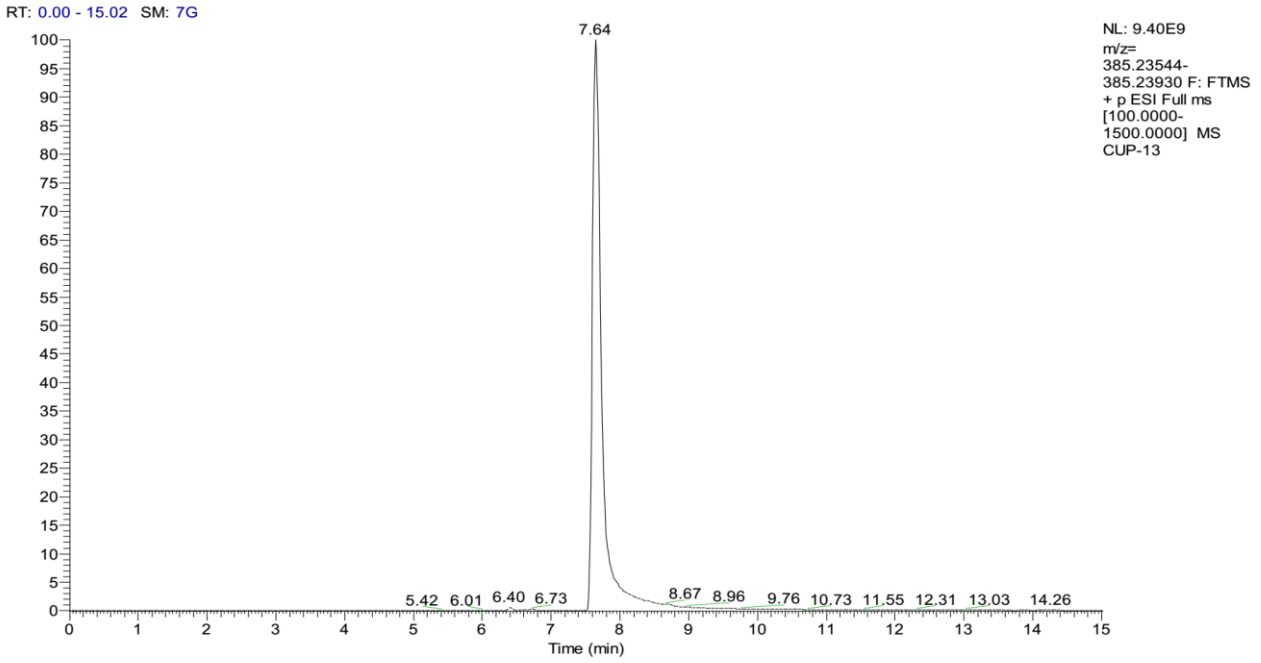

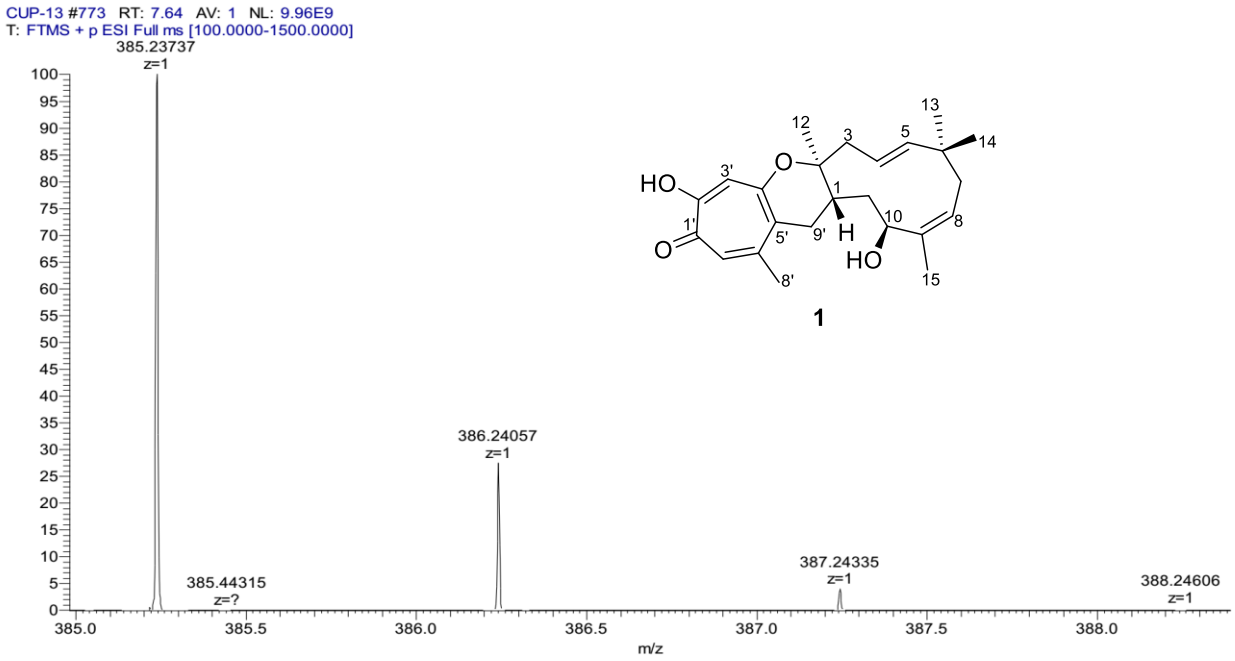

1

m/z	Theo. Mass	Delta (ppm)	RDB equiv.	Composition	
385.23737	385.23734	0.09	8.5	C24 H33 O4	M+H

Figure S24. HRESIMS data of **1**.

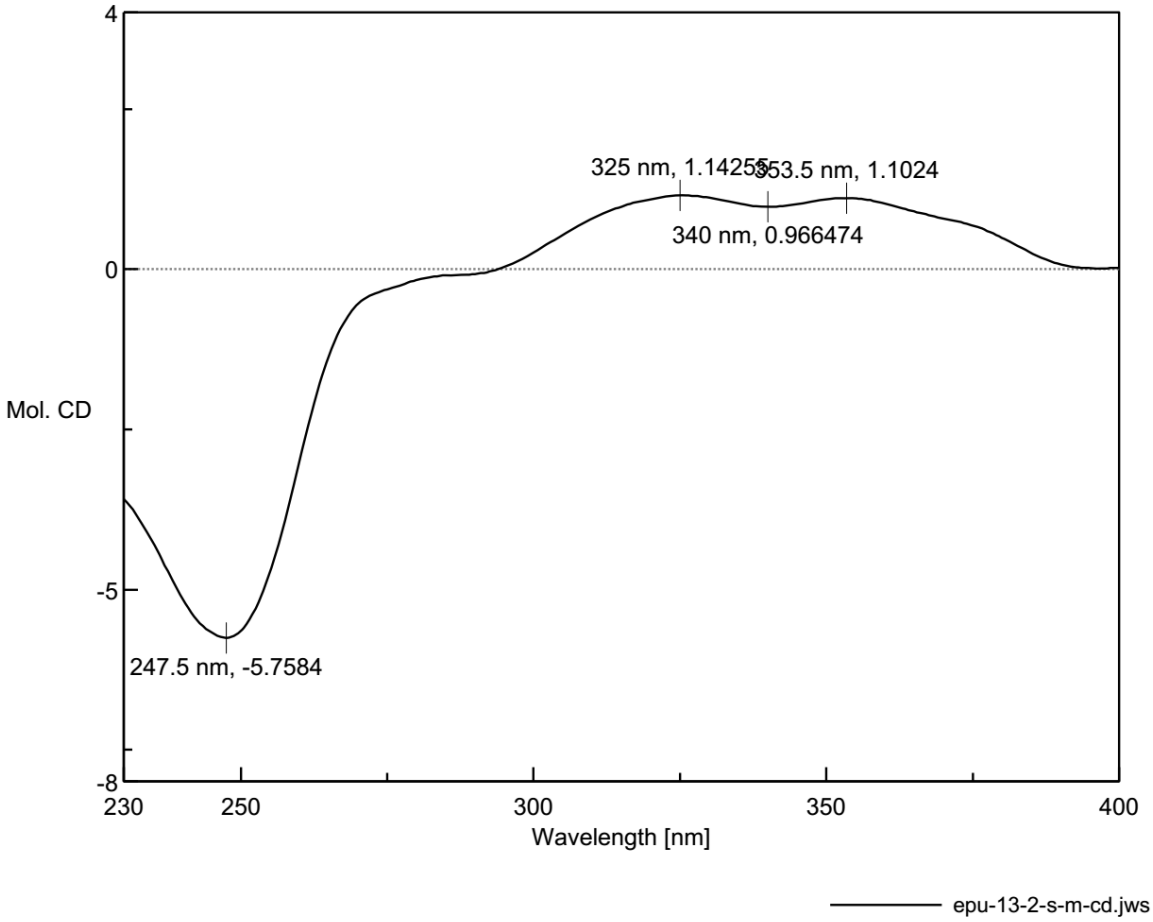

[Measurement Information]	
Instrument Name	J-815
Model Name	J-815
Serial No.	A024461168
Accessory	Standard
Accessory S/N	A024461168
Cell Length	1 mm
Measurement date	2019/6/11 15:23
Photometric Mode	CD, HT, Abs
Measure Range	400 - 230 nm
Data pitch	0.5 nm
Sensitivity	Standard
D.I.T.	1 sec
Bandwidth	2.00 nm
Start Mode	Immediately
Scanning Speed	100 nm/min
Baseline Correction	Baseline
Shutter Control	Auto
CD Detector	PMT
PMT Voltage	Auto
Accumulations	2
Solvent	CHCl3
Concentration	0.1 (w/v)%

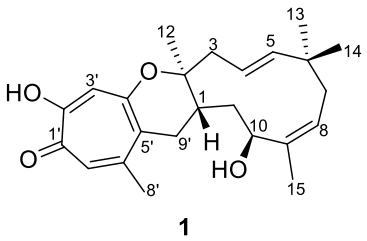

1

Figure S25. CD spectrum of **1** in $CDCl_3$.

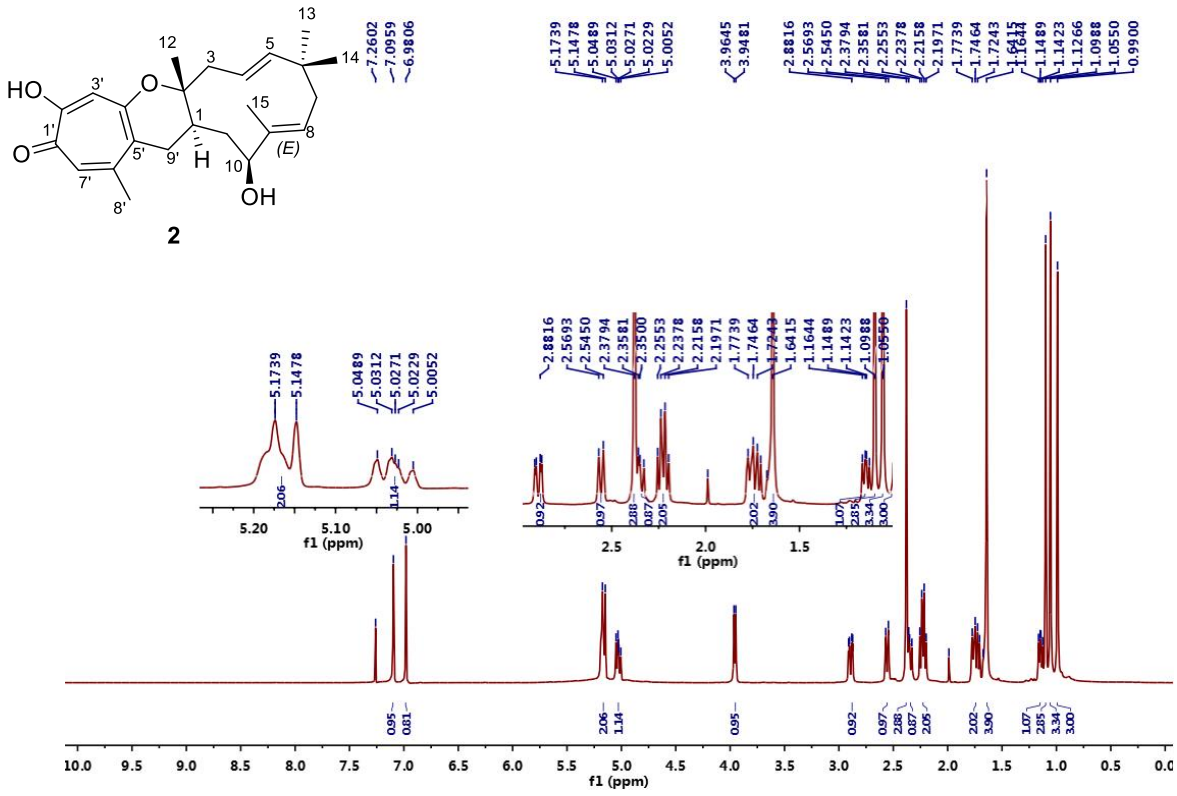

Figure S26. ^{1}H NMR (600MHz) spectrum of **2** in $CDCl_3$.

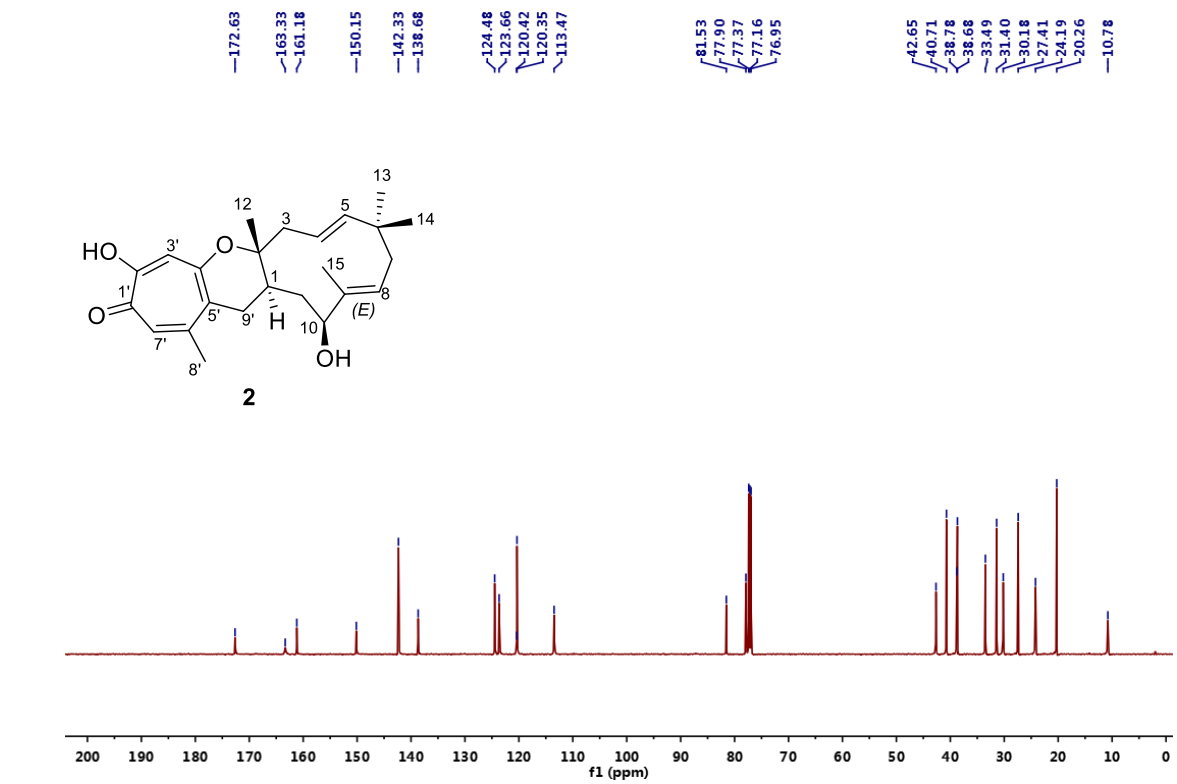

Figure S27. ^{13}C NMR (150MHz) spectrum of **2** in $CDCl_3$.

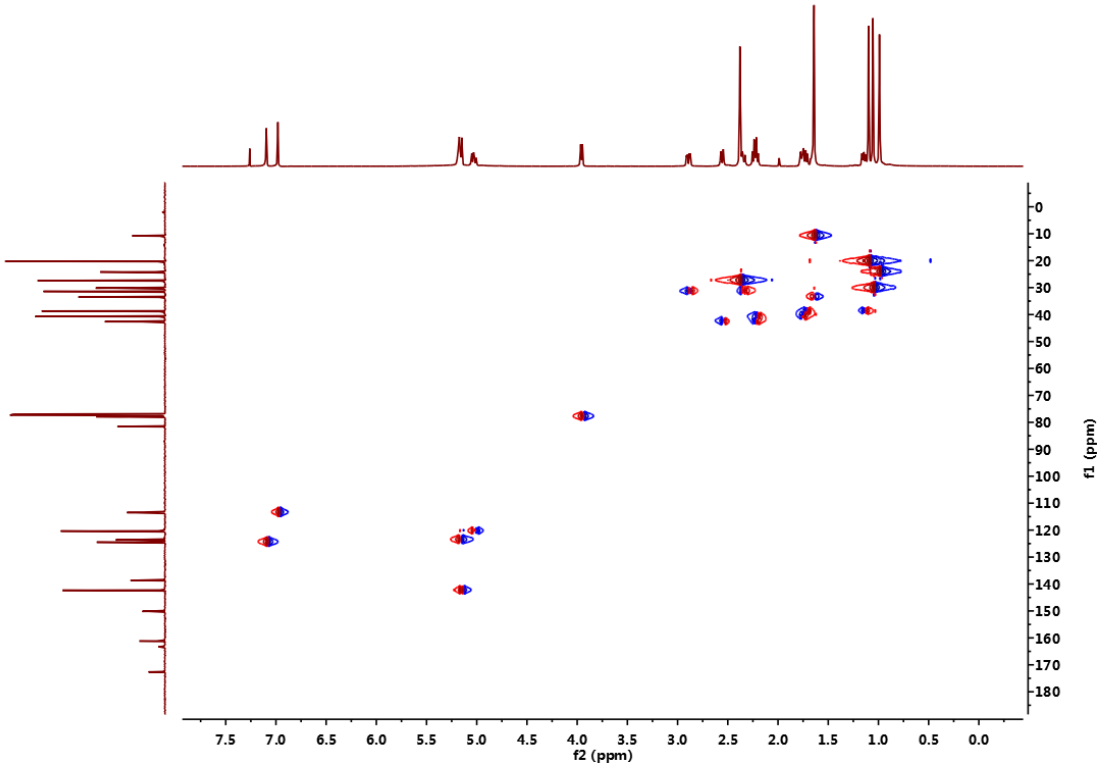

Figure S28. HSQC (600MHz) spectrum of **2** in $CDCl_3$.

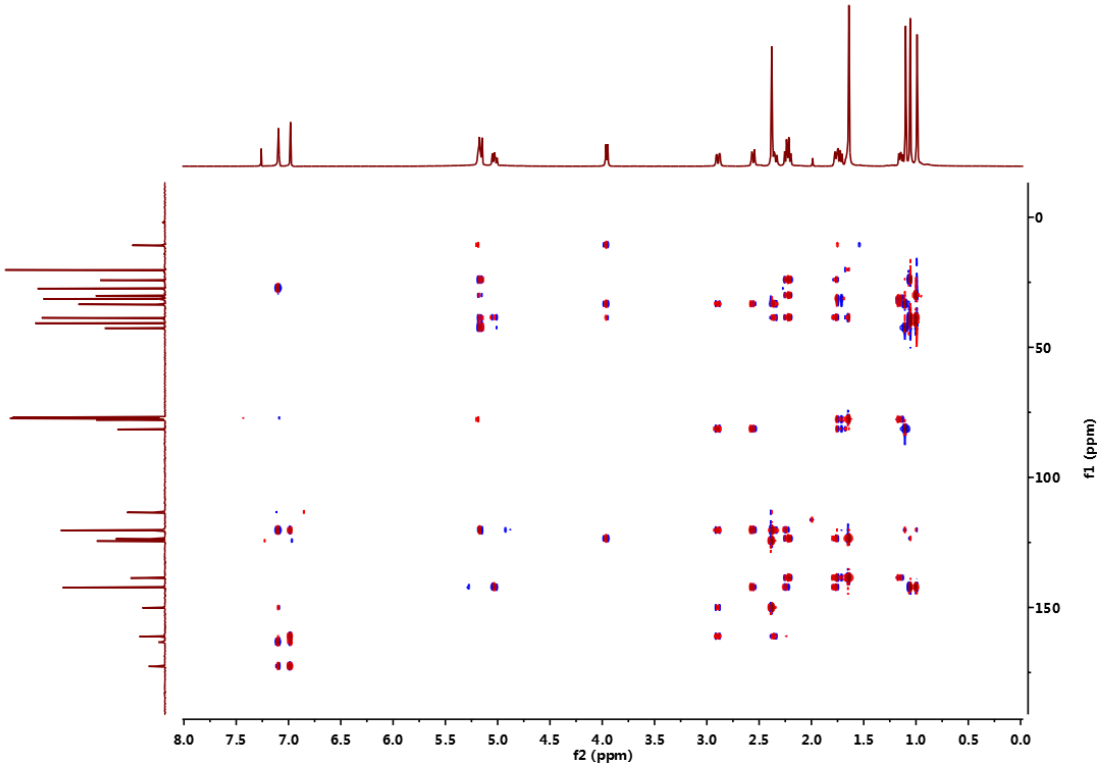

Figure S29. HMBC (600MHz) spectrum of **2** in $CDCl_3$.

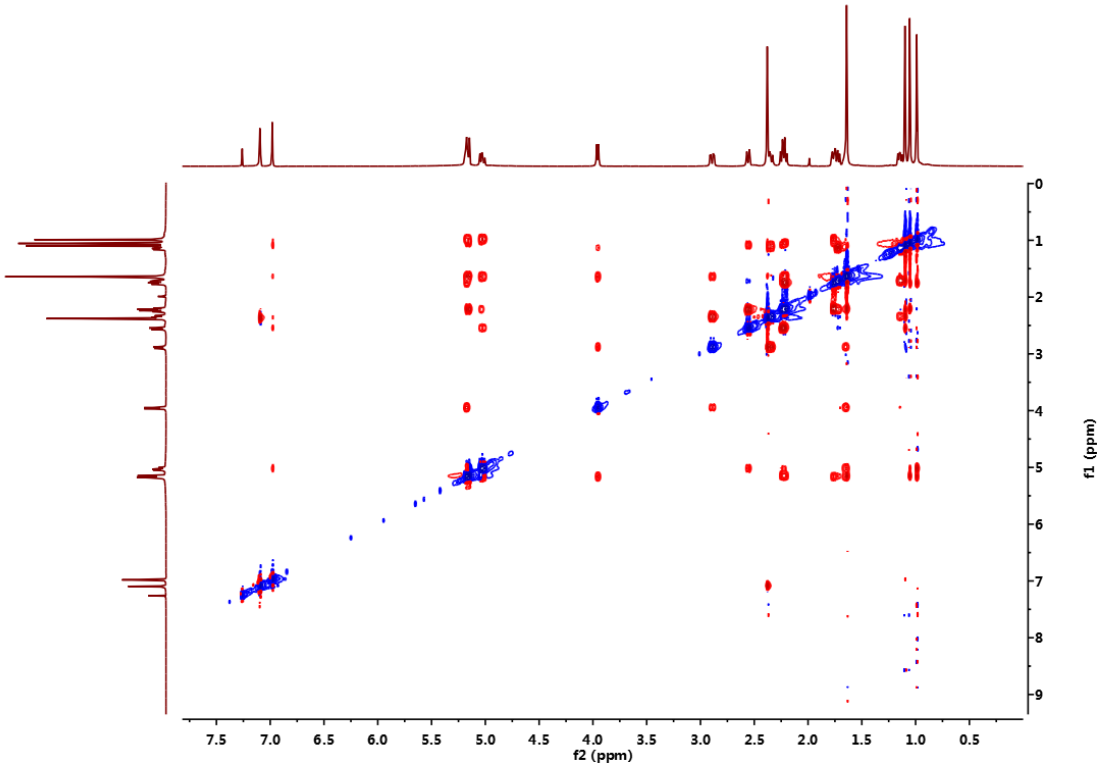

Figure S30. NOESY (600MHz) spectrum of **2** in $CDCl_3$.

Thermo Qexactive Focus Report

compound NO. : hum-jy-9
Method : LCMS(compound)-low

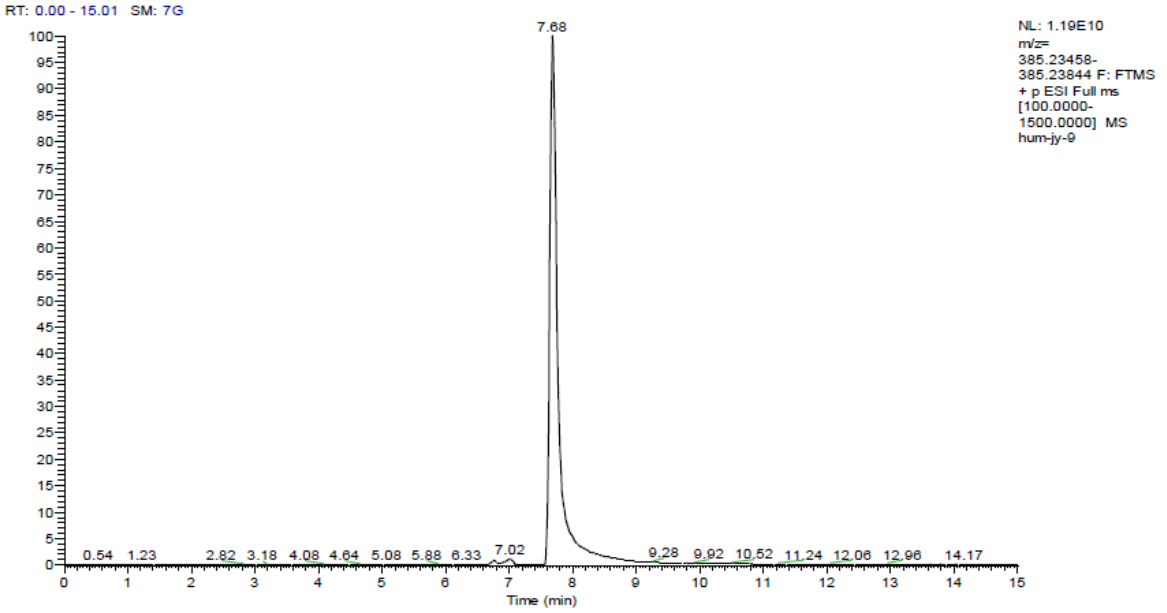

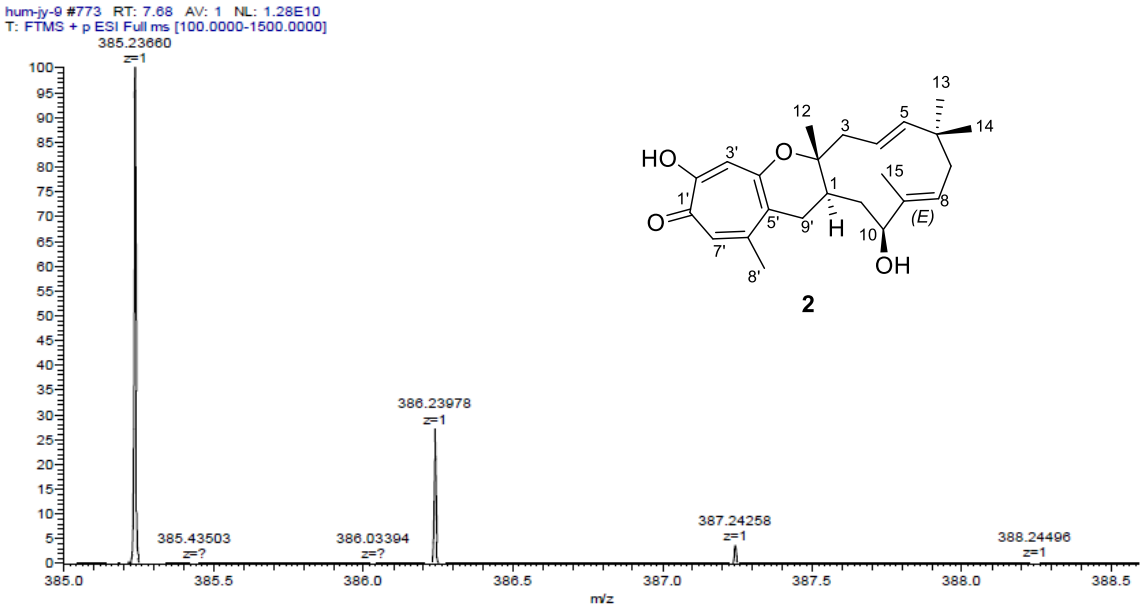

2

m/z	Theo. Mass	Delta (ppm)	RDB equiv.	Composition	
385.23660	385.23734	-1.91	8.5	C24 H33 O4	M+H

Figure S31. HRESIMS spectrum of **2**.

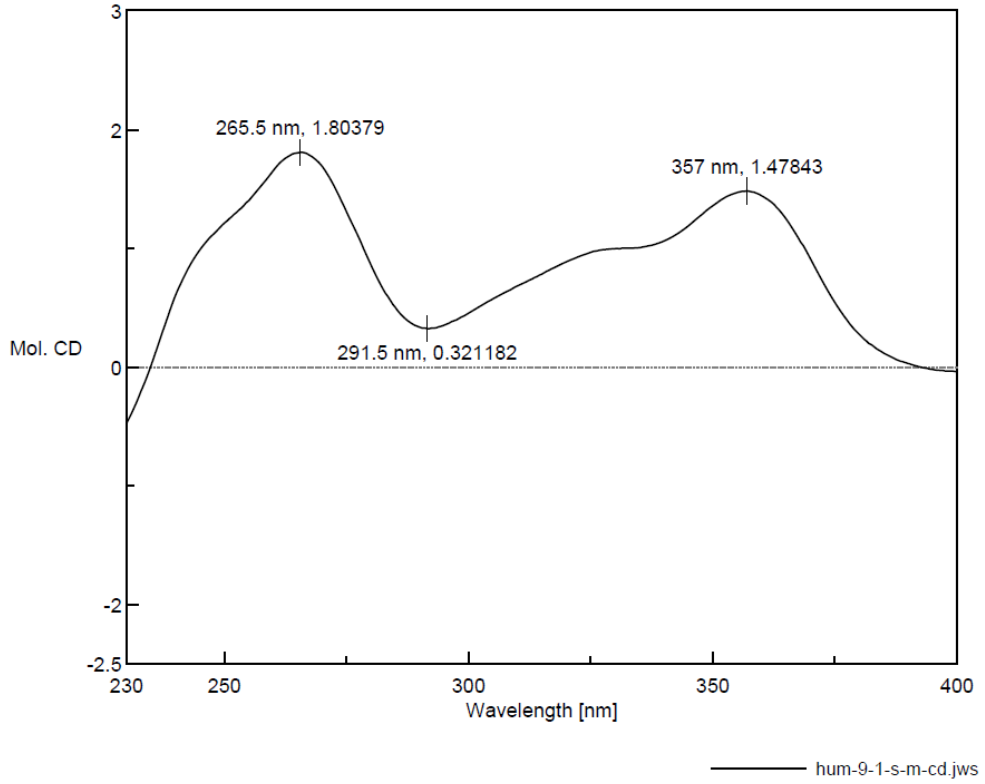

[Measurement Information]

Instrument Name	J-815
Model Name	J-815
Serial No.	A024461168
Accessory	Standard
Accessory S/N	A024461168
Cell Length	1 mm
Measurement date	2019/6/6 15:11
Photometric Mode	CD, HT, Abs
Measure Range	400 - 230 nm
Data pitch	0.5 nm
Sensitivity	Standard
D.I.T.	1 sec
Bandwidth	2.00 nm
Start Mode	Immediately
Scanning Speed	100 nm/min
Baseline Correction	Baseline
Shutter Control	Auto
CD Detector	PMT
PMT Voltage	Auto
Accumulations	2
Solvent	CHCl3
Concentration	0.2 (w/v)%

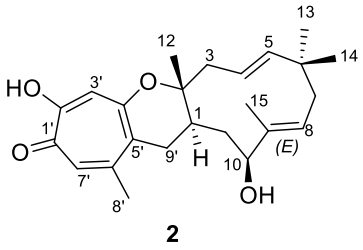

2

Figure S32. CD spectrum of **2** in $CDCl_3$.

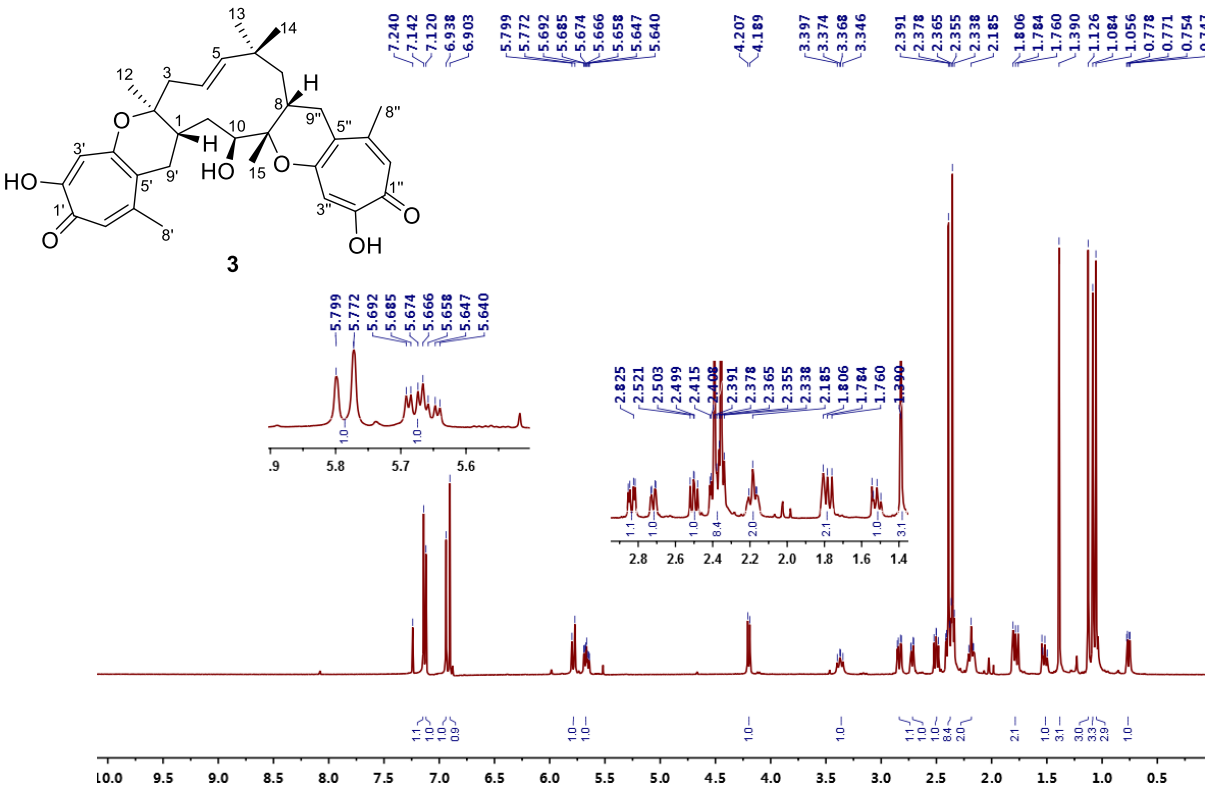

Figure S33. ^{1}H NMR (600MHz) spectrum of **3** in $CDCl_3$.

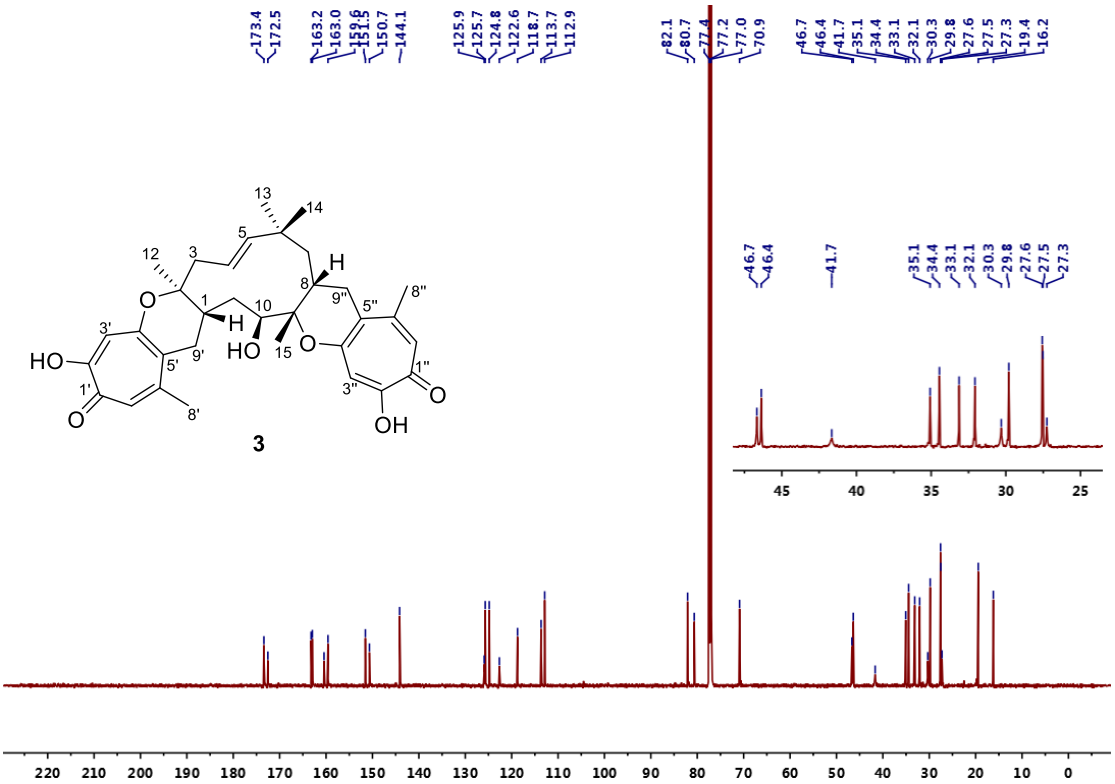

Figure S34. ^{13}C NMR (150MHz) spectrum of **3** in $CDCl_3$.

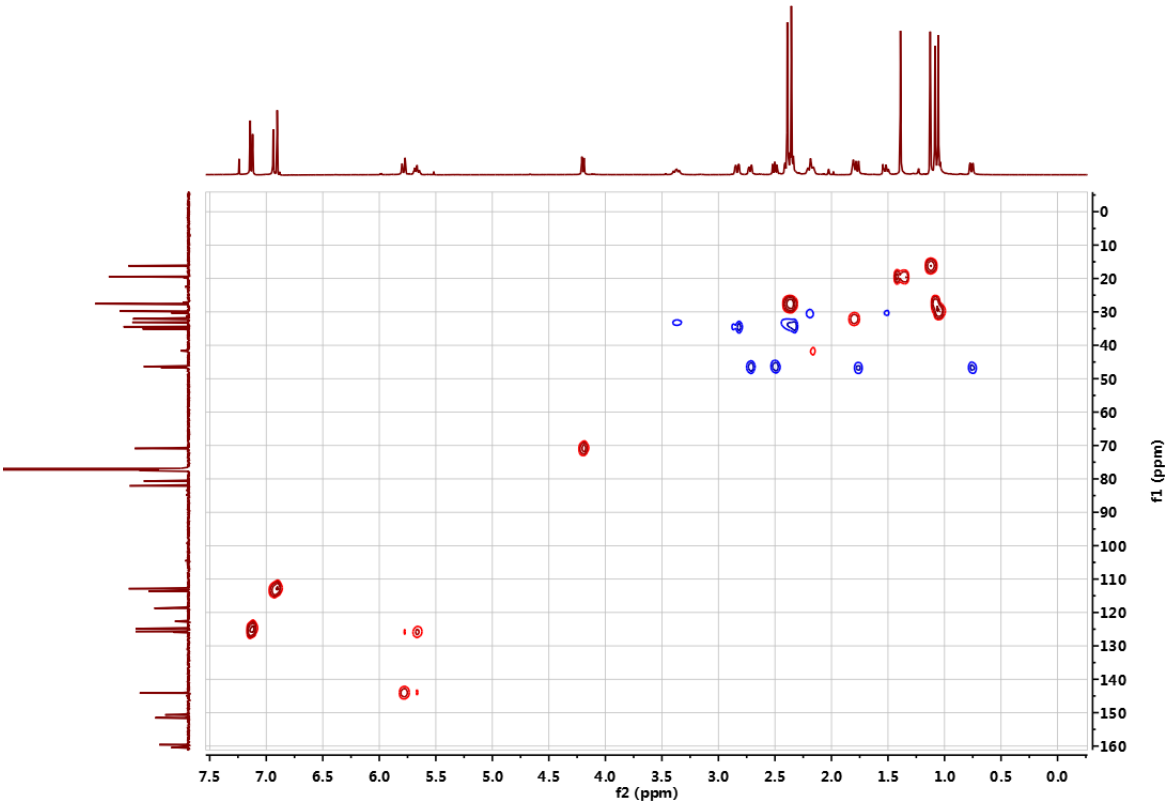

Figure S35. HSQC (600MHz) spectrum of **3** in $CDCl_3$.

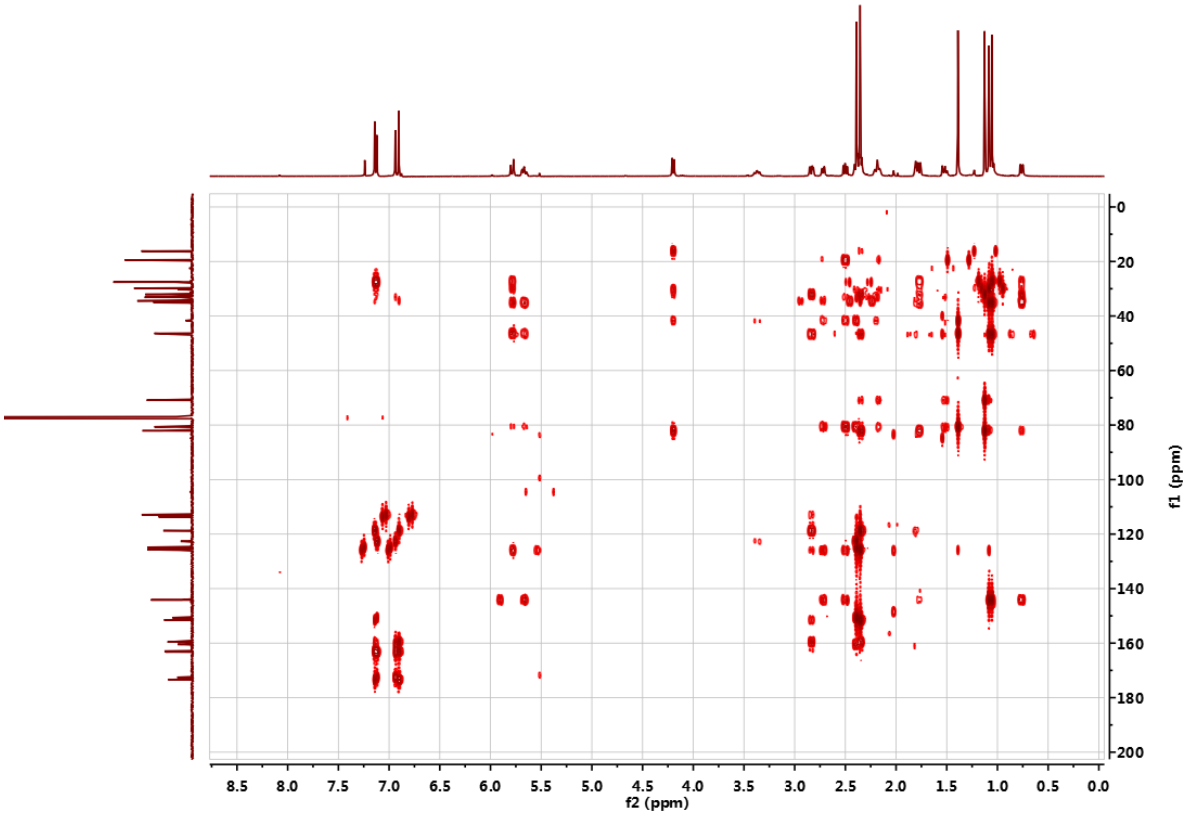

Figure S36. HMBC (600MHz) spectrum of **3** in $CDCl_3$.

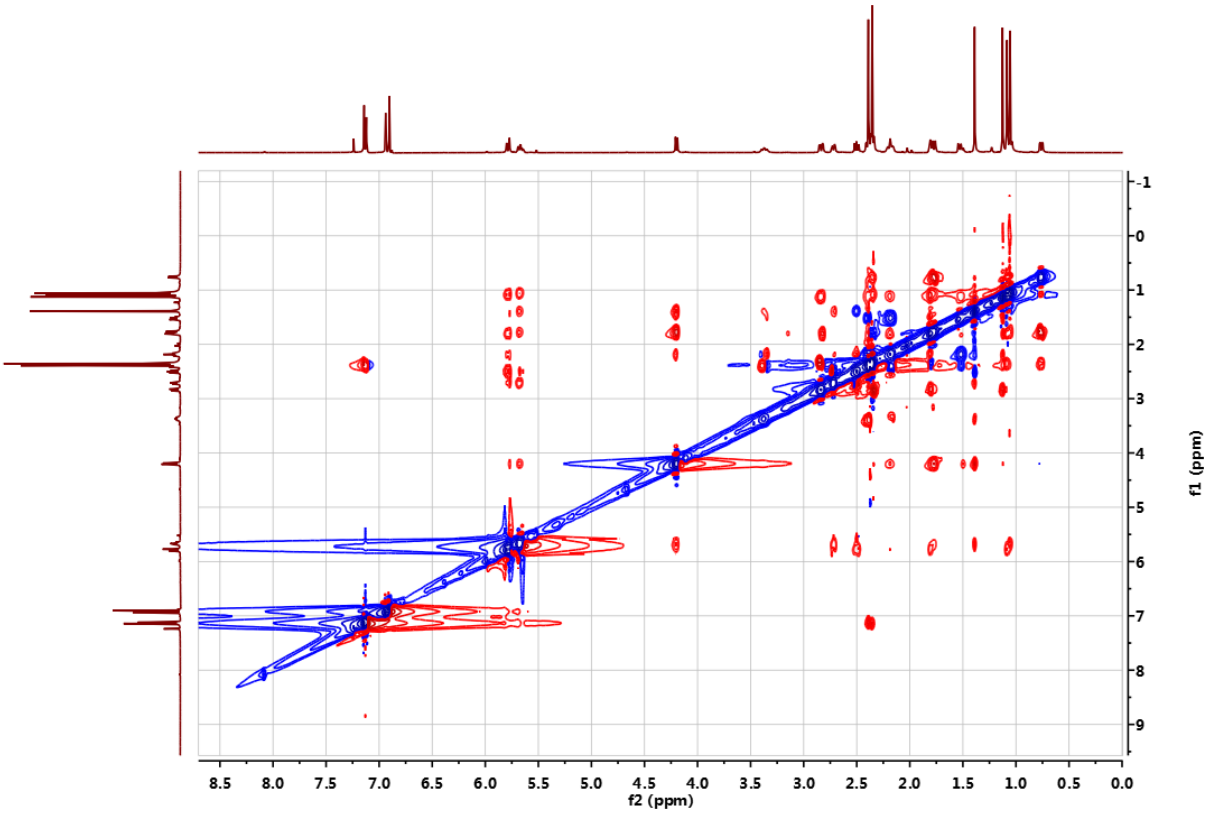

Figure S37. NOESY (600MHz) spectrum of **3** in $CDCl_3$.

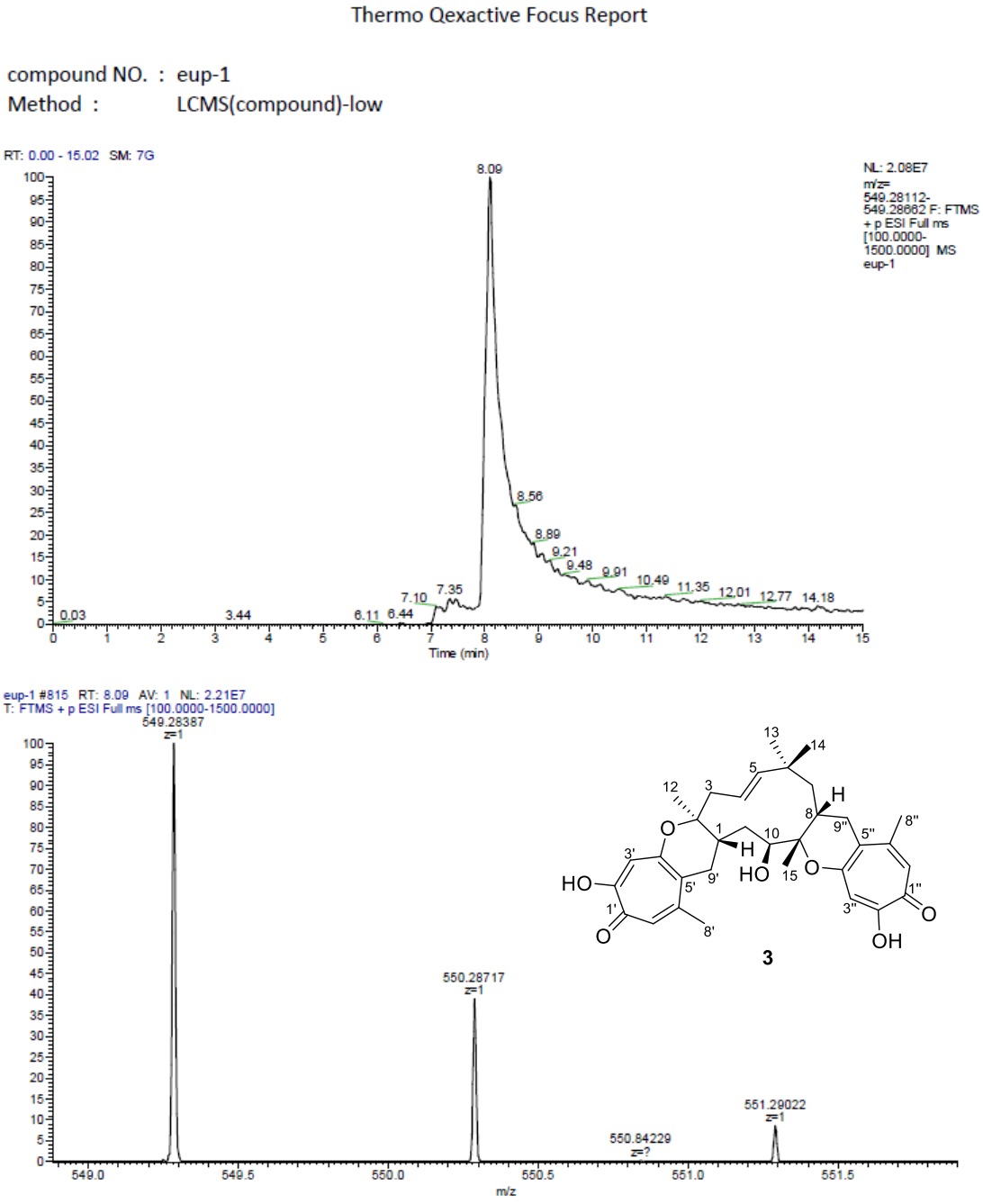

m/z	Theo. Mass	Delta (ppm)	RDB equiv.	Composition	
549.28387	549.28468	-1.47	13.5	C33 H41 O7	M+H

Figure S38. HRESIMS spectrum of **3**.

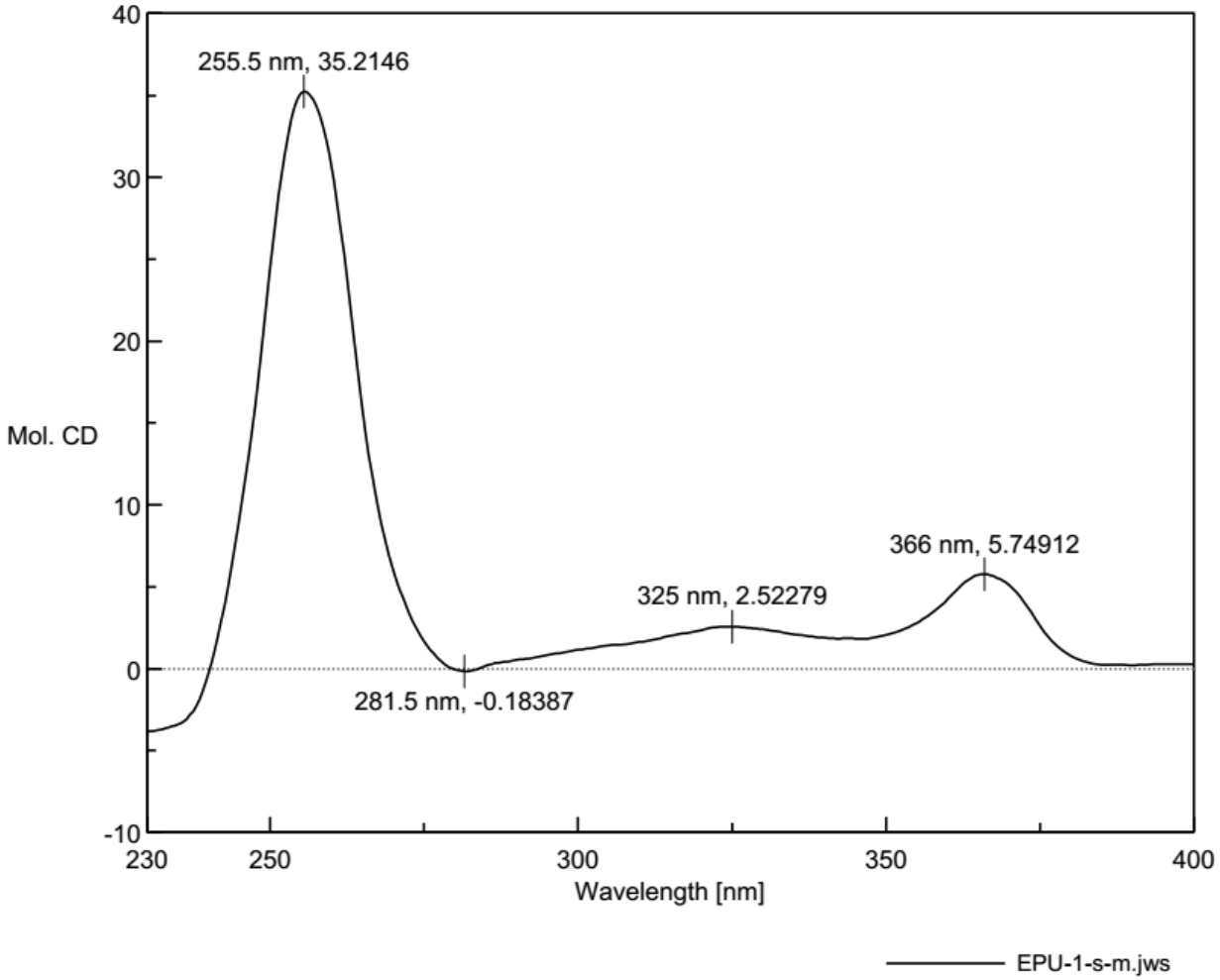

[Measurement Information]	
Instrument Name	J-815
Model Name	J-815
Serial No.	A024461168
Accessory	Standard
Accessory S/N	A024461168
Cell Length	1 mm
Measurement date	2019/5/23 9:06
Photometric Mode	CD, HT, Abs
Measure Range	400 - 230 nm
Data pitch	0.5 nm
Sensitivity	Standard
D.I.T.	1 sec
Bandwidth	2.00 nm
Start Mode	Immediately
Scanning Speed	100 nm/min
Baseline Correction	Baseline
Shutter Control	Auto
CD Detector	PMT
PMT Voltage	Auto
Accumulations	2
Solvent	CHCl3
Concentration	0.1 (w/v)%

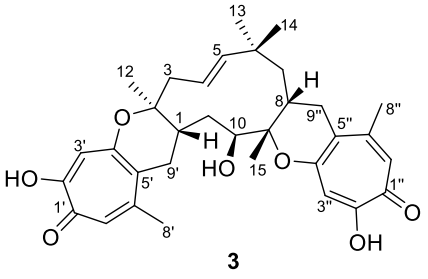

3

Figure S39. CD spectrum of **3** in $CDCl_3$.

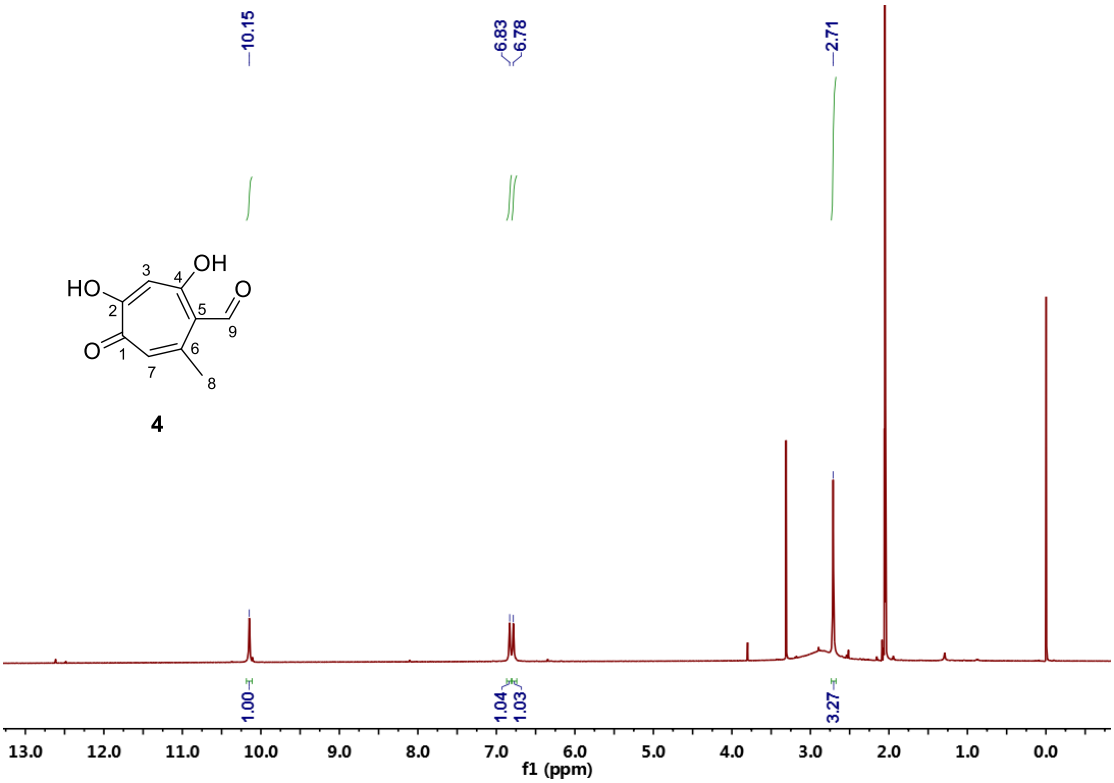

Figure S40. ^{1}H NMR (600MHz) spectrum of **4** in acetone-d_6.

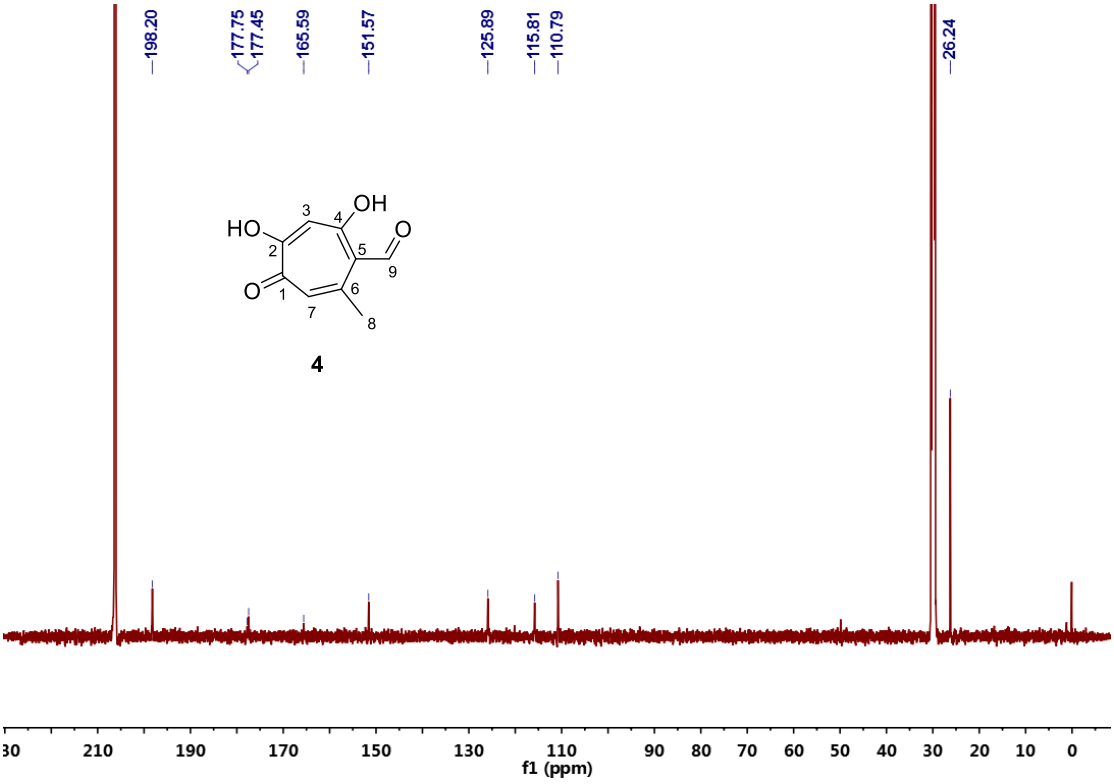

Figure S41. ^{13}C NMR (150MHz) spectrum of **4** in acetone-d_6.

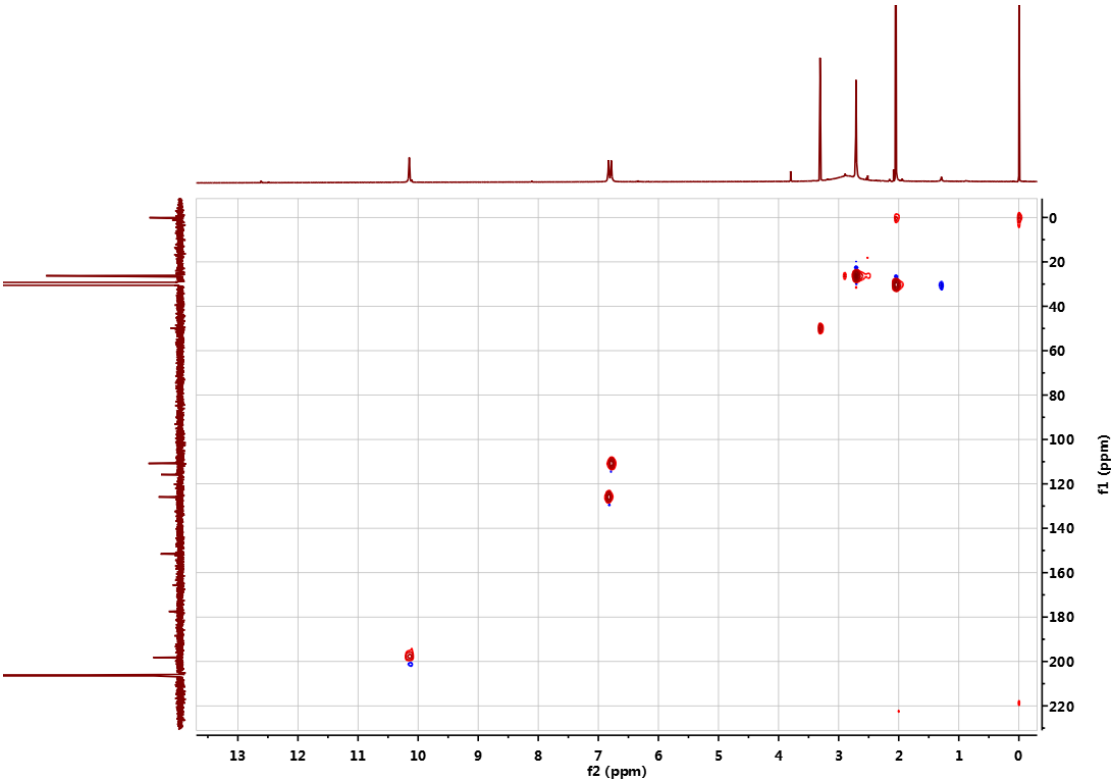

Figure S42. HSQC (600MHz) spectrum of **4** in acetone-d_6.

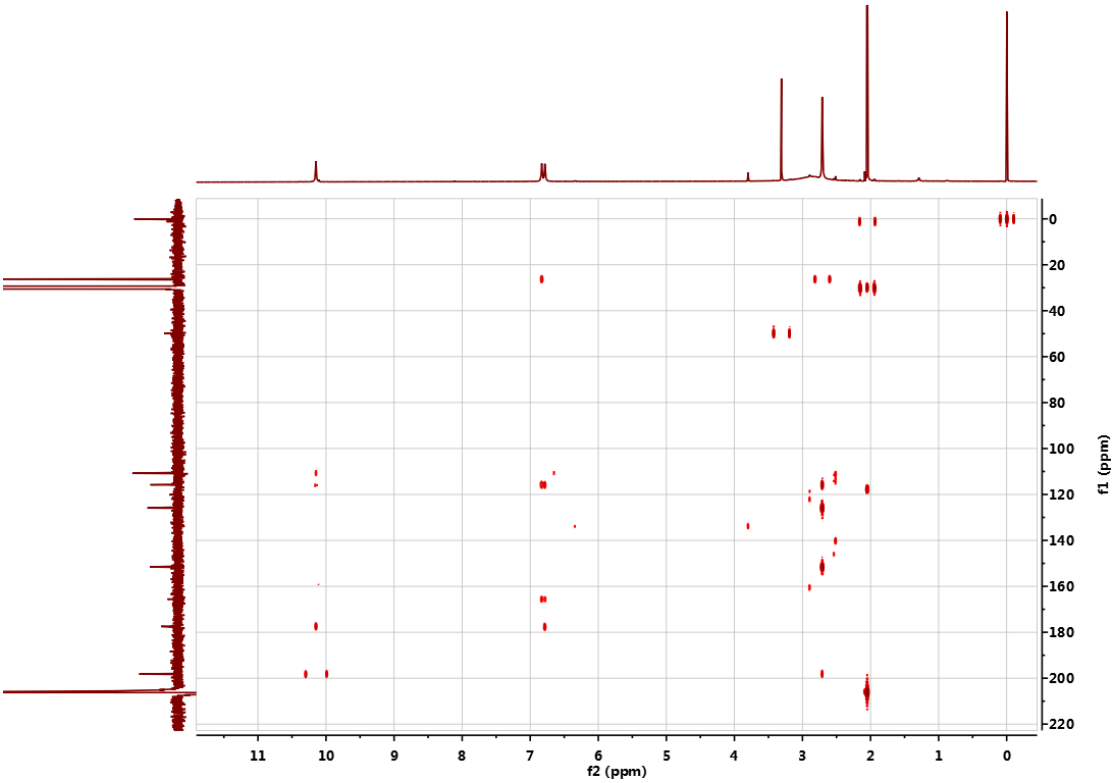

Figure S43. HMBC (600MHz) spectrum of **4** in acetone-d_6.

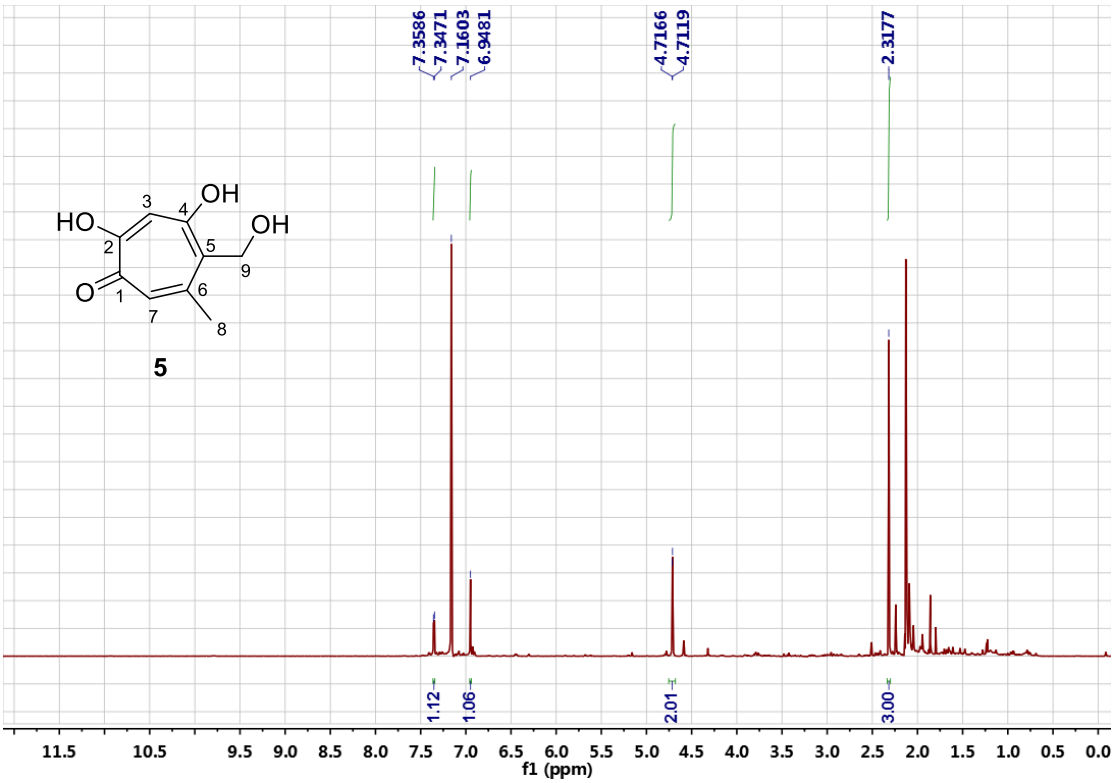

Figure S44. ^{1}H NMR (600MHz) spectrum of **5** in a mixture of C_6D_6 and $(CD_3)_2SO$ (4:1).

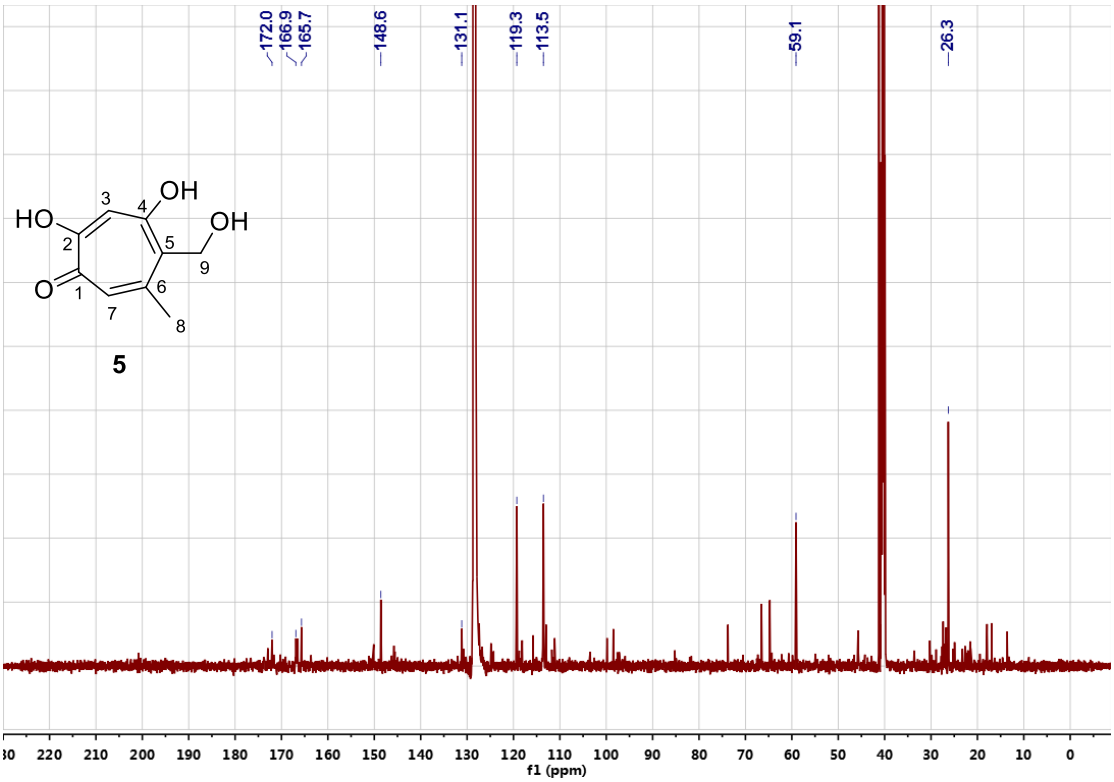

Figure S45. ^{13}C NMR (150MHz) spectrum of **5** in a mixture of C_6D_6 and $(CD_3)_2SO$ (4:1).

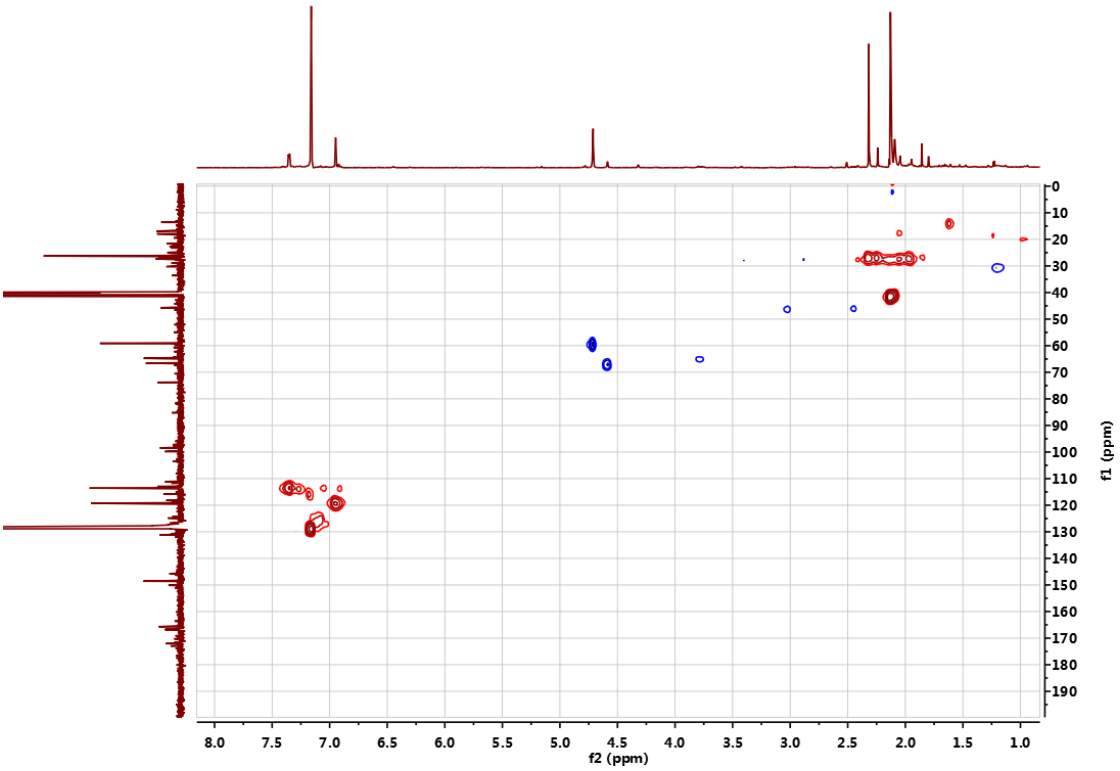

Figure S46. HSQC (600MHz) spectrum of **5** in a mixture of C_6D_6 and $(CD_3)_2SO$ (4:1).

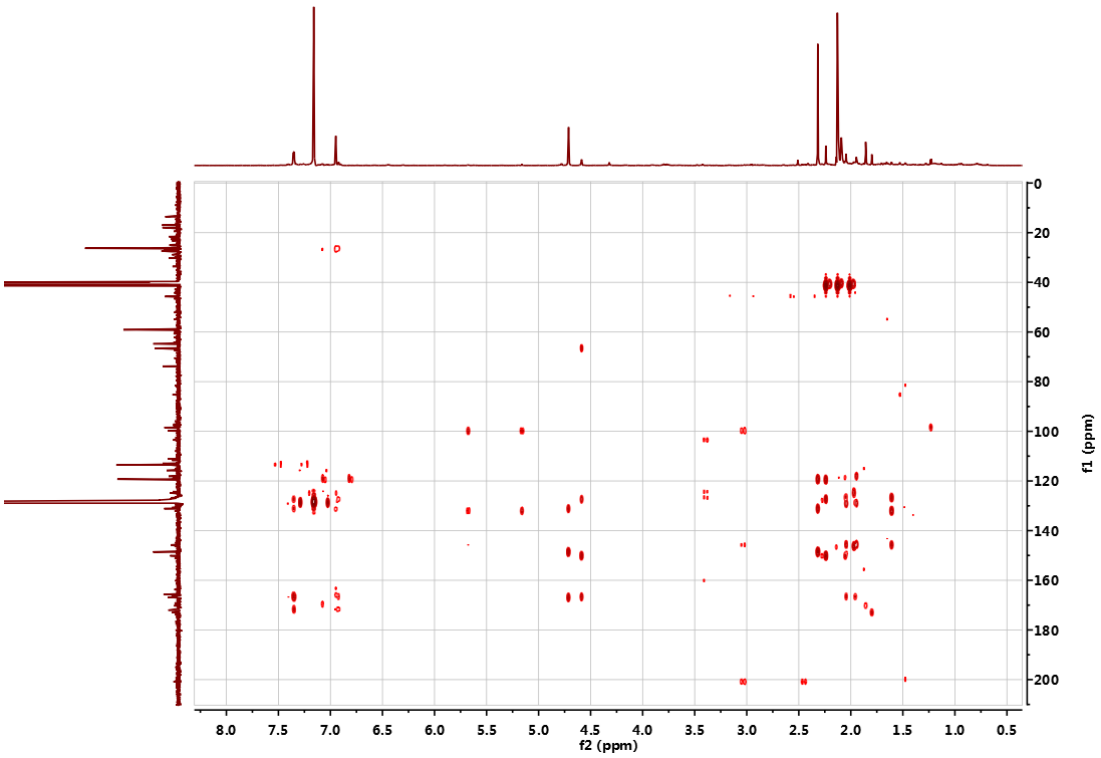

Figure S47. HMBC (600MHz) spectrum of **5** in a mixture of C_6D_6 and $(CD_3)_2SO$ (4:1).

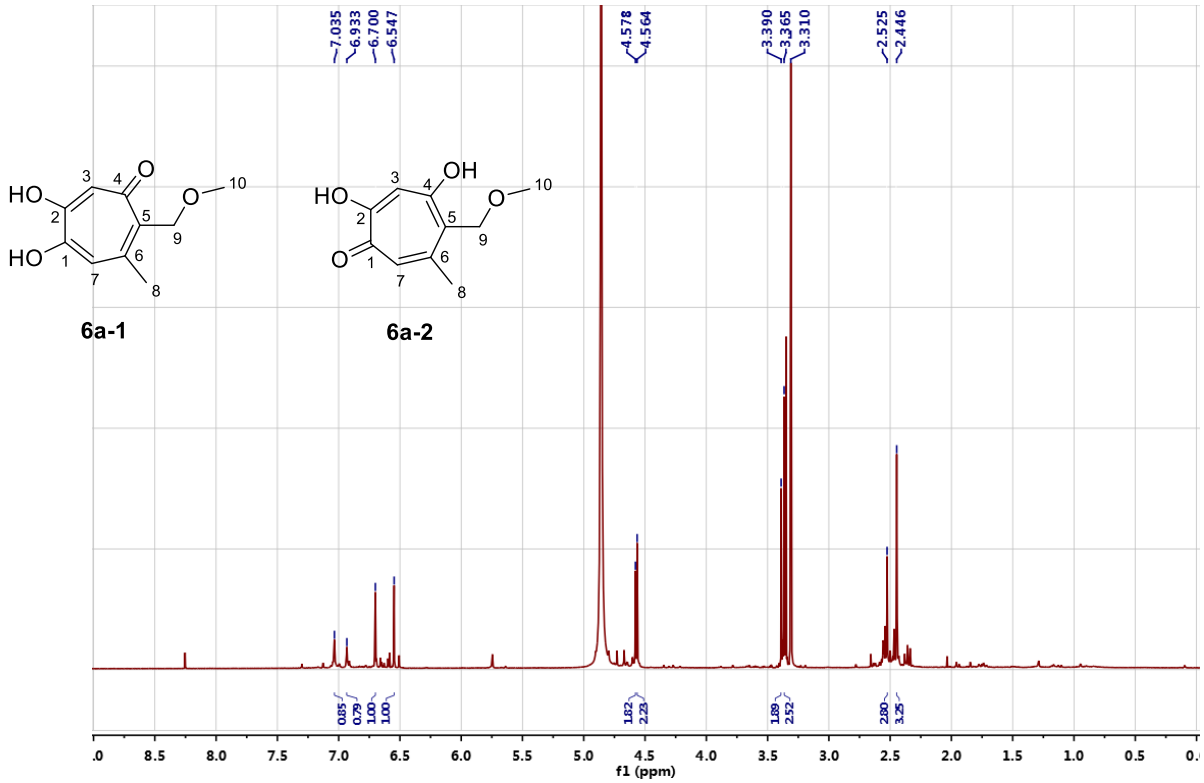

Figure S48. ^{1}H (600MHz) NMR spectrum of **6a** in CD_3OD.

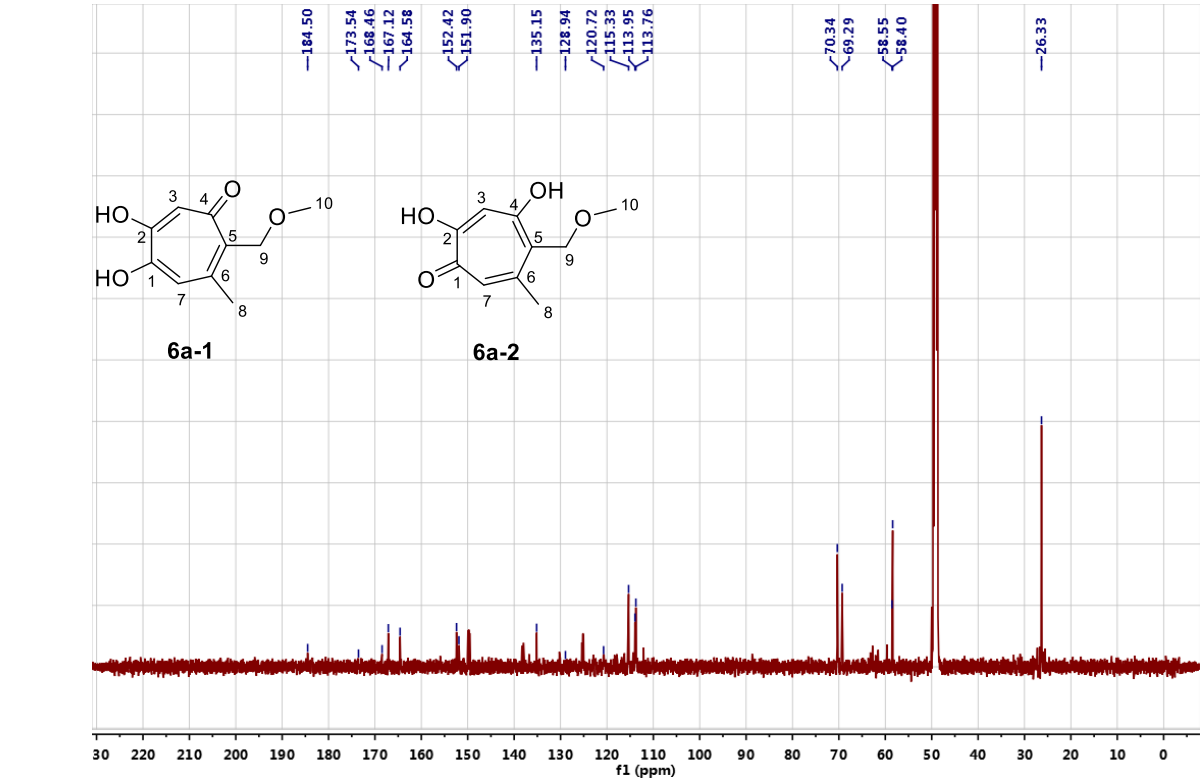

Figure S49. ^{13}C (150MHz) NMR spectrum of **6a** in CD_3OD.

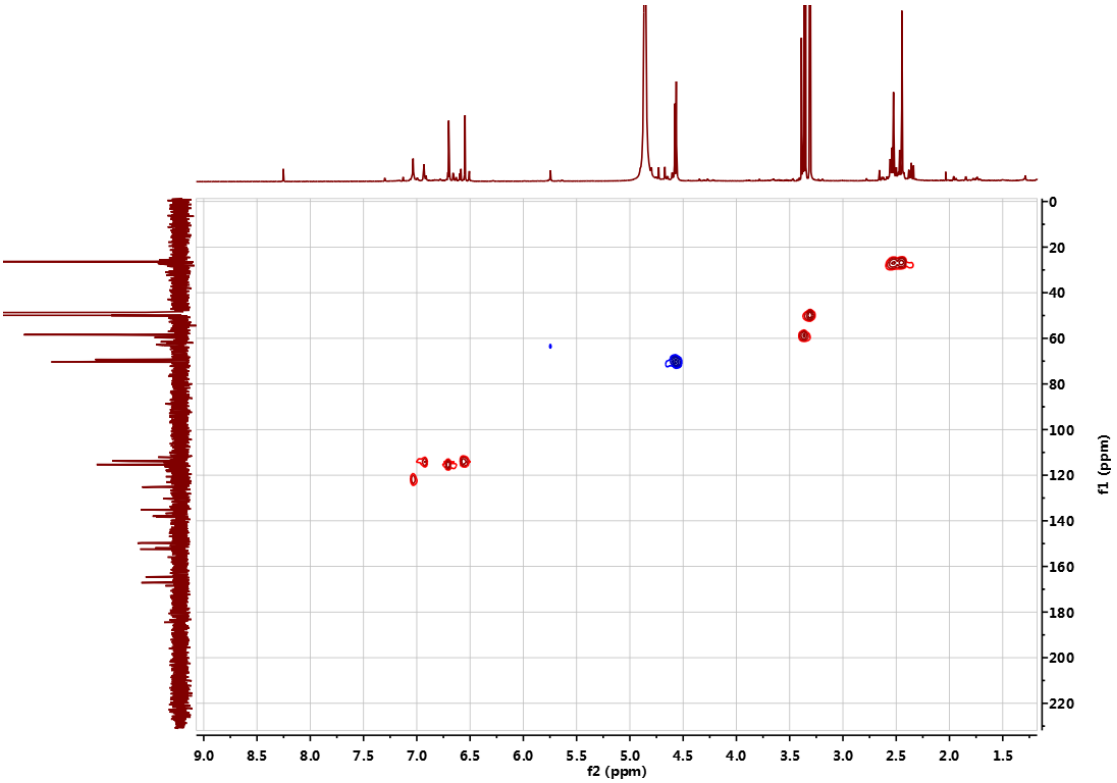

Figure S50. HSQC (600MHz) spectrum of **6a** in CD_3OD.

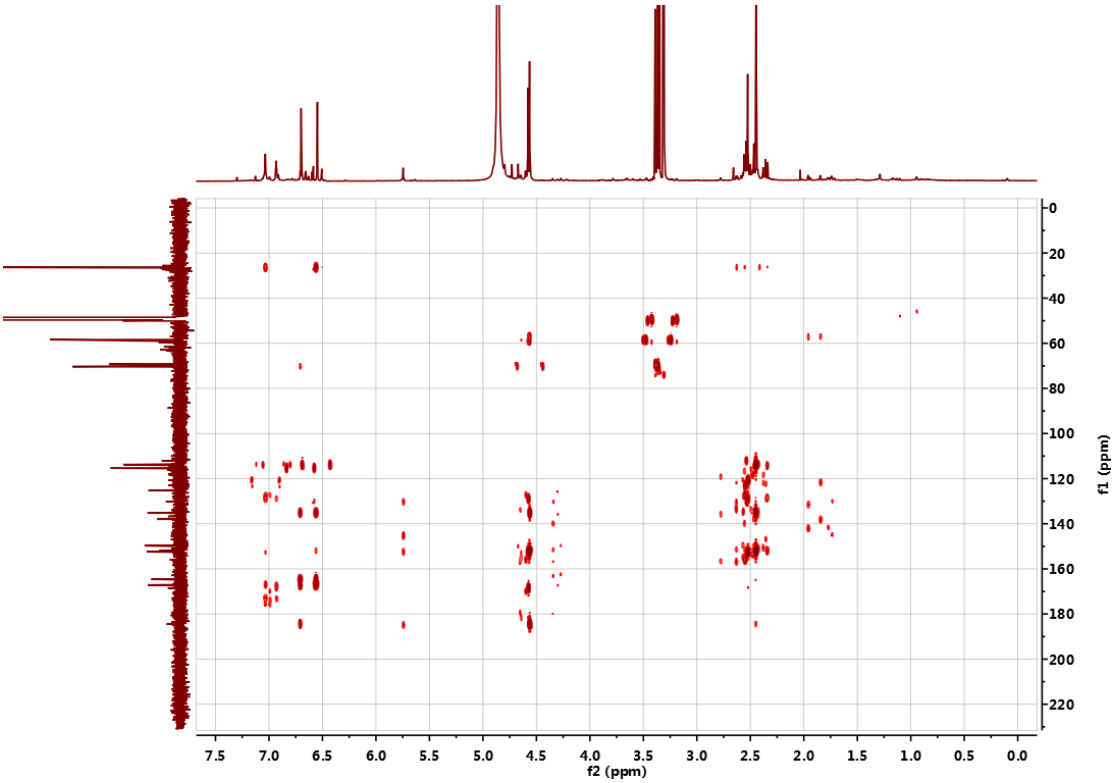

Figure S51. HMBC (600MHz) spectrum of **6a** in CD_3OD.

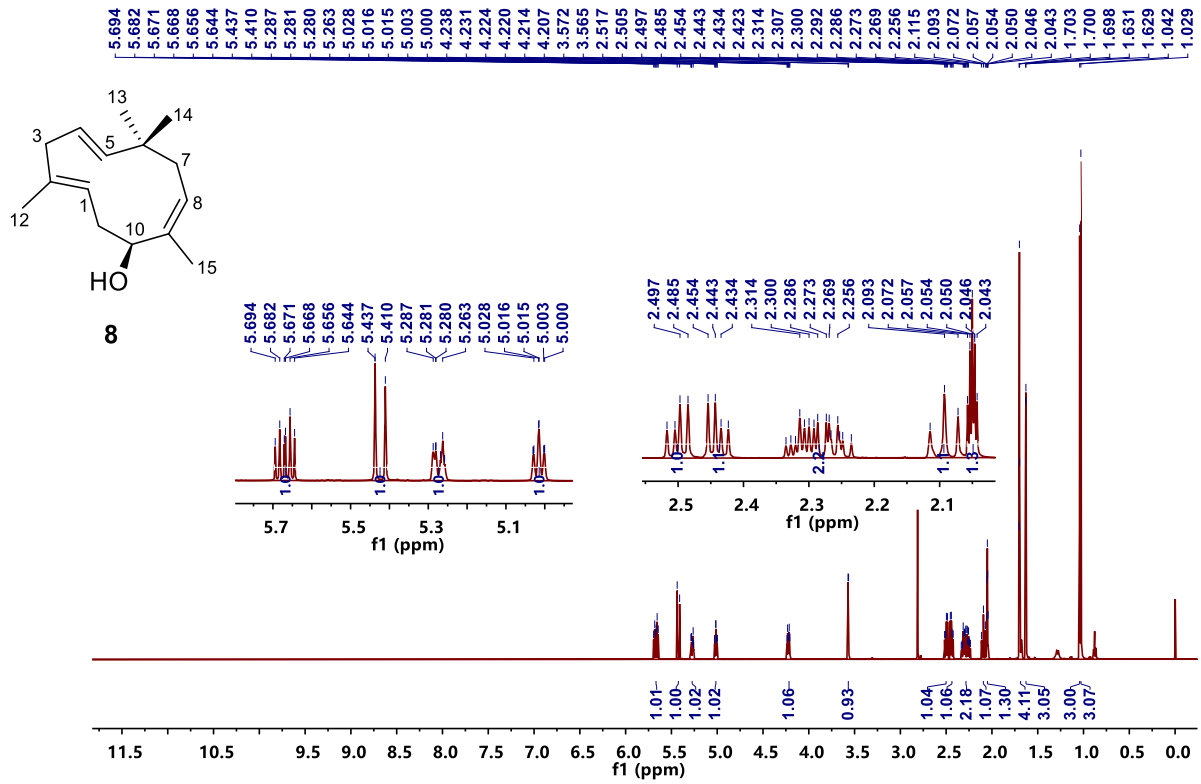

Figure S52. ^{1}H NMR (600MHz) spectrum of **8** in acetone-d_6.

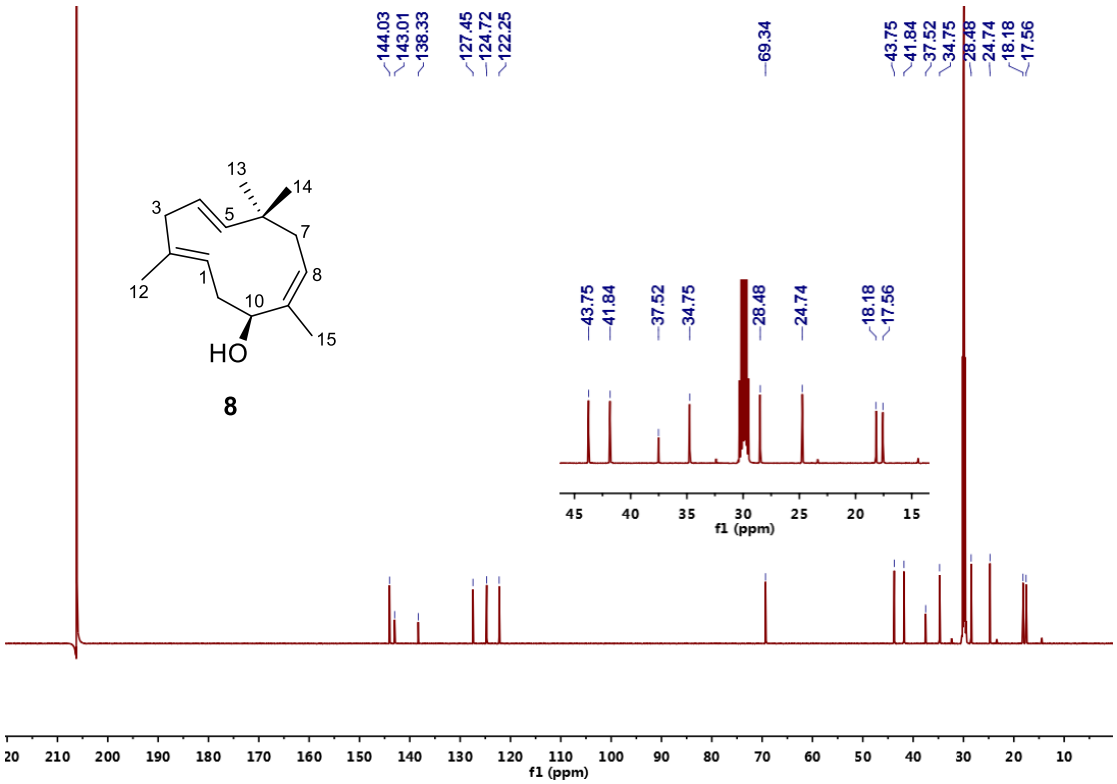

Figure S53. ^{13}C NMR (150MHz) spectrum of **8** in acetone-d_6.

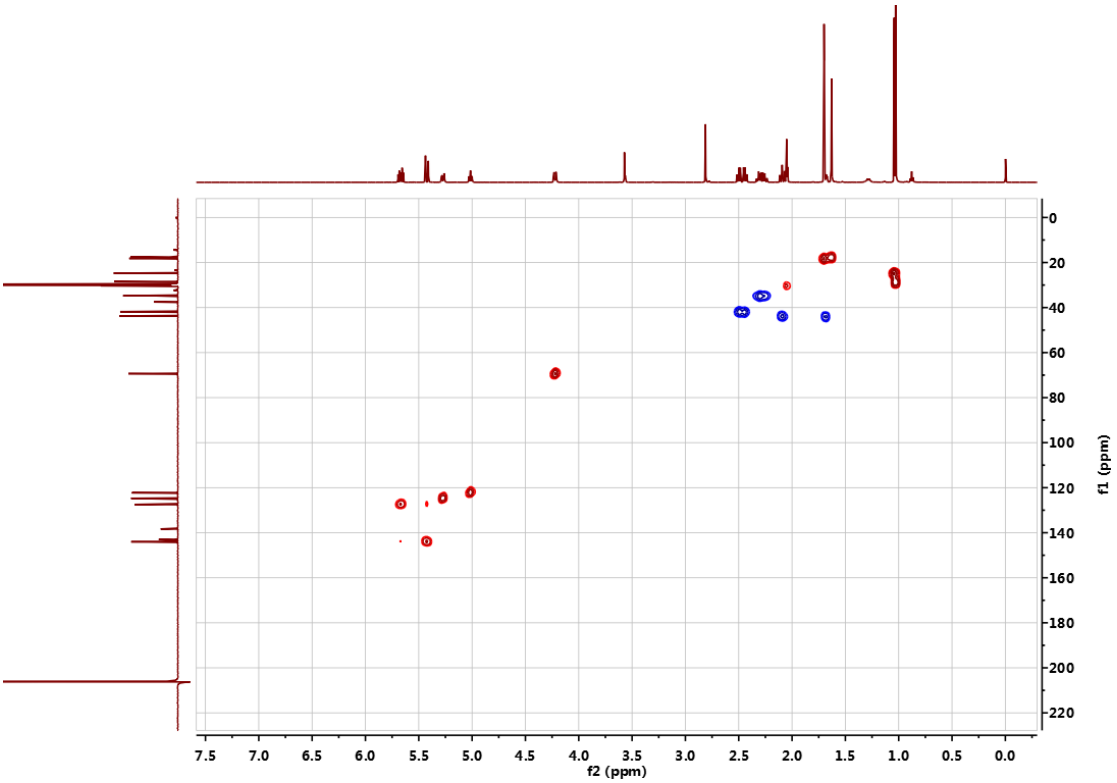

Figure S54. HSQC (600MHz) spectrum of **8** in acetone-d_6.

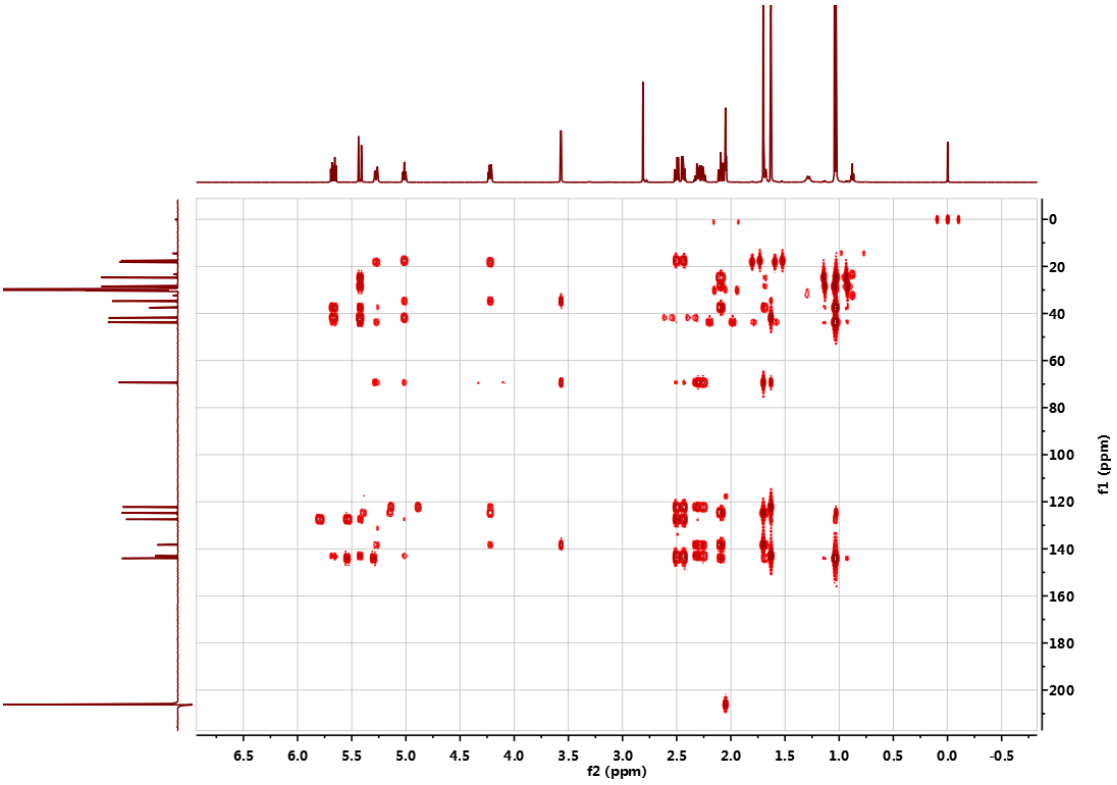

Figure S55. HMBC (600MHz) spectrum of **8** in acetone-d_6.

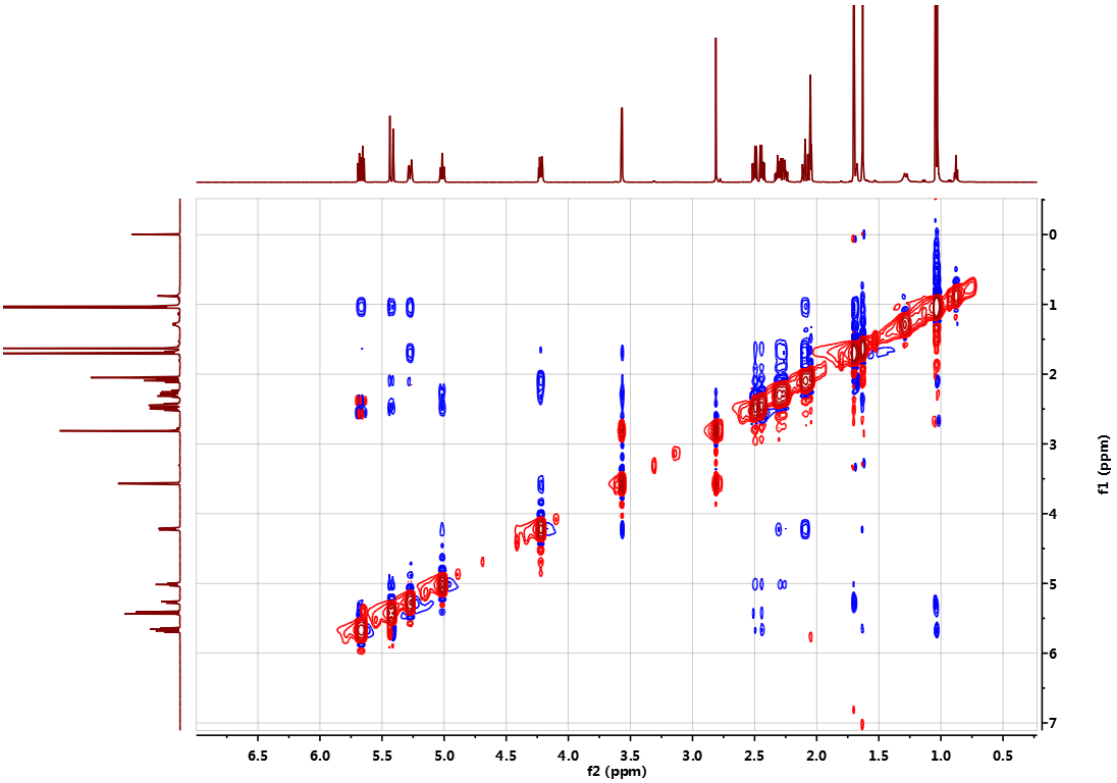

Figure S56. NOESY (600MHz) spectrum of **8** in acetone-d_6.

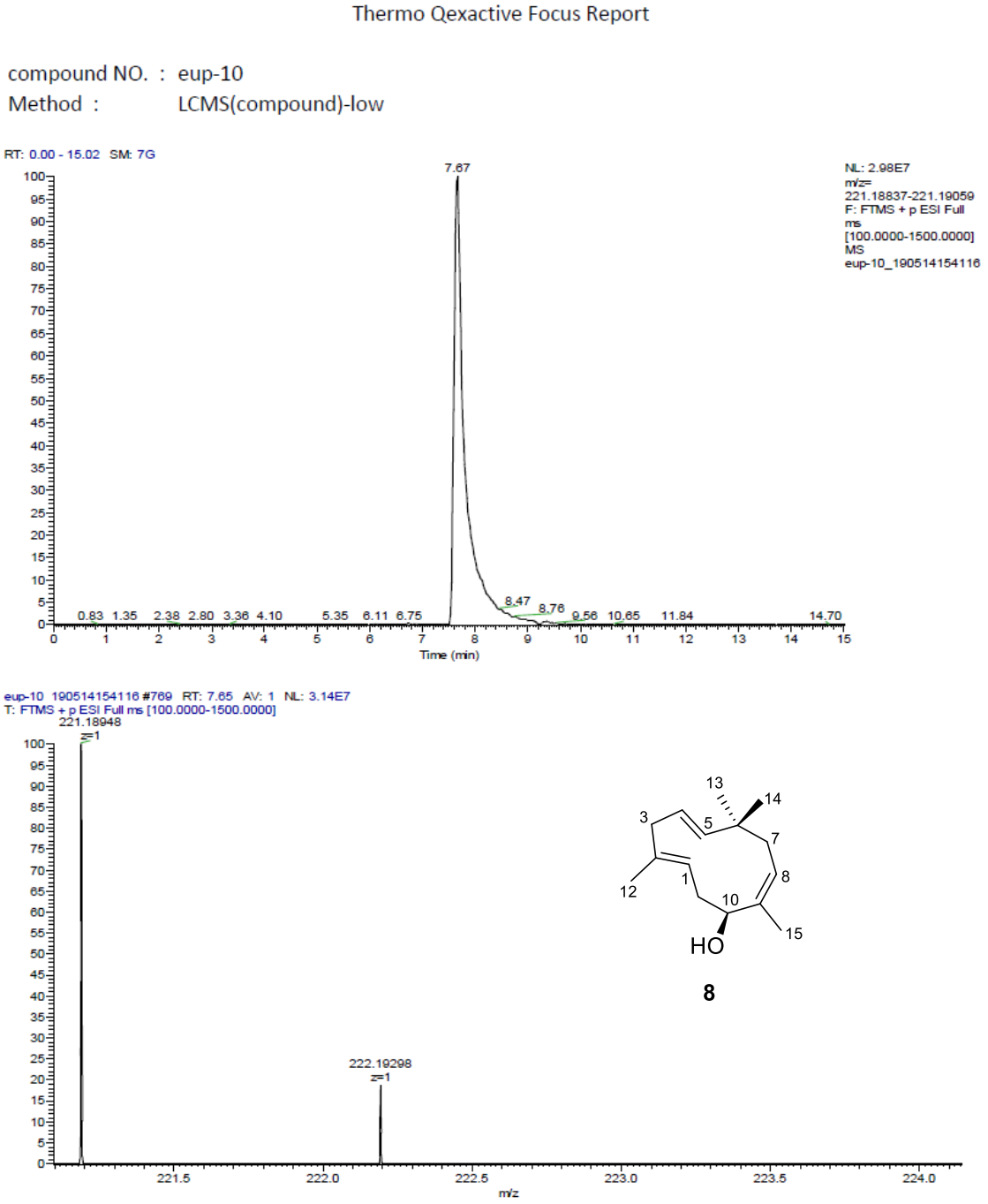

m/z	Theo. Mass	Delta (ppm)	RDB equiv.	Composition	
221.18948	221.18999	-2.31	3.5	C15 H25 O	M+H

Figure S57. HRESIMS spectrum of **8**.

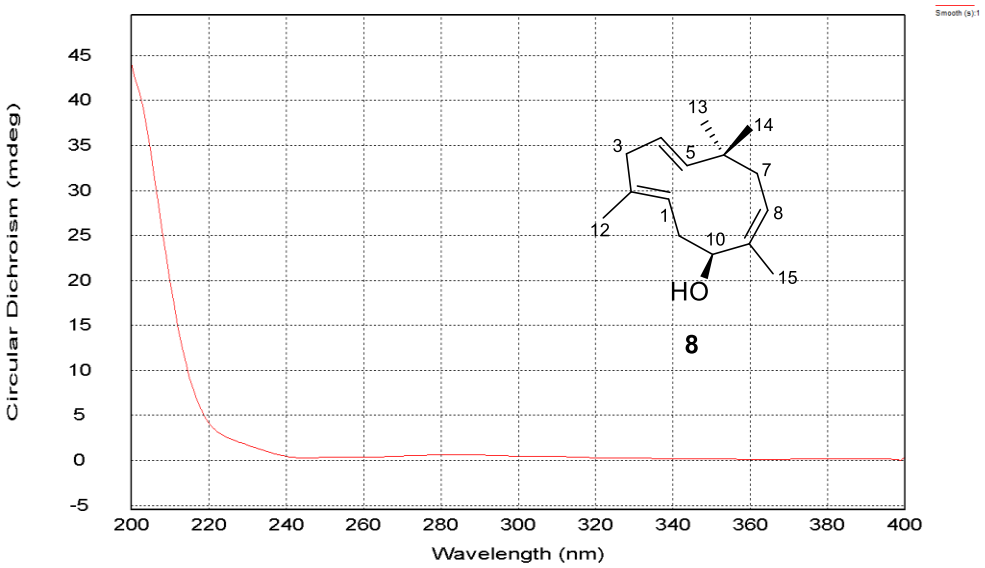

Figure S58. Experimental CD spectrum of **8**.

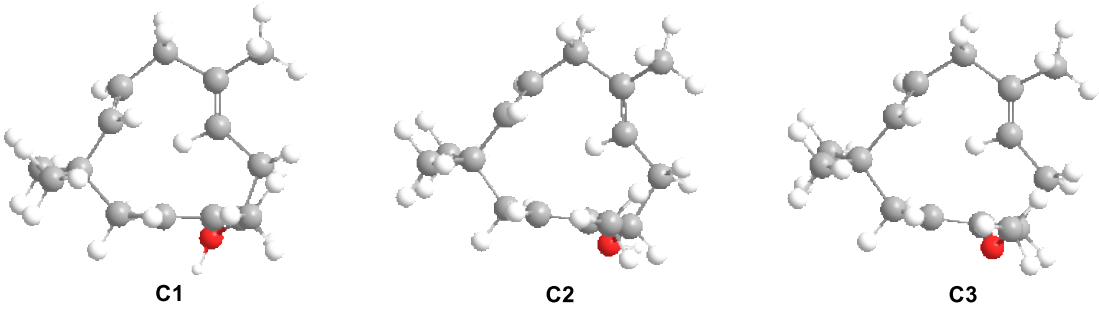

Figure S59. WB97XD/DGDZVP optimized three lowest energy 3D conformers of *S*-**8**.

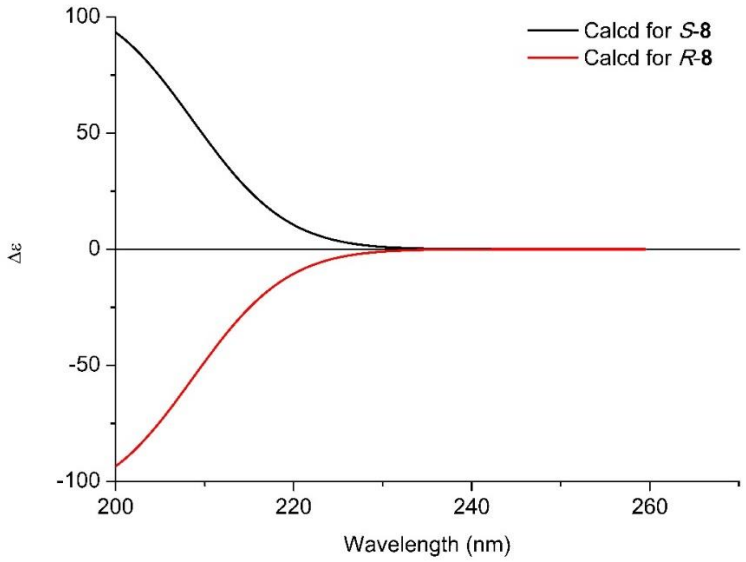

Figure S60. Calculated ECD spectra of *R*-**8** (red) and *S*-**8** (black).

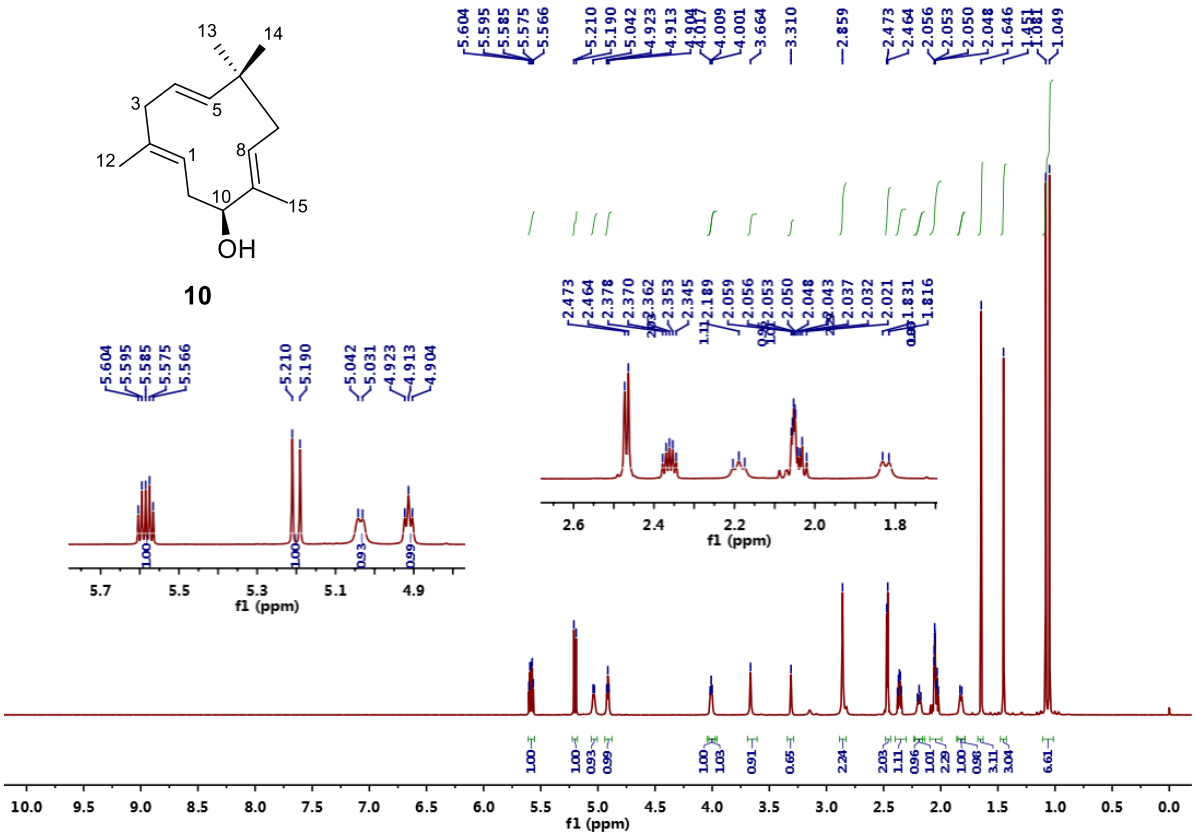

Figure S61. ^{1}H NMR (800MHz) spectrum of **10** in acetone-d_6.

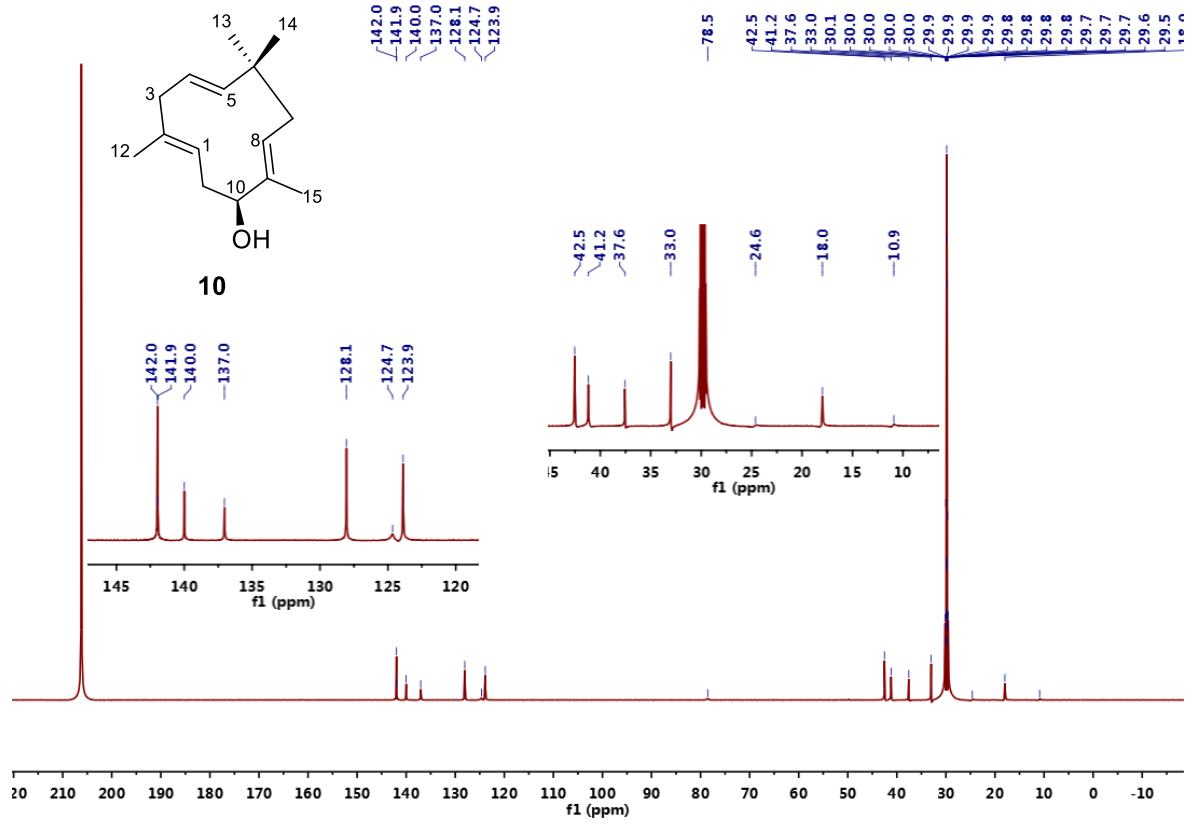

Figure S62. ^{13}C NMR (200MHz) spectrum of **10** in acetone-d_6.

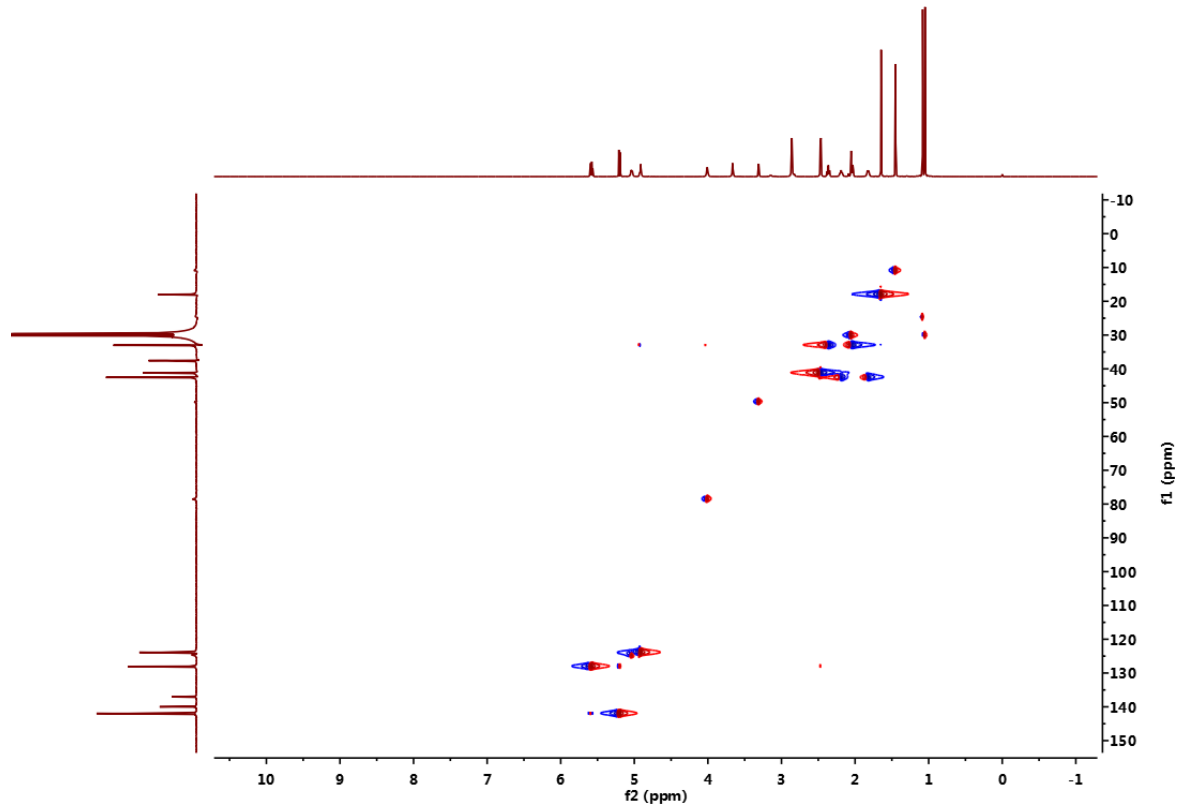

Figure S63. HSQC (800MHz) spectrum of **10** in acetone-d_6.

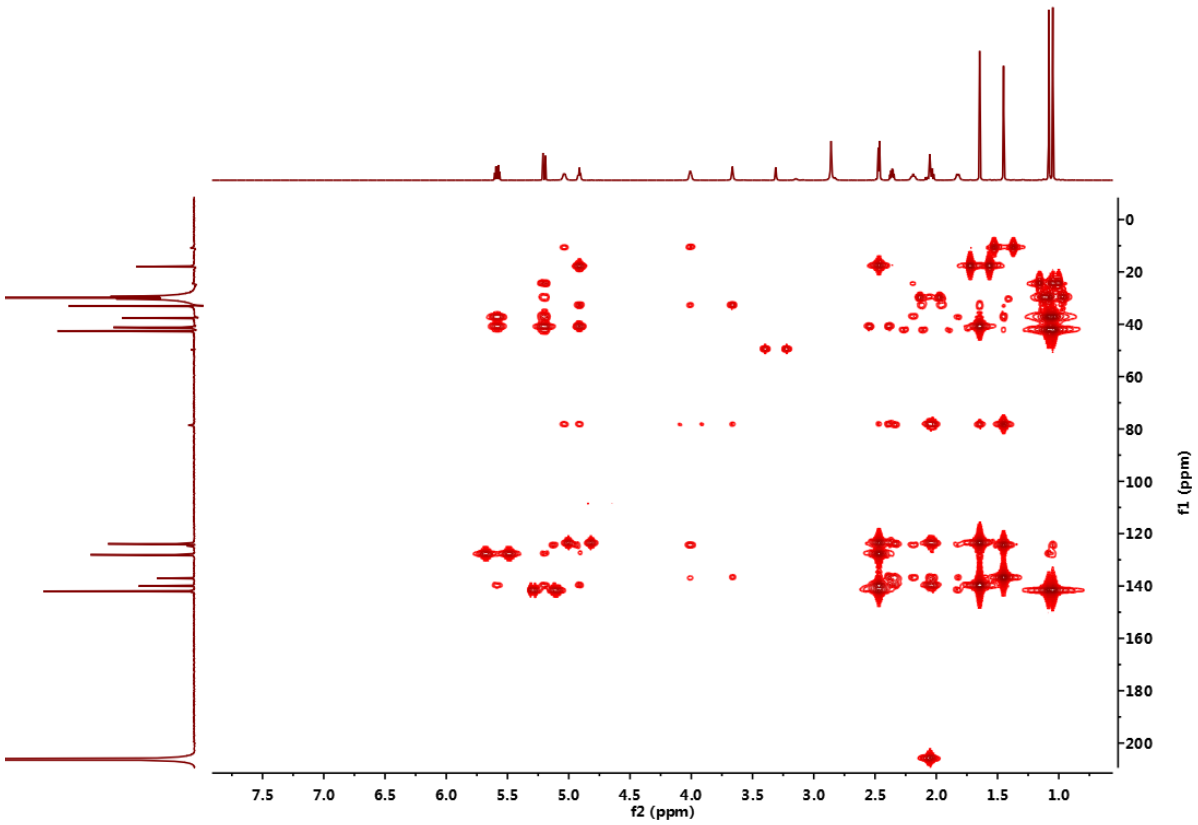

Figure S64. HMBC (800MHz) spectrum of **10** in acetone-d_6.

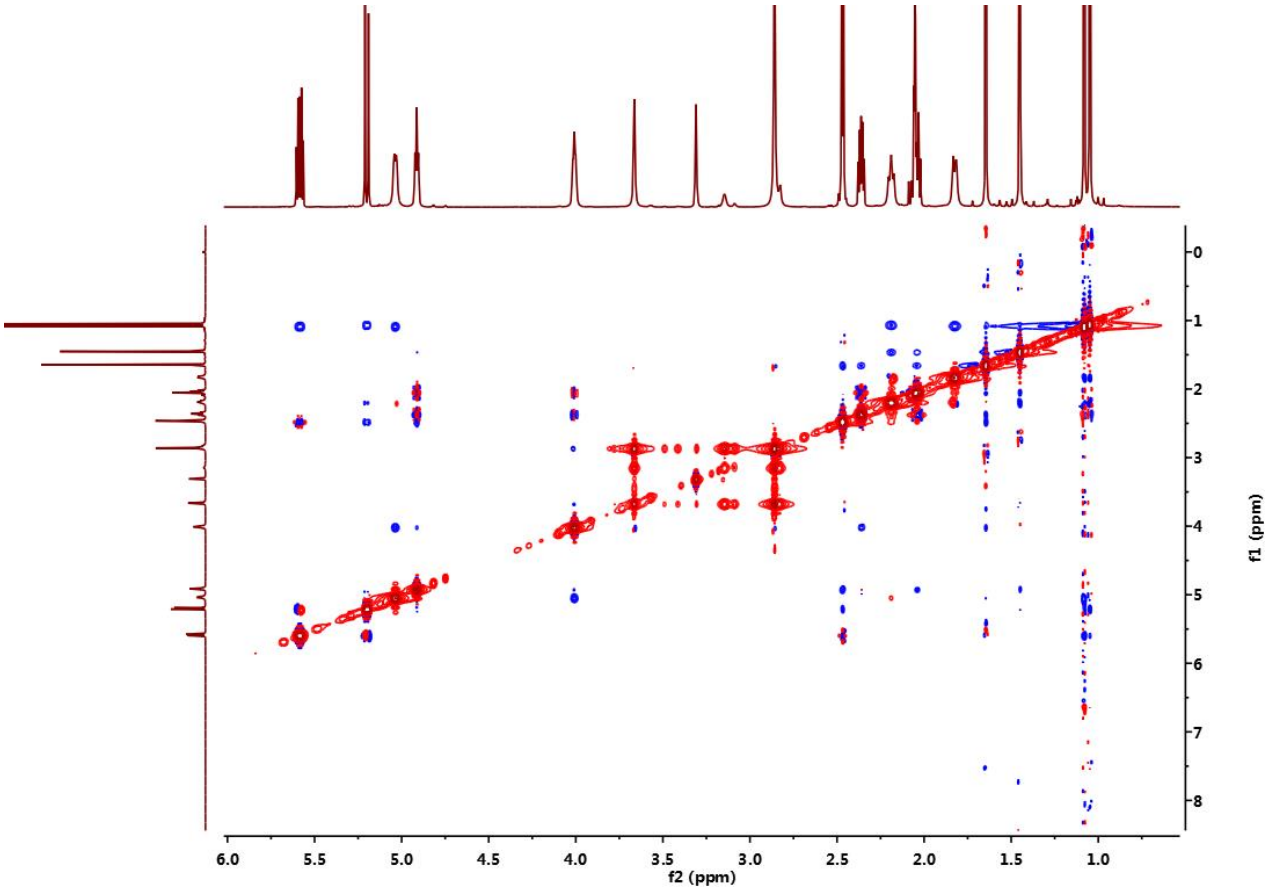

Figure S65. NOESY (800MHz) spectrum of **10** in acetone-d_6.

Thermo Qexactive Focus Report

compound NO. : Hum-125A

Method : LCMS(compound)-low

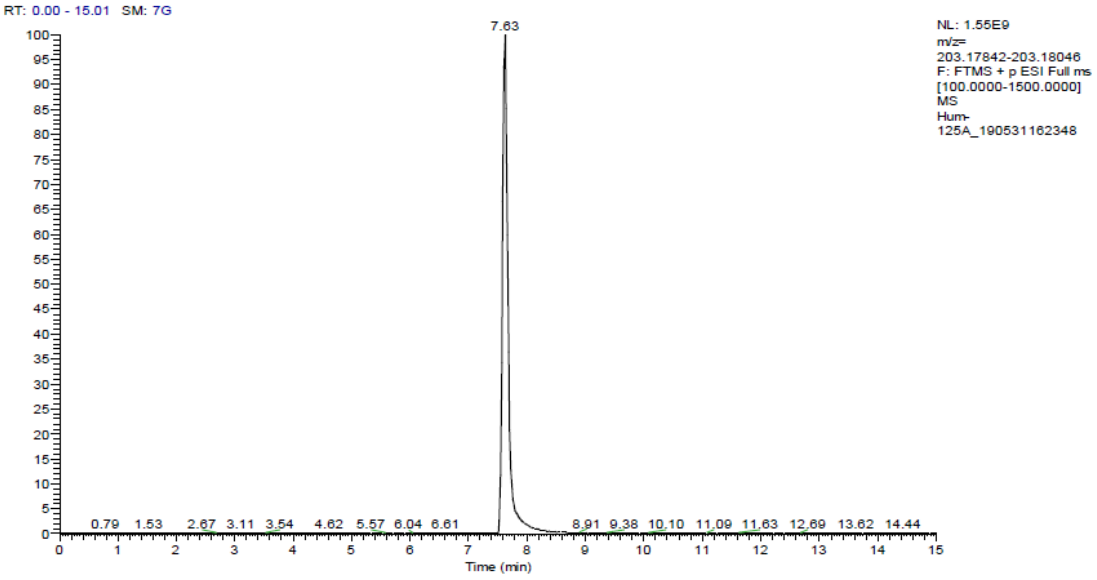

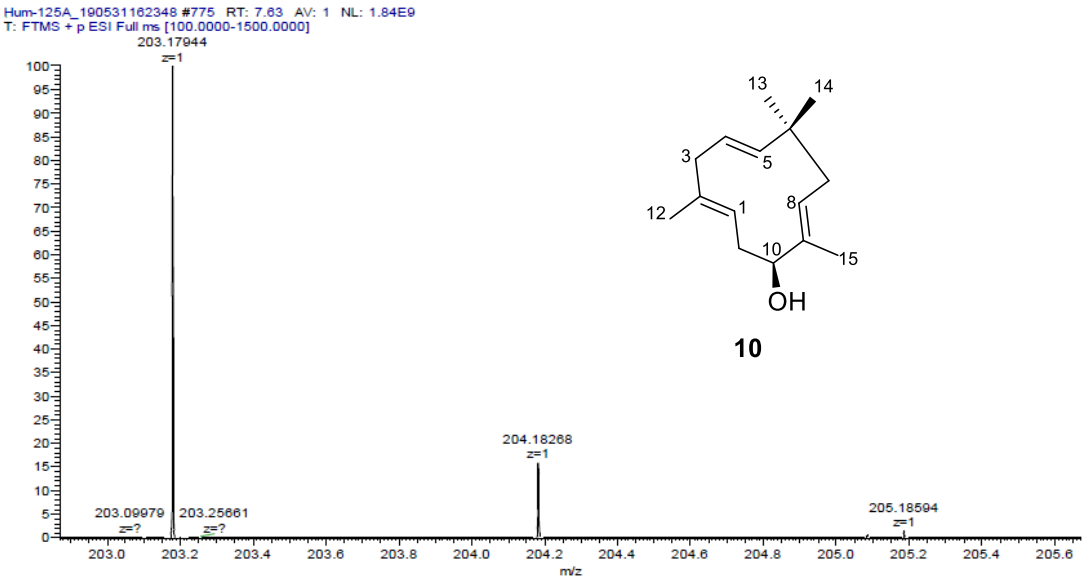

10

m/z	Theo. Mass	Delta (ppm)	RDB equiv.	Composition	
203.17944	203.17943	0.06	4.5	C15 H23	M+H-H_2O

Figure S66. HRESIMS spectrum of **10**.

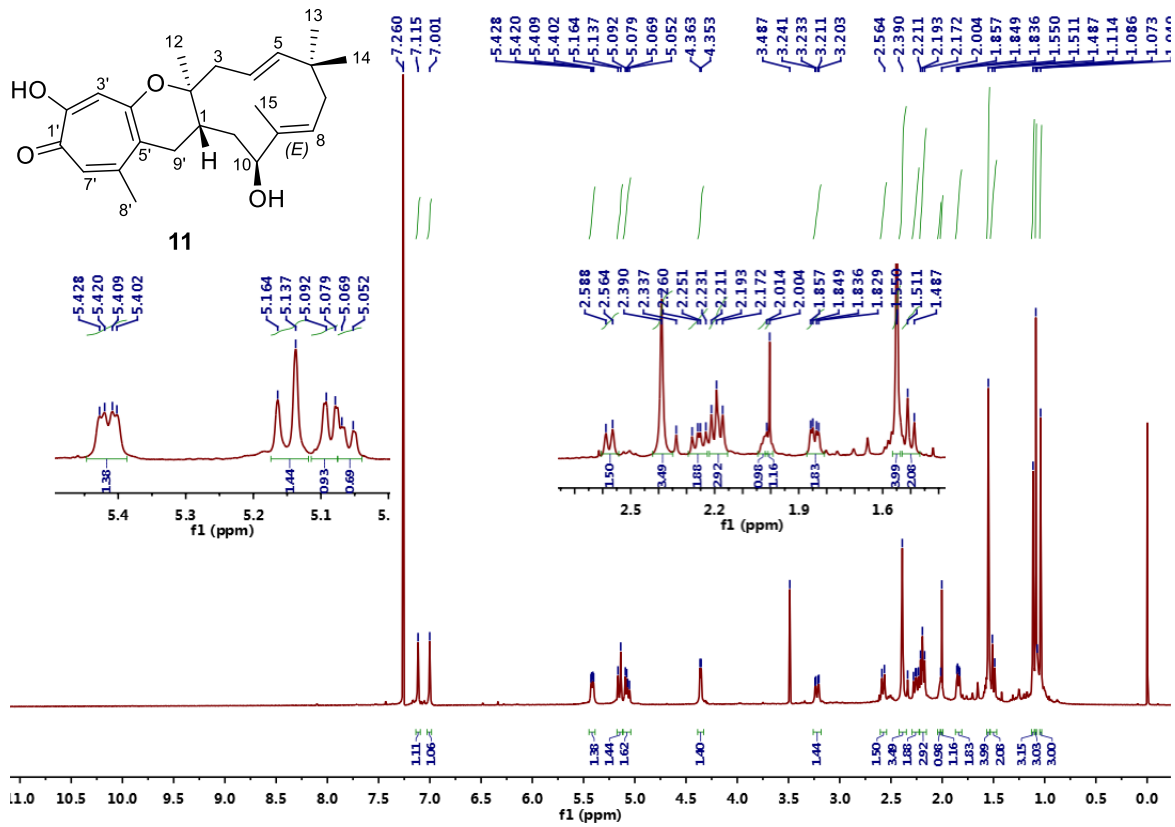

Figure S67. ^{1}H NMR (600MHz) spectrum of **11** in $CDCl_3$.

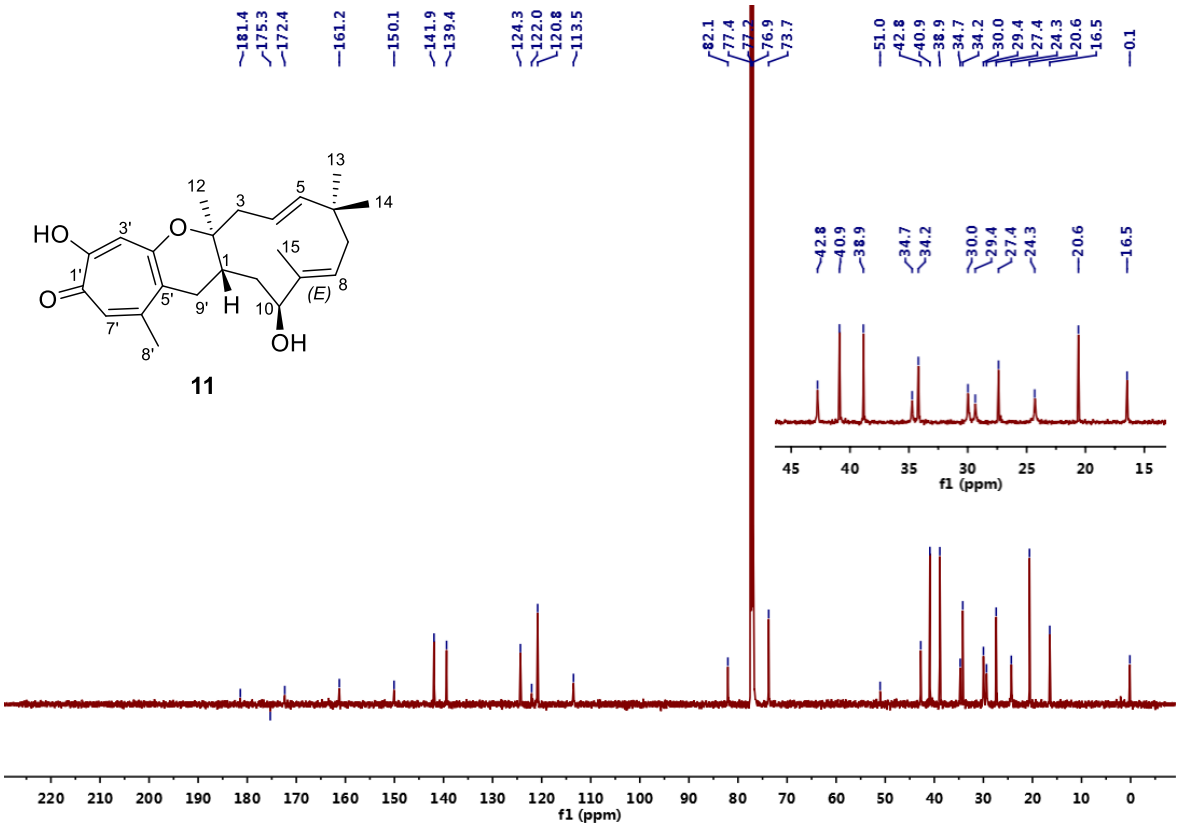

Figure S68. ^{13}C NMR (150MHz) spectrum of **11** in $CDCl_3$.

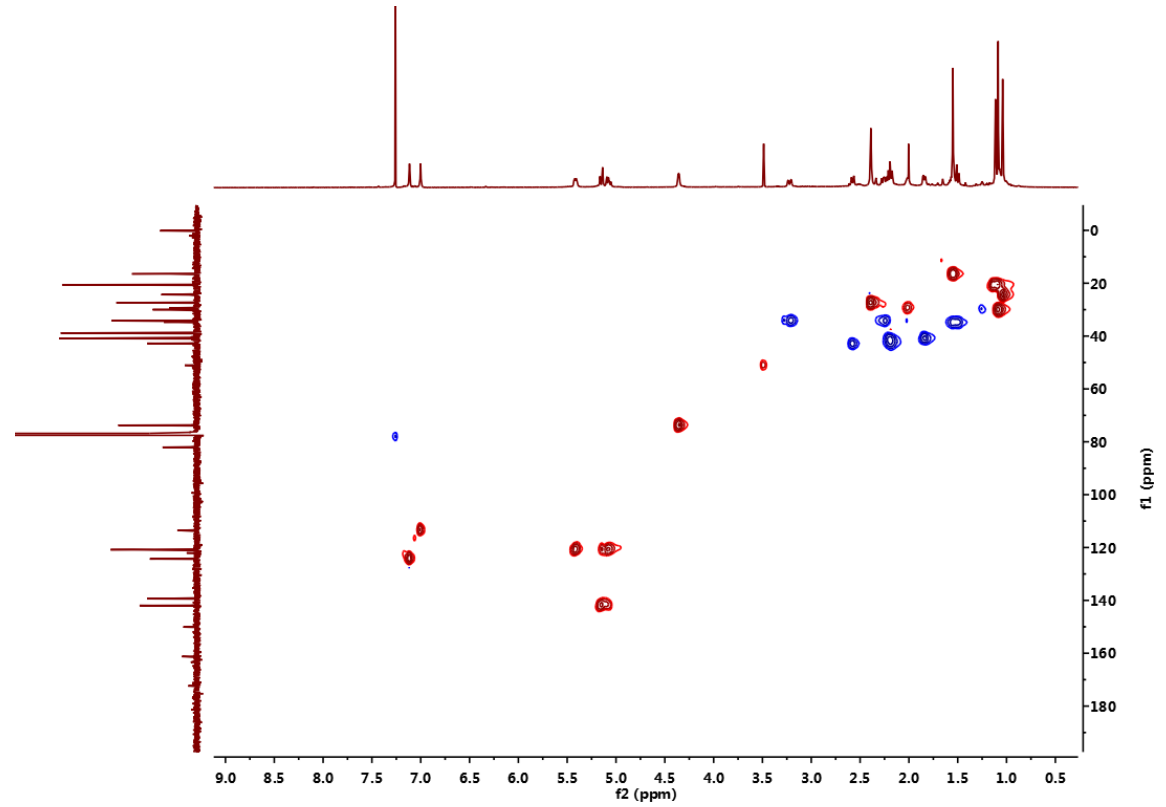

Figure S69. HSQC (600MHz) spectrum of **11** in $CDCl_3$.

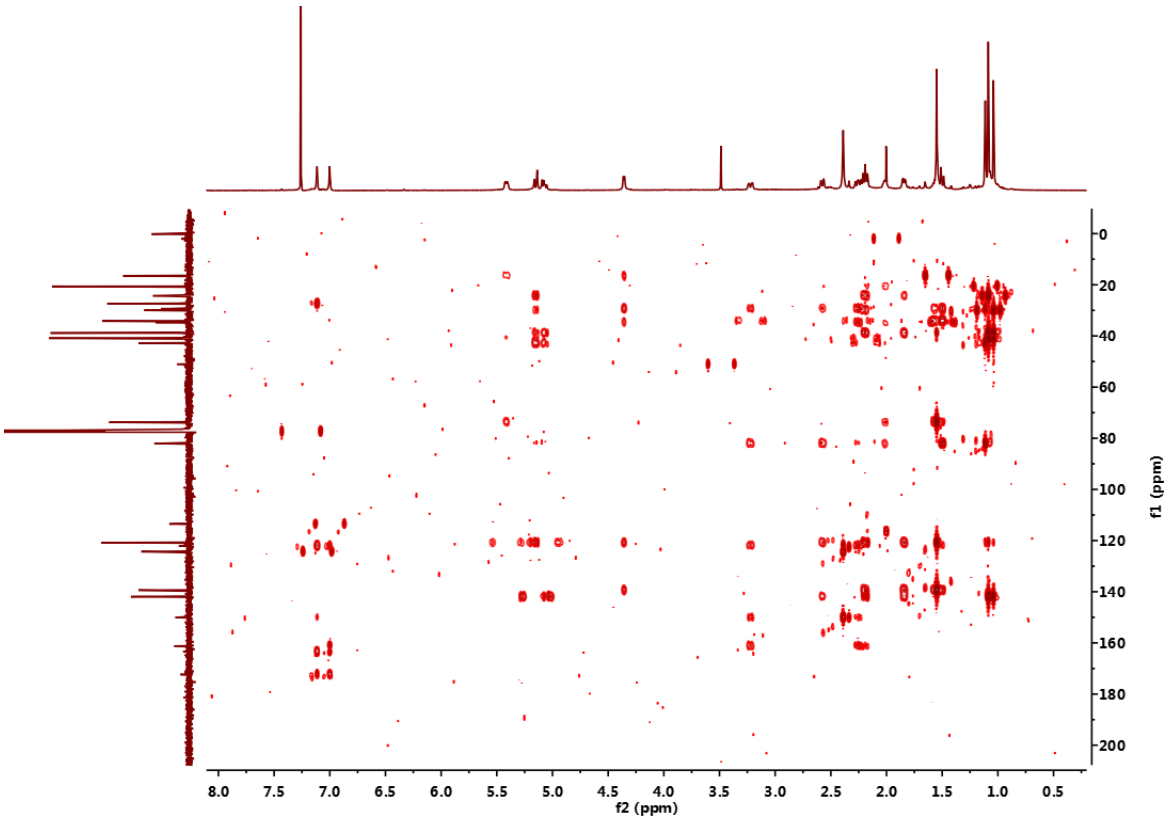

Figure S70. HMBC (600MHz) spectrum of **11** in $CDCl_3$.

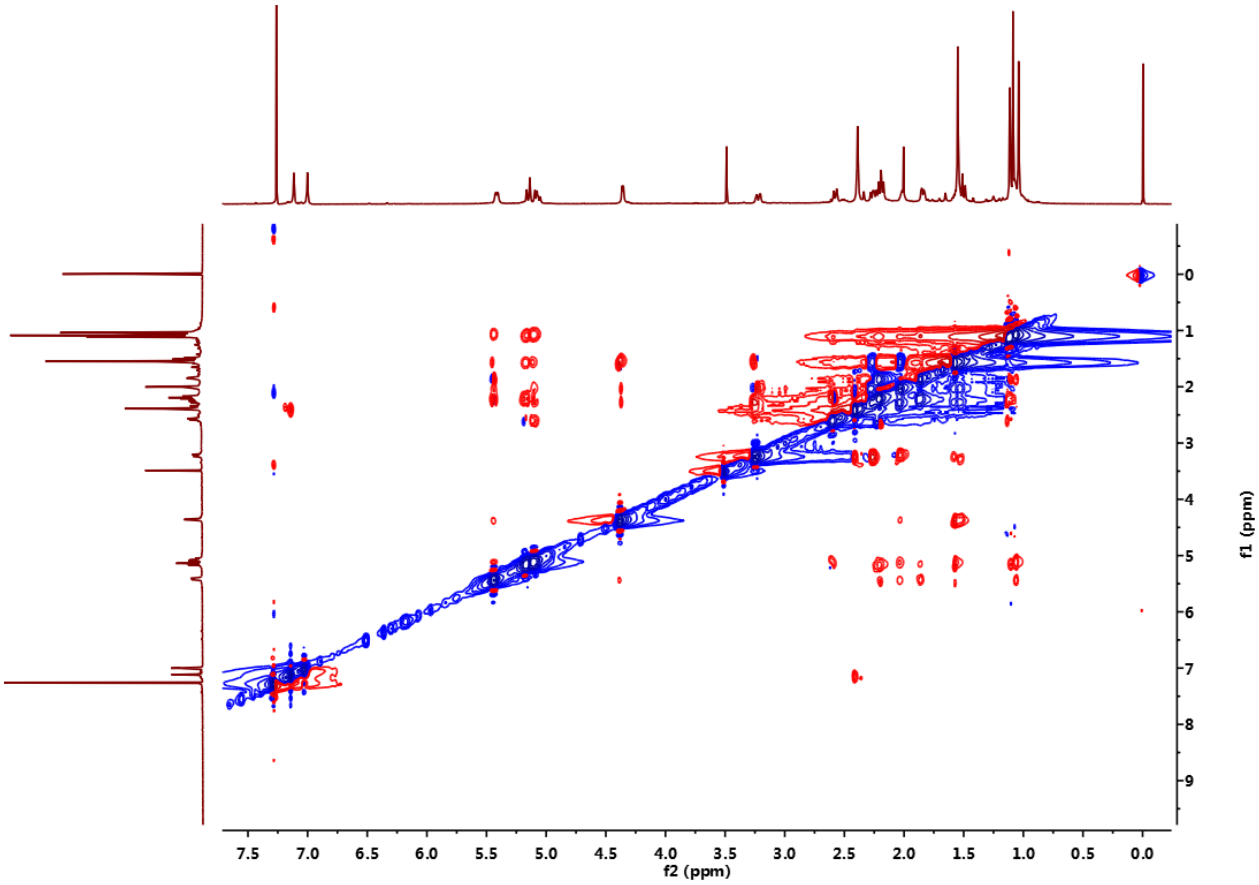

Figure S71. NOESY (600MHz) spectrum of **11** in $CDCl_3$.

Thermo Qexactive Focus Report

compound NO. : hum-jy-125b
Method : LCMS(compound)-low

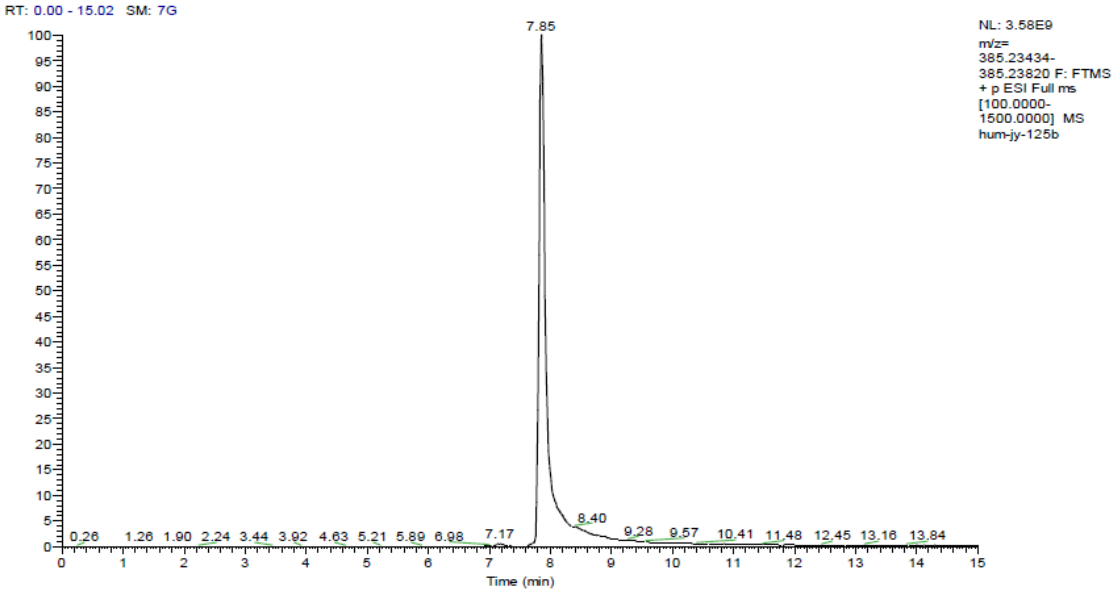

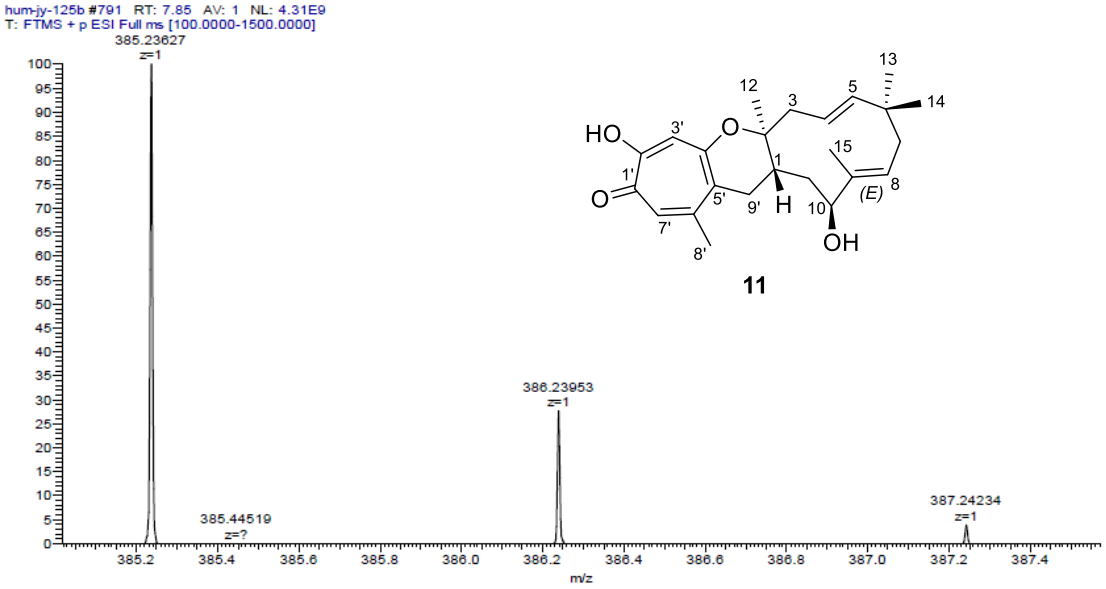

11

m/z	Theo. Mass	Delta (ppm)	RDB equiv.	Composition	
385.23627	385.23734	-2.77	8.5	C24 H33 O4	M+H

Figure S72. HRESIMS spectrum of **11**.

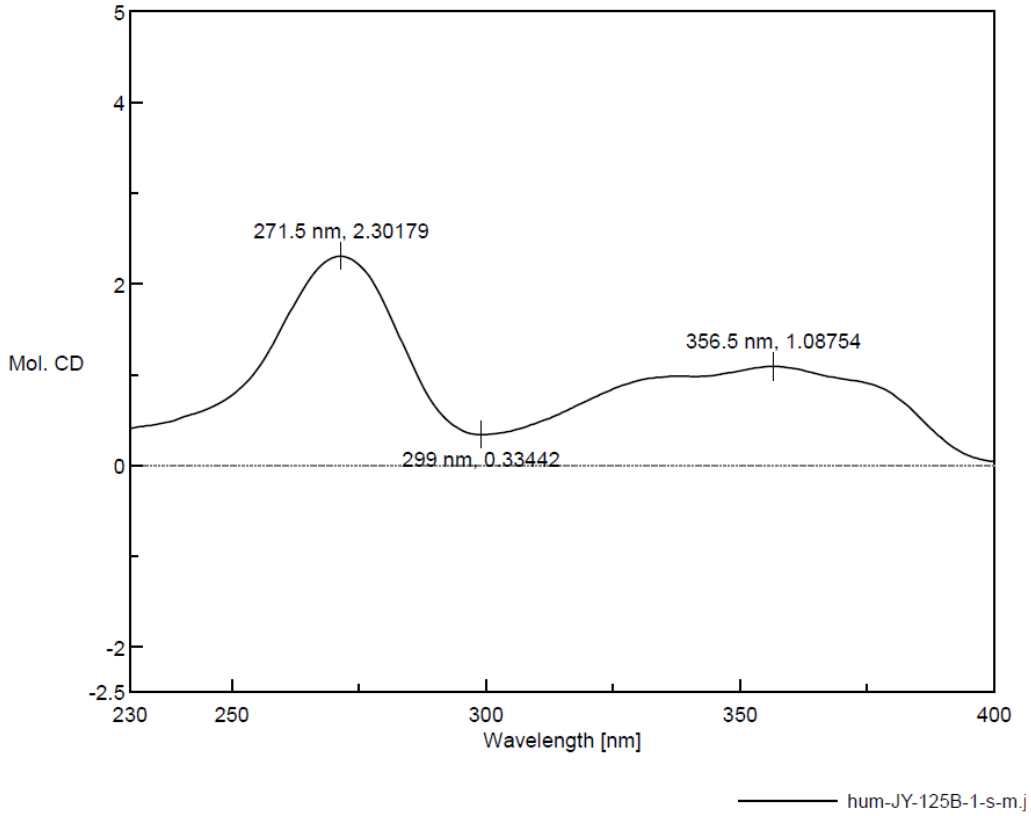

[Measurement Information]

Instrument Name	J-815
Model Name	J-815
Serial No.	A024461168
Accessory	Standard
Accessory S/N	A024461168
Cell Length	1 mm
Measurement date	2019/6/6 14:50
Photometric Mode	CD, HT, Abs
Measure Range	400 - 230 nm
Data pitch	0.5 nm
Sensitivity	Standard
D.I.T.	1 sec
Bandwidth	2.00 nm
Start Mode	Immediately
Scanning Speed	100 nm/min
Baseline Correction	Baseline
Shutter Control	Auto
CD Detector	PMT
PMT Voltage	Auto
Accumulations	2
Solvent	CHCl3
Concentration	0.2 (w/v)%

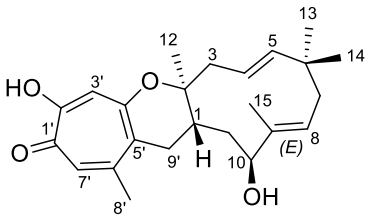

11

Figure S73. CD spectrum of **11** in $CDCl_3$.

References

1. Yan, D.; Chen, Q.; Gao, J.; Bai, J.; Liu, B.; Zhang, Y.; Zhang, L.; Zhang, C.; Zou, Y.; Hu, Y., Complexity and diversity generation in the biosynthesis of fumiquinazoline-related peptidyl alkaloids. *Organic Letters* **2019,** *21* (5), 1475-1479.

2. Gao, S.-S.; Zhang, T.; Garcia-Borras, M.; Hung, Y.-S.; Billingsley, J. M.; Houk, K. N.; Hu, Y.; Tang, Y., Biosynthesis of heptacyclic duclauxins requires extensive redox modifications of the phenalenone aromatic polyketide. *Journal of the American Chemical Society* **2018,** *140* (22), 6991-6997.

3. Bai, J.; Yan, D.; Zhang, T.; Guo, Y.; Liu, Y.; Zou, Y.; Tang, M.; Liu, B.; Wu, Q.; Yu, S.; Tang, Y.; Hu, Y., A cascade of redox reactions generates complexity in the biosynthesis of the protein phosphatase-2 inhibitor rubratoxin A. *Angewandte Chemie-International Edition* **2017,** *56* (17), 4782-4786.

4. Zhai, Y.; Li, Y.; Zhang, J.; Zhang, Y.; Ren, F.; Zhang, X.; Liu, G.; Liu, X.; Che, Y., Identification of the gene cluster for bistropolone-humulene meroterpenoid biosynthesis in *Phoma* sp. *Fungal Genetics and Biology* **2019,** *129*, 7-15.

5. El-Elimat, T.; Raja, H. A.; Ayers, S.; Kurina, S. J.; Burdette, J. E.; Mattes, Z.; Sabatelle, R.; Bacon, J. W.; Colby, A. H.; Grinstaff, M. W.; Pearce, C. J.; Oberlies, N. H., Meroterpenoids from *Neosetophoma sp.*: A dioxa 4.3.3 propellane ring system, potent cytotoxicity, and prolific expression. *Organic Letters* **2019,** *21* (2), 529-534.

6. Mayerl, F.; Gao, Q.; Huang, S.; Klohr, S. E.; Matson, J. A.; Gustavson, D. R.; Pirnik, D. M.; Berry, R. L.; Fairchild, C.; Rose, W. C., Eupenifeldin, a novel cytotoxic bistropolone from *Eupenicillium brefeldianum*. *Journal of Antibiotics* **1993,** *46* (7), 1082-1088.

7. Zhang, J.; Liu, L.; Wang, B.; Zhang, Y.; Wang, L.; Lie, X.; Che, Y., Phomanolides A and B from the fungus *Phoma* sp.: meroterpenoids derived from a putative tropolonic sesquiterpene via hetero-Diels-Alder reactions. *Journal of Natural Products* **2015,** *78* (12), 3058-3066.

8. al Fahad, A.; Abood, A.; Simpson, T. J.; Cox, R. J., The Biosynthesis and Catabolism of the Maleic Anhydride Moiety of Stipitatonic Acid. *Angewandte Chemie-International Edition* **2014,** *53* (29), 7519-7523.

9. Grau, E.; Mecking, S., Polyterpenes by ring opening metathesis polymerization of caryophyllene and humulene. *Green Chemistry* **2013,** *15* (5), 1112-1115.

10. Spartan 14, Wavefunction, Inc.: Irvine, CA.

11. Frisch, M. J.; Trucks, G. W.; Schlegel, H. B.; Scuseria, G. E.; Robb, M. A.; Cheeseman, J. R.; Scalmani, G.; Barone, V.; Petersson, G. A.; Nakatsuji, H.; et al. Gaussian 16 Revision A.03. 2016. Frisch, M. J.; Trucks, G. W.; Schlegel, H. B.; Scuseria, G. E.; Robb, M. A.; Cheeseman, J. R.; Scalmani, G.; Barone, V.; Petersson, G. A.; Nakatsuji, H.; Li, X.; Caricato, M.; Marenich, A. V.; Bloino, J.; Janesko, B. G.; Gomperts, R.; Mennucci, B.; Hratchian, H. P.; Ortiz, J. V.; Izmaylov, A. F; Sonnenberg, J. L.; Williams-Young, D.; Ding, F.; Lipparini, F.; Egidi, F.; Goings, J.; Peng, B.; Petrone, A.; Henderson, T.; Ranasinghe, D.; Zakrzewski, V. G.; Gao, J.; Rega, N.; Zheng, G.; Liang, W.; Hada, M.; Ehara, M.; Toyota, K.; Fukuda, R.; Hasegawa, J.; Ishida, M.; Nakajima, T.; Honda, Y.; Kitao, O.; Nakai, H.; Vreven, T.; Throssell, K.; Montgomery Jr., J. A.; Peralta, J. E.; Ogliaro, F.; Bearpark, M. J.; Heyd, J. J.; Brothers, E. N.; Kudin, K. N.; Staroverov, V. N.; Keith, T. A.; Kobayashi, R.; Normand, J.; Raghavachari, K.; Rendell, A. P.; Burant, J. C.; Iyengar, S. S.; Tomasi, J.; Cossi, M.; Millam, J. M.; Klene, M.; Adamo, C.; Cammi, R.; Ochterski, J. W.; Martin, R. L.; Morokuma, K.; Farkas, O.; Foresman, J. B.; Fox, D. J. Gaussian 16 Revision A.03. **2016**.

12. Cai, P.; Smith, D.; Cunningham, B.; Brown-Shimer, S.; Katz, B.; Pearce, C.; Venables, D.; Houck, D., Epolones: Novel sesquiterpene-tropolones from fungus OS-F69284 that induce erythropoietin in human cells. *Journal of Natural Products* **1998,** *61* (6), 791-795.

13. Adlington, R. M.; Baldwin, J. E.; Mayweg, A. V. W.; Pritchard, G. J., Biomimetic cycloaddition approach to tropolone natural products via a tropolone ortho-quinone methide. *Organic Letters* **2002,** *4* (17), 3009-3011.

14. Schrödinger Release 2017-2: MacroModel, version 11.2.014; Schrödinger, LLC: New York. **2017**.

15. Ernzerhof, M.; Scuseria, G. E., Assessment of the Perdew-Burke-Ernzerhof exchange-correlation functional. *Journal of Chemical Physics* **1999,** *110* (11), 5029-5036.

16. Adamo, C.; Barone, V., Toward reliable density functional methods without adjustable parameters: The PBE0 model. *Journal of Chemical Physics* **1999,** *110* (13), 6158-6170.

17. Grimme, S.; Antony, J.; Ehrlich, S.; Krieg, H., A consistent and accurate ab initio parametrization of density functional dispersion correction (DFT-D) for the 94 elements H-Pu. *Journal of Chemical Physics* **2010,** *132* (15), 154104.

18. Grimme, S.; Ehrlich, S.; Goerigk, L., Effect of the Damping Function in Dispersion Corrected Density Functional Theory. *Journal of Computational Chemistry* **2011,** *32* (7), 1456-1465.

19. Weigend, F.; Ahlrichs, R., Balanced basis sets of split valence, triple zeta valence and quadruple zeta valence quality for H to Rn: Design and assessment of accuracy. *Physical Chemistry Chemical Physics* **2005,** *7* (18), 3297-3305.

20. Mardirossian, N.; Head-Gordon, M., Thirty years of density functional theory in computational chemistry: an overview and extensive assessment of 200 density functionals. *Molecular Physics* **2017,** *115* (19), 2315-2372.

21. Grimme, S., Supramolecular Binding Thermodynamics by Dispersion-Corrected Density Functional Theory. *Chemistry-a European Journal* **2012,** *18* (32), 9955-9964.

22. Li, Y.-P.; Gomes, J.; Sharada, S. M.; Bell, A. T.; Head-Gordon, M., Improved Force-Field Parameters for QM/MM Simulations of the Energies of Adsorption for Molecules in Zeolites and a Free Rotor Correction to the Rigid Rotor Harmonic Oscillator Model for Adsorption Enthalpies. *Journal of Physical Chemistry C* **2015,** *119* (4), 1840-1850.

23. Ignacio Funes-Ardoiz, & Robert S. Paton. (2018, September 26). GoodVibes: version 2.0.3 (Version v2.0.3). Zenodo.

24. Liu, J. W.; Zhang, M. Y.; Yan, Y. M.; Wei, X. Y.; Dong, L.; Zhu, Y. X.; Cheng, Y. X., Characterization of sesquiterpene dimers from *Resina commiphora* that promote Adipose-derived stem cell proliferation and differentiation. *Journal of Organic Chemistry* **2018,** *83* (5), 2725-2733.

25. Qin, D. P.; Pan, D. B.; Xiao, W.; Li, H. B.; Yang, B.; Yao, X. J.; Dai, Y.; Yu, Y.; Yao, X. S., Dimeric cadinane sesquiterpenoid derivatives from *Artemisia annua*. *Organic Letters* **2018,** *20* (2), 453-456.

26. Zhang, Y.-L.; Zhou, X.-W.; Wu, L.; Wang, X.-B.; Yang, M.-H.; Luo, J.; Luo, J.-G.; Kong, L.-Y., Isolation, structure elucidation, and absolute configuration of syncarpic acid-conjugated terpenoids from *Rhodomyrtus tomentosa*. *Journal of Natural Products* **2017,** *80* (4), 989-998.

27. Hou, J. Q.; Guo, C.; Zhao, J. J.; Dong, Y. Y.; Hu, X. L.; He, Q. W.; Zhang, B. B.; Yan, M.; Wang, H., Anti-inflammatory meroterpenoids from *Baeckea frutescens*. *Journal of Natural Products* **2017,** *80* (8), 2204-2214.

28. Ma, S. G.; Gao, R. M.; Li, Y. H.; Jiang, J. D.; Gong, N. B.; Li, L.; Lu, Y.; Tang, W. Z.; Liu, Y. B.; Qu, J.; Lu, H. N.; Li, Y.; Yu, S. S., Antiviral spirooliganones A and B with unprecedented skeletons from the roots of *Illicium oligandrum*. *Organic Letters* **2013,** *15* (17), 4450-4453.

29. Liang, W. J.; Geng, C. A.; Zhang, X. M.; Chen, H.; Yang, C. Y.; Rong, G. Q.; Zhao, Y.; Xu, H. B.; Wang, H.; Zhou, N. J.; Ma, Y. B.; Huang, X. Y.; Chen, J. J., (+/-)-Paeoveitol, a pair of new norditerpene enantiomers from *Paeonia veitchii*. *Organic Letters* **2014,** *16* (2), 424-427.

30. Fu, H. Z.; Luo, Y. M.; Li, C. J.; Yang, J. Z.; Zhang, D. M., Psidials A-C, three unusual meroterpenoids from the leaves of *Psidium guajava* L. *Organic Letters* **2010,** *12* (4), 656-659.

31. Gao, Y.; Wang, G. Q.; Wei, K.; Hai, P.; Wang, F.; Liu, J. K., Isolation and biomimetic synthesis of (+/-)-guajadial B, a novel meroterpenoid from *Psidium guajava*. *Organic Letters* **2012,** *14* (23), 5936-5939.

32. Xu, G.; Yang, X. W.; Wu, C. Y.; Li, X. N.; Su, J.; Deng, X.; Li, Y.; Qin, H. B.; Yang, L. X.; Zhao, Q. S., Przewalskone: a cytotoxic adduct of a danshenol type terpenoid and an icetexane diterpenoid via hetero-Diels-Alder reaction from *Salvia przewalskii*. *Chem Commun (Camb)* **2012,** *48* (37), 4438-4440.

33. Gao, C.; Han, L.; Zheng, D.; Jin, H.; Gai, C.; Wang, J.; Zhang, H.; Zhang, L.; Fu, H., Dimeric abietane diterpenoids and sesquiterpenoid lactones from *Teucrium viscidum*. *Journal of Natural Products* **2015,** *78* (4), 630-638.

34. Li, Y.; Niu, S.; Sun, B.; Liu, S.; Liu, X.; Che, Y., Cytosporolides A-C, antimicrobial meroterpenoids with a unique peroxylactone skeleton from *Cytospora* sp. *Organic Letters* **2010,** *12* (14), 3144-3147.

35. Spence, J. T.; George, J. H., Structural reassignment of cytosporolides A-C via biomimetic synthetic studies and reinterpretation of NMR data. *Organic Letters* **2011,** *13* (19), 5318-5321.

36. Liu, L.; Liu, S.; Jiang, L.; Chen, X.; Guo, L.; Che, Y., Chloropupukeananin, the first chlorinated pupukeanane derivative, and its precursors from *Pestalotiopsis fici*. *Organic Letters* **2008,** *10* (7), 1397-1400.

37. Liu, L.; Han, Y.; Xiao, J.; Li, L.; Guo, L.; Jiang, X.; Kong, L.; Che, Y., Chlorotheolides A and B, spiroketals generated via Diels–Alder reactions in the Endophytic fungus *Pestalotiopsis theae*. *Journal of Natural Products* **2016,** *79* (10), 2616-2623.

38. Ding, G.; Zhang, F.; Chen, H.; Guo, L.; Zou, Z.; Che, Y., Pestaloquinols A and B, isoprenylated epoxyquinols from *Pestalotiopsis* sp. *Journal of Natural Products* **2011,** *74* (2), 286-291.

39. Rivera-Chávez, J.; Zacatenco-Abarca, J.; Morales-Jiménez, J.; Martínez-Aviña, B.; Hernández-Ortega, S.; Aguilar-Ramírez, E., Cuautepestalorin, a 7,8-dihydrochromene–oxoisochromane adduct bearing a hexacyclic scaffold from *Pestalotiopsis* sp. IQ-011. *Organic Letters* **2019,** *21* (10), 3558-3562.

40. Chen, Y.; Jiang, N.; Wei, Y. J.; Li, X.; Ge, H. M.; Jiao, R. H.; Tan, R. X., Citrofulvicin, an antiosteoporotic polyketide from *Penicillium velutinum*. *Organic Letters* **2018,** *20* (13), 3741-3744.

41. Zhao, H.; Chen, G.-D.; Zou, J.; He, R.-R.; Qin, S.-Y.; Hu, D.; Li, G.-Q.; Guo, L.-D.; Yao, X.-S.; Gao, H., Dimericbiscognienyne A: A meroterpenoid dimer from *Biscogniauxia* sp. with new skeleton and its activity. *Organic Letters* **2017,** *19* (1), 38-41.

42. Lu, Z.-Y.; Lin, Z.-J.; Wang, W.-L.; Du, L.; Zhu, T.-J.; Fang, Y.-C.; Gu, Q.-Q.; Zhu, W.-M., Citrinin dimers from the halotolerant fungus *Penicillium citrinum* B-57. *Journal of Natural Products* **2008,** *71* (4), 543-546.

43. Arnone, A.; Nasini, G.; Panzeri, W.; Pava, O. V. d.; Malpezzi, L., Acremine G, dimeric metabolite from cultures of *Acremonium byssoides* A20. *Journal of Natural Products* **2008,** *71* (1), 146-149.

44. Liu, L.; Li, Y.; Li, L.; Cao, Y.; Guo, L.; Liu, G.; Che, Y., Spiroketals of *Pestalotiopsis fici* provide evidence for a biosynthetic hypothesis involving diversified Diels–Alder reaction cascades. *The Journal of Organic Chemistry* **2013,** *78* (7), 2992-3000.

45. Yang, M.-H.; Gu, M.-L.; Han, C.; Guo, X.-J.; Yin, G.-P.; Yu, P.; Kong, L.-Y., Aureochaeglobosins A–C, three [4 + 2] adducts of chaetoglobosin and aureonitol derivatives from *Chaetomium globosum*. *Organic Letters* **2018,** *20* (11), 3345-3348.

46. Ren, J.; Niu, S.; Li, L.; Geng, Z.; Liu, X.; Che, Y., Identification of oxaphenalenone ketals from the Ascomycete fungus *Neonectria* sp. *Journal of Natural Products* **2015,** *78* (6), 1316-1321.

47. Wu, P.; Xue, J.; Yao, L.; Xu, L.; Li, H.; Wei, X., Bisacremines E–G, three polycyclic dimeric acremines produced by *Acremonium persicinum* SC0105. *Organic Letters* **2015,** *17* (19), 4922-4925.

48. Kusumi, T.; Ichikawa, A.; Kakisawa, H.; Tsunakawa, M.; Konishi, M.; Oki, T., The structures of quartromicins A1, A2, and A3: novel macrocyclic antiviral antibiotics possessing four tetronic acid moieties. *Journal of the American Chemical Society* **1991,** *113* (23), 8947-8948.

49. Bunyapaiboonsri, T.; Veeranondha, S.; Boonruangprapa, T.; Somrithipol, S., Ramiferin, a bisphenol-sesquiterpene from the fungus *Kionochaeta ramifera* BCC 7585. *Phytochemistry Letters* **2008,** *1* (4), 204-206.

50. Pittayakhajonwut, P.; Theerasilp, M.; Kongsaeree, P.; Rungrod, A.; Tanticharoen, M.; Thebtaranonth, Y., Pughiinin A, a sesquiterpene from the fungus *Kionochaeta pughii* BCC 3878. *Planta Medica* **2002,** *68* (11), 1017-1019.

51. Che, Y.; Wang, B.; Zhang, Y.; Zhang, J. New *Phoma* XZ068 used for preparing compound eupenifeldin is preserved at Chinese culture collection committee general microbiology center with accession No. CGMCC No.10481. CN105238702-A; CN105238702-B.

52. Ayers, S.; Zink, D. L.; Powell, J. S.; Brown, C. M.; Grund, A.; Bills, G. F.; Platas, G.; Thompson, D.; Singh, S. B., Noreupenifeldin, a tropolone from an unidentified ascomycete. *Journal of Natural Products* **2008,** *71* (3), 457-459.

53. Ainsworth, A. M.; Chicarellirobinson, M. I.; Copp, B. R.; Fauth, U.; Hylands, P. J.; Holloway, J. A.; Latif, M.; Obeirne, G. B.; Porter, N.; Renno, D. V.; Richards, M.; Robinson, N., Xenovulene A, a novel GABA-benzodiazepine receptor-binding compound produced by *Acremonium strictum*. *Journal of Antibiotics* **1995,** *48* (7), 568-573.

54. Qi, Q.-Y.; Bao, L.; Ren, J.-W.; Han, J.-J.; Zhang, Z.-Y.; Li, Y.; Yao, Y.-J.; Cao, R.; Liu, H.-W., Sterhirsutins A and B, two new heterodimeric sesquiterpenes with a new skeleton from the culture of *Stereum hirsutum* collected in Tibet Plateau. *Organic Letters* **2014,** *16* (19), 5092-5095.

55. Yang, X.-W.; Li, Y.-P.; Su, J.; Ma, W.-G.; Xu, G., Hyperjapones A-E, terpenoid polymethylated acylphloroglucinols from *Hypericum japonicum*. *Organic Letters* **2016,** *18* (8), 1876-1879.

56. Harris, G. H.; Hoogsteen, K.; Silverman, K. C.; Raghoobar, S. L.; Bills, G. F.; Lingham, R. B.; Smith, J. L.; Dougherty, H. W.; Cascales, C.; Pelaez, F., Isolation and structure determination of pycnidione, a novel bistropolone stromelysin inhibitor from a *Phoma* sp. *Tetrahedron* **1993,** *49* (11), 2139-2144.

57. Wright, A. D.; Lang-Unnasch, N., Potential antimalarial lead structures from fungi of marine origin. *Planta Medica* **2005,** *71* (10), 964-966.

58. Pornpakakul, S.; Roengsumran, S.; Deechangvpart, S.; Petsom, A.; Muangsin, N.; Ngamroinavanich, N.; Sriubolmas, N.; Chalchit, N.; Ohta, T., Diaporthichalasin, a novel CYP3A4 inhibitor from an endophytic *Diaporthe* sp. *Tetrahedron Letters* **2007,** *48* (4), 651-655.

59. Kaneko, M.; Matsuda, D.; Ohtawa, M.; Fukuda, T.; Nagamitsu, T.; Yamori, T.; Tomoda, H., Potentiation of bleomycin in Jurkat cells by fungal pycnidione. *Biological & Pharmaceutical Bulletin* **2012,** *35* (1), 18-28.

60. Hsiao, C.-J.; Hsiao, S.-H.; Chen, W.-L.; Guh, J.-H.; Hsiao, G.; Chan, Y.-J.; Lee, T.-H.; Chung, C.-L., Pycnidione, a fungus-derived agent, induces cell cycle arrest and apoptosis in A549 human lung cancer cells. *Chemico-Biological Interactions* **2012,** *197* (1), 23-30.

61. Weenen, H.; Nkunya, M. H. H.; Elfadl, A. A.; Harkema, S.; Zwanenburg, B., Lucidene, a bis(benzopyranyl) sesquiterpene from *Uvaria lucida* ssp *lucida*. *Journal of Organic Chemistry* **1990,** *55* (17), 5107-5109.